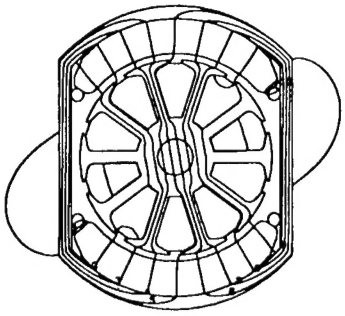

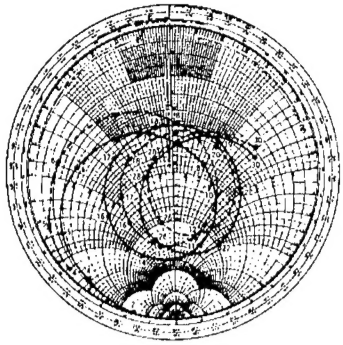

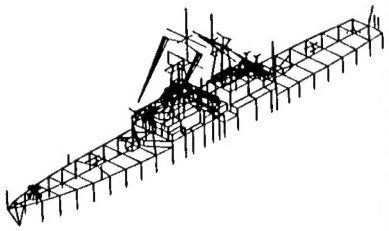

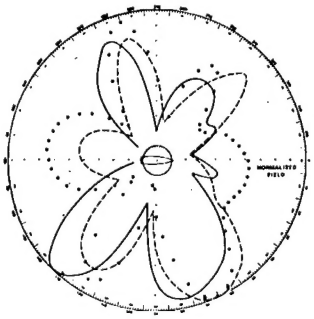

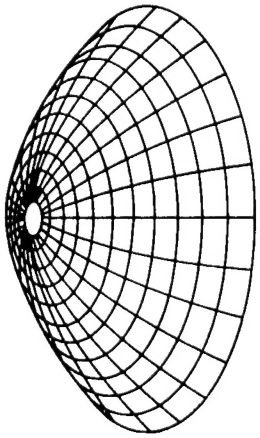

APPLIED COMPUTATIONAL ELECTROMAGNETICS SOCIETY JOURNAL

November 1999
Vol. 14 No. 3

ISSN 1054-4887

GENERAL PURPOSE AND SCOPE. The Applied Computational Electromagnetics Society Journal_hereinafter known as the ***ACES Journal*** is devoted to the exchange of information in computational electromagnetics, to the advancement of the state-of-the-art, and to the promotion of related technical activities. A primary objective of the information exchange is the elimination of the need to "re-invent the wheel" to solve a previously-solved computational problem in electrical engineering, physics, or related fields of study. The technical activities promoted by this publication include code validation, performance analysis, and input/output standardization; code or technique optimization and error minimization; innovations in solution technique or in data input/output; identification of new applications for electromagnetics modeling codes and techniques; integration of computational electromagnetics techniques with new computer architectures; and correlation of computational parameters with physical mechanisms.

SUBMISSIONS. The ***ACES Journal*** welcomes original, previously unpublished papers, relating to **applied computational electromagnetics**.

Typical papers will represent the computational electromagnetics aspects of research in electrical engineering, physics, or related disciplines. However, papers which represent research in **applied computational electromagnetics** itself are equally acceptable.

Contributions may be sent to the Editors-in-Chief, Dr. Ahmed Kishk or Dr. Allen Glisson

Department of EE
University of Mississippi
University, MS, 38677 USA
Phone: 662-232-5385 (Ahmed)
Phone: 662-232-5353 (Allen)
Fax: 662-232-7231
email:ahmed@olemiss.edu
email:aglisson@olemiss.edu. See "Information for Authors" on the back cover.

SUBSCRIPTIONS. All members of the Applied Computational Electromagnetics Society (**ACES**) who have paid their subscription fees are entitled to receive the ***ACES Journal*** with a minimum of three issues per calendar year.

Visit us on line at: http://aces.ee.olemiss.edu

Back issues, when available, are $15.00 each. Subscriptions to **ACES**, orders for back issues of the ***ACES Journal*** and changes of addresses should be sent to:

Dr. Richard W. Adler
ACES Executive Officer
ECE Department, Code ECAB
Naval Postgraduate School
833 Dyer Road, Room 437
Monterey, CA 93943-5121 USA

Allow four week's advance notice for change of address. Claims for missing issues will not be honored because of insufficient notice or address change or loss in mail unless the secretary is notified within 60 days for USA and Canadian subscribers or 90 days for subscribers in other countries, from the last day of the month of publication. For information regarding reprints of individual papers or other materials, see "Information for Authors".

LIABILITY. Neither ACES or the ***ACES Journal*** editors are responsible for any consequence of misinformation or claims, express or implied, in any published material in an ***ACES Journal*** issue. This also applies to advertising, for which only camera-ready copies are accepted. Authors are responsible for information contained in their papers. If any material submitted for publication includes material which has already been published elsewhere, it is the author's responsibility to obtain written permission to reproduce such material.

APPLIED COMPUTATIONAL ELECTROMAGNETICS SOCIETY Journal

November 1999
Vol. 14 No. 3

ISSN 1054-4887

The ACES Journal is abstracted in INSPEC, in Engineering Index, and in DTIC.

The second, third, fourth, and fifth illustrations on the front cover have been obtained from Lawrence Livermore National laboratory.

The first illustration on the front cover has been obtained from FLUX2D software, CEDRAT S.S. France, MAGSOFT Corporation, New York.

THE APPLIED COMPUTATIONAL ELECTROMAGNETICS SOCIETY

JOURNAL EDITORS

THE APPLIED COMPUTATIONAL ELECTROMAGNETICS SOCIETY

JOURNAL

Vol. 14 No. 3 November1999

TABLE OF CONTENTS

Predicting MoM Error Currents by Inverse Application of Residual E-Fields

André P.C. Fourie, Derek C. Nitch, and Alan R. Clark

Abstract— **This paper presents a methodology to predict *a posteriori* the error associated with a Method-of-Moments solution. The discussion is limited to a one dimensional pulse basis function wire-based implementation, but is easily extended. A Formulation for Error Prediction based on the relationship between the error in the boundary conditions and the error in the solution is presented, and validated by an over-segmented problem. The formulation is then used in a normally-segmented solution to predict the error by means of a linear interpolation of the calculated current which results in a smoother boundary condition error. The results show that this normally-segmented methodology predicts the error current within 5% of the "accurate" error current obtained by a 20:1 oversegmentation of the problem. Further work needs to be performed to extend this to the multidimensional case, although no technical difficulties are expected with this.**

I. Introduction

In a method of moments (MoM) solution to an electromagnetic problem, the structure currents are calculated to ensure that the boundary conditions are satisfied in some sense, usually at specific match points (point matching) or over specific domains in an average, or weighted average, manner.

The boundary condition to be satisfied—when using a MoM for perfectly conducting wires—is that the total tangential **E**-field should be zero at all points on the wire. A current which ensures zero tangential **E**-fields in a continuous sense on all wires would be accurate in accordance with the uniqueness theorem.

Many researchers have recognized that the accuracy of a method must be related to how well the boundary conditions are met by a specific solution (Hsaio & Kleinman 1996, Meyer & Davidson 1996). The exact relationship between the error in the boundary conditions and the error in the observable quantities has not been defined and has also not been used to gain an estimate of solution (or method) accuracy. This study investigates the possibility of getting such a relationship and then formulates approximations which allow its incorporation in MoM (and other methods) with the lowest computational overhead.

II. Formulation for Error Prediction (FEP)

The obvious relationship between the error in the boundary conditions and the error in the solution is quite clear in the following formulation for perfectly conducting wires (Thiele 1973):

Suppose we have obtained a current solution, $I(s)$, where

$$I(s) = I_a(s) + I_e(s) \tag{1}$$

The authors are with the Department of Electrical Engineering, University of the Witwatersrand, Johannesburg, Wits, 2050 South Africa.

and $I_a(s)$ is the accurate solution and $I_e(s)$ is the error associated with the solution $I(s)$.

If we have the continuous (and assumed accurate for the moment) relationship between the current and the excitation then

$$L_{op} I_a(s) = V(s) \tag{2}$$

where L_{op} is the linear operator (Pocklington's equation is an example for wire problems) which defines the excitation tangential to the wire, $V(s)$. Pocklington's equation is usually solved using the Method-of-Moments. In the case of a point matching solution, this results in a tangential **E**-field error of zero *only* at the match points. At any other point on the structure there *will* be a tangential **E**-field error.

If pulse weighting functions were used in the MoM solution, then it is likely that there will be a tangential **E**-field error at any point on the structure—the tangential **E**-field error will be zero only in the average sense.

The tangential **E**-field *errors* found on the structure are defined to be the *residuals*. The tangential **E**-field from the inaccurate current, $I(s)$, is:

$$L_{op} I(s) = V(s) + V_e(s) \tag{3}$$

where $V_e(s)$ is the tangential **E**-field residual (or error) on the wires. Combining equations (1) and (3), and from the linearity of the operator and superposition it follows that

$$L_{op} I_e(s) = V_e(s) \tag{4}$$

The inverse of equation (4) will allow the error current $I_e(s)$ to be obtained from the **E**-field residual (error), $V_e(s)$.

$$I_e(s) = L_{op}^{-1} V_e(s) \tag{5}$$

We shall call the above mathematical development the Formulation for Error Prediction (FEP) for later reference. Once the error currents have been found, the errors in secondary parameters such as radiation pattern or input impedance are easily quantified. This may be done, for example, by using the error current to obtain near/far fields at the same points as the full solution values were computed. This will produce "error fields" which places a bound on the error in the computed field values. Errors in other parameters such as input impedance, etc. may be obtained in a similar manner.

This somewhat trivial proof indicates that the error in any solution may, in principle, be calculated exactly provided that:

- The residual **E**-field over the structure can be calculated continuously and accurately.

1054-4887

- An accurate continuous operator L_{op} and its inverse exist.

In practice the following obstacles to using this result are apparent:

- Calculation of the residual **E**-field over the structure can be computationally time intensive.
- The operator is normally discretized as an interaction matrix and hence is neither continuous nor accurate.

III. Using the FEP to obtain accurate error currents.

The graphs which follow illustrate an investigation using the FEP for a specific problem. A dipole antenna of length $\ell = 0.5\lambda$ and with radius, $a = 0.005\lambda$ was excited with an incident **E**-field of 1 V/m.

A simple MoM program was written which uses pulse basis functions and point matching. The convergence of the method is shown in Figure 1. The method clearly converges to a stable answer when around 100 to 200 segments are used for the dipole. The Formulation for Error Prediction

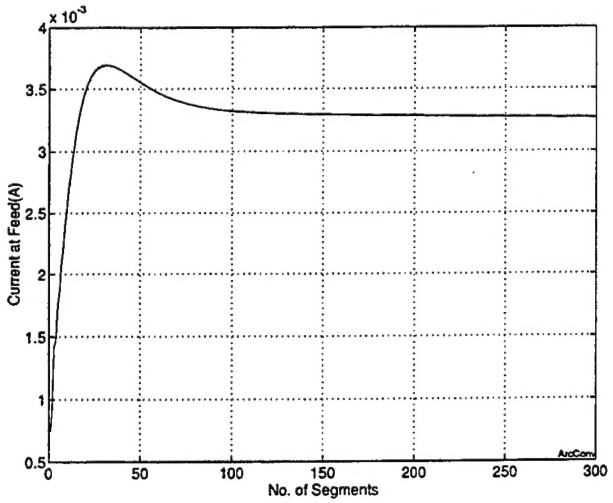

Fig. 1. The feed current magnitude for a variation in number of segments of a dipole with $\ell = 0.5\lambda$ and $a = 0.005\lambda$ using pulse basis functions and point matching.

(FEP) is illustrated by considering the current from the 200 segment problem to be the "accurate" current. Two "inaccurate" currents were obtained by solving the same problem with only 10 and 20 segments.

The residual **E**-fields from these two inaccurate solutions were then obtained at 200 points across the dipole (i.e. at many more points than the match points). Figure 2 shows the residual **E**-field magnitude for a 10 segment solution and a 20 segment solution, which clearly demonstrates that the boundary conditions are exactly met at the match points, but also shows a significant error (50V/m for a 1V/m excitation) at other points. The residual **E**-fields in Figure 2 can be applied as an *excitation vector* on the same geometry divided into 200 segments to yield the error current in accordance with the FEP as stated in equations (4) and (5). Figure 3 shows this graphically. It is clear

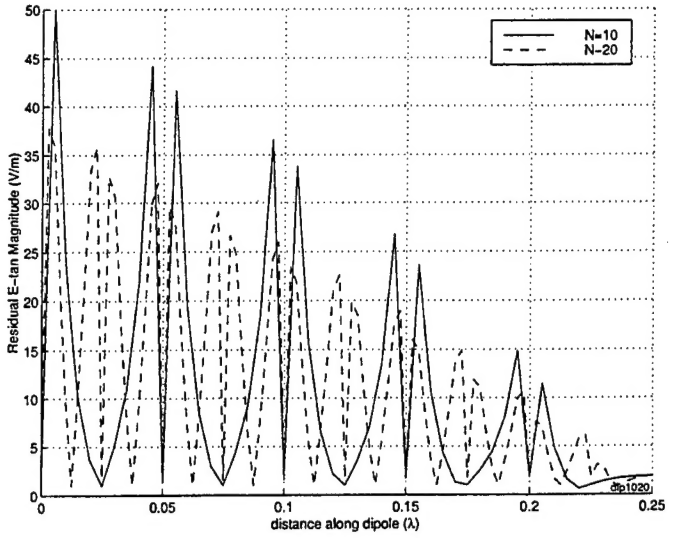

Fig. 2. The magnitude of the residual **E**-fields obtained for a 10 and 20 segment dipole with $\ell = 0.5\lambda$ and $a = 0.005\lambda$ using pulse basis functions and point matching.

from these figures that sum of the inaccurate current (obtained from the 10 segment solution) and the error current (obtained by applying the residual **E**-fields via FEP) is practically equal to the "accurate" current obtained from the 200 segment case. The 200 segment inverse interaction matrix hence represents an accurate and pseudo-continuous inverse operator, L_{op}, and the 200 point discretization of the residual **E**-field a pseudo-continuous representation on the error, $E_e(s)$. Figure 3 illustrates the principle behind

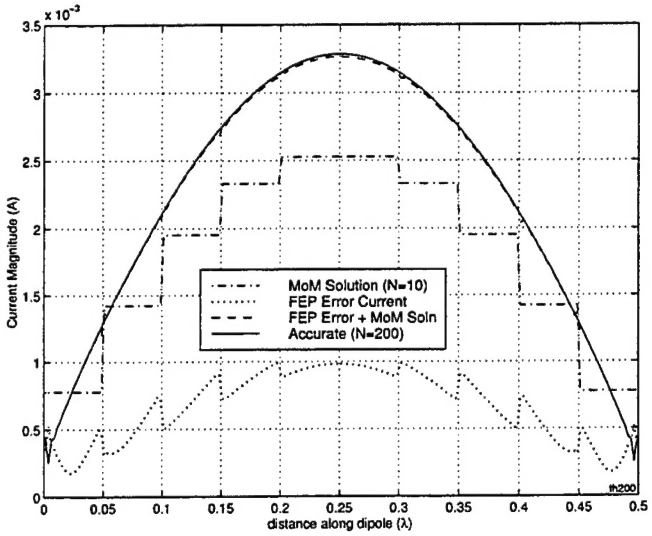

Fig. 3. The current magnitude to prove the FEP for a 10 segment dipole with $\ell = 0.5\lambda$ and $a = 0.005\lambda$ using pulse basis functions and point matching.

error prediction by inverse application of the residual **E**-fields as excitations to produce an error current. The computational effort does not render it suitable as a general tool for error prediction—oversegmenting a problem by a factor of 20 in order to obtain an error estimate is clearly unproductive! The technique may however, be useful as

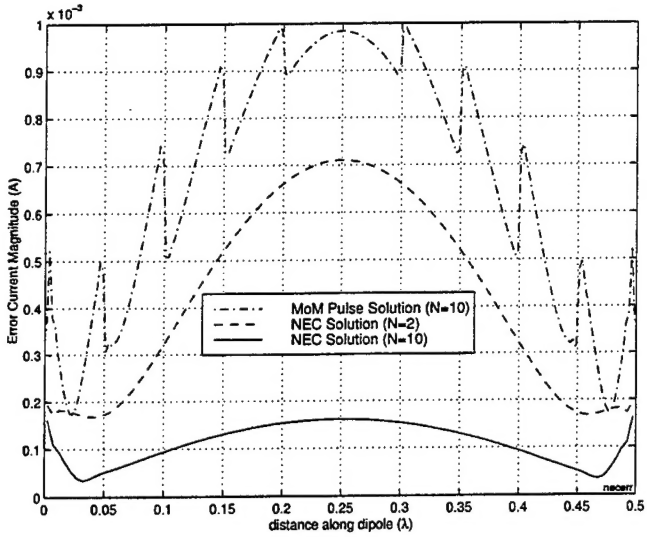

Fig. 4. The error current associated with NEC2 solutions for a 2, 10 segment dipole , as compared to the 10 segment MoM solution using pulses with $\ell = 0.5\lambda$ and $a = 0.005\lambda$.

a research tool; different basis and/or weighting functions, for instance, may be compared in terms of absolute error currents. Such an exercise was performed to compare the NEC2 (Burke & Poggio 1981) basis functions with pulse basis functions. The same dipole antenna was simulated using NEC2 with 2 and 10 segments and the error currents obtained using the same procedure, by applying the tangential **E**-field errors as an excitation to an oversegmented wire of the same dimensions. The error currents associated with these two cases are shown in Figure 4, together with the 10 segment MoM problem, presented earlier. Comparing these currents indicates that NEC2 basis functions achieve roughly the same accuracy for 2 segments as pulse basis functions do for 10 segments. This may be expected since NEC2 uses a superpositioned sine, cosine and a constant term as its basis function, which is quite suitable for approximating the currents on a dipole.

IV. Using FEP *without* oversegmentation

The previous section showed that the FEP may be used to obtain accurate error currents with major computational overheads associated with overdiscretizing the problem. We now attempt to use the same FEP without the requirement to increase the problem discretization. The main problem with the FEP is that although it is possible to calculate the residual accurately, only N excitations may be used to excite the error currents. It is hence necessary to reduce the residual over each segment to a single value. The first approximation to the accurate FEP was to obtain the residual **E**-fields at 100 points on the dipole and use the average value of ten samples applied as $E_e(s)$ on the original 10 segment problem[1]. Results from using this method were not satisfactory, since the large oscillations in residual **E**-field evident in Figure 2 require a finer discretization in order to obtain a reasonable estimate—which defeats the objective. It should be noted that the estimate was not inaccurate as a result of insufficient field point samples when averaging, since increasing the samples to 200 and 400 did not improve matters.

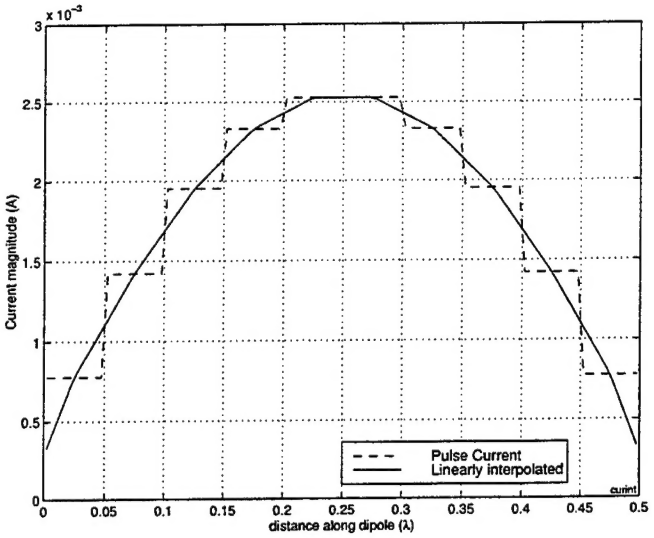

Fig. 5. The current obtained for a 10 segment dipole with $\ell = 0.5\lambda$ and $a = 0.005\lambda$ using pulse basis functions and point matching and a linear interpolation to the original pulse current.

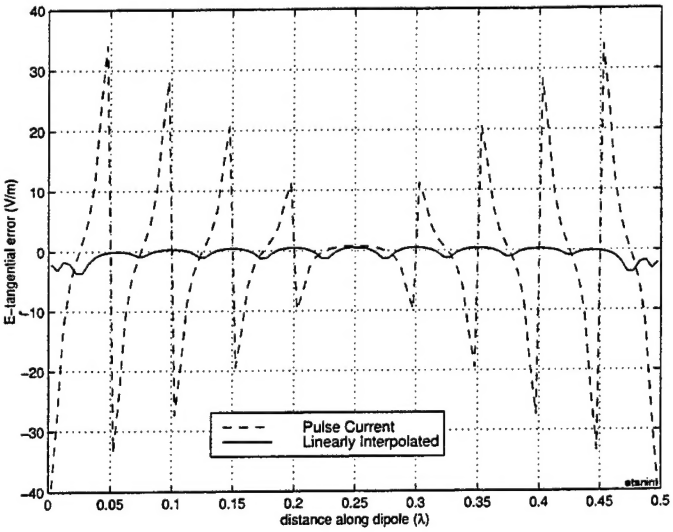

Fig. 6. The tangential **E**-field magnitude from a 10 segment dipole with $\ell = 0.5\lambda$ and $a = 0.005\lambda$ using pulse basis functions and point matching as well as the tangential **E**-field from a linear approximation to the original pulse current

We recognized that the large oscillations in the residual **E**-fields were mainly due to the pulse basis functions which are discontinuous at segment boundaries. Rather than solving the problem with different basis functions to

[1]Note that using an "average value" is meaningful for a point matching MoM (using Dirac delta weighting functions), however, if pulse weighting functions are used, the error residual computed would be zero. In the case of the pulse weighting function, one sample per segment may result in a more appropriate segment error. It stands to reason that the method used to obtain the segment residual must employ a function other than that of the actual testing functions used in the MoM solution.

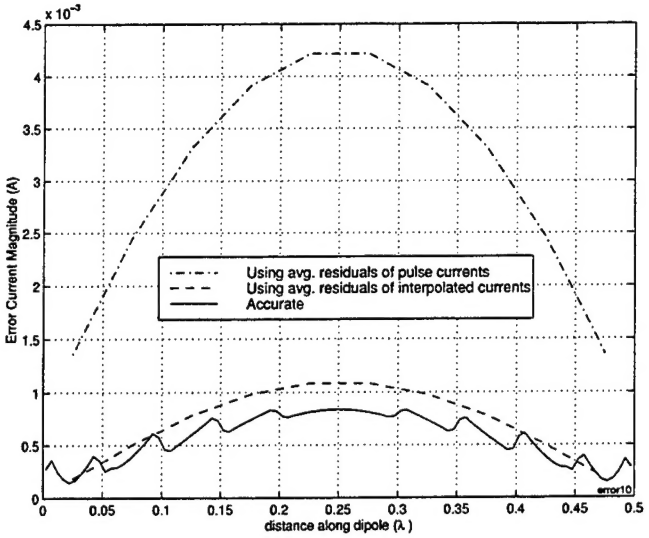

Fig. 7. Error current from applying the averaged **E**-tangential fields obtained from the pulse currents and the linearly interpolated currents as an excitation to the 10 segment problem. The accurate error current obtained earlier is also shown for comparison.

ensure smooth residual **E**-field behaviour, we performed curve fitting to the *actual pulse current solution* before calculating the residual **E**-fields via FEP. Figure 5 shows the original pulse currents obtained from the MoM together with a linear approximation to these currents, which clearly offer a smoother current solution. Figure 6 compares the residual **E**-field due to the original pulse currents as well as to the linearly interpolated currents (using only 10 segments). The residuals from the interpolated currents are clearly much less oscillatory than those resulting from the actual pulse solution.

The average (over a segment) of the residual **E**-fields associated with the linearly interpolated current shown in Figure 6 was applied to the original 10 segment problem to obtain error currents without increasing problem discretization. Figure 7 shows the effectiveness of this approach. Using the average residual **E**-fields obtained from the linearly interpolated currents provides a good estimate of the accuracy of the solution.

It should be noted that, in general, the linear interpolation of the pulse basis function solution will not necessarily yield a more accurate current representation. (It was also not the purpose.) The interpolated current was merely used to produce better behaved (less oscillatory) residuals. These residuals can be averaged over one segment to yield a residual **E**-field vector of the same order as the problem discretization (10 values in our example). The FEP can, hence, be used with the same size matrix, and if matrix factorization is used, without much additional computational effort.

V. Conclusion

The FEP is definitely suitable for research purposes when applying it "accurately" by increasing the problem discretization. An error prediction scheme for estimating the errors associated with run-of-the-mill simulations using MoM, however, would not be useful if problem order is increased. This is mainly due to memory limitations (since matrix storage space is proportional to N^2) and to computational limitations (since execution time is proportional to N^3). The latter part of this limited study shows that a reasonable estimate may be obtained without using finer problem discretization provided that the behaviour of the **E**-field residuals are smooth over a segment. This is true even if a discontinuous current due to simple basis functions is artificially smoothed by interpolation to achieve better behaviour of residual **E**-fields.

It seems to us that the relationship between residual **E**-field smoothness and required problem discretization must obey normal sampling criteria for the FEP to provide reasonable error estimates. Problem discretization should allow the residual **E**-field curve shape to be retained by the error excitation vector for good estimates. Residual **E**-field variations along a wire with a period of the order of the segment length (0.05λ for 10 segments) are the result of non-physical behaviour of currents at segment boundaries; it should hence, in principle, always be possible to "smooth" current behaviour to obtain slower variations in residuals (changes in the order of a wavelength should be more realistic).

The interpolation approach also illustrates a very interesting aspect of the behaviour of the residual **E**-fields: the large, fast, oscillations are purely associated with local, non-physical current behaviour. Smoothing the current results in much lower variations in the residual **E**-fields, which render them more suitable for error prediction. The interpolated currents are not, however, inherently more accurate—at least in terms of errors in overall magnitude—but they do seem to be a more natural representation of current shape, which one would expect. In the cases investigated here, current interpolation was done in order to obtain error estimates with lower computational overheads. The opposite is clearly also possible: currents may be obtained using some crude basis functions and can then be smoothed *a posteriori* (or altered) while using the FEP method to measure whether a more accurate answer was obtained.

Naturally, errors in the secondary parameters such as input impedance or radiation pattern, etc. can be derived from the error currents using the existing relationships between currents and these parameters—allowing for "error bars" to be placed on these parameters.

References

Burke, G. J. & Poggio, A. J. (1981), Numerical Electromagnetics Code (NEC)—Method of Moments, Tech. doc. 116, Naval Oceans Systems Centre, San Diego, CA.

Hsaio, G. C. & Kleinman, R. E. (1996), 'Error control in numerical solution of boundary integral equations', *Applied Computational Electromagnetics Society Journal* **11**(1), 32–36.

Meyer, F. J. C. & Davidson, D. B. (1996), 'A-posteriori error estimates for two-dimensional electromagnetic field computations: Boundary elements and finite elements', *Applied Computational Electromagnetics Society Journal* **11**(2), 40–50.

Thiele, G. A. (1973), Wire antennas, *in* R. Mitra, ed., 'Computer techniques for Electromagnetics', Pergamon Press, chapter 2, pp. 7–19.

On the Iteration of Surface Currents and the Magnetic Field Integral Equation

Daniel D. Reuster, Ph.D. and Gary A. Thiele, Ph.D.
Department of Electrical Engineering
University of Dayton
Dayton, OH 45469-0226

Paul W. Eloe, Ph.D.
Department of Mathematics
University of Dayton
Dayton, OH 45469-2316

Abstract - In an effort to mathematically validate the convergence properties of various surface current-iterative methods, the magnetic field integral equation is analyzed for its contraction mapping properties. The analysis is performed first on the general integral operators and then on the matrices representing the discrete forms of the integral operators associated with the different iterative methods. The contraction mapping properties are determined by investigating the spectral radius of each linear operator. Conditions for the verification and validation of these iterative methods are provided, along with mathematical checks for the existence of spurious modes and the existence of internal resonance.

1. Introduction

Throughout the past decade, a variety of surface current-iterative methods [1-6] have been proposed to solve electromagnetic scattering and radiation problems involving the Magnetic Field Integral Equation (MFIE) and related integral equations. Most of these methods were developed as alternatives to the traditional Method of Moments (MoM) [7,8] solution, which involve the inversion of a dense (*most often complex*) matrix. While each of the methods showed some computational advantages, each also introduced a new issue of concern: that of convergence. For the most part, the convergence of these iterative methods has been shown by numerical example, but little mathematical analysis has been offered for the understanding of why these methods converge to the correct solution. Oftentimes convergence is simply claimed when the delta change in iterations falls below some pre-set limit. In the following paper, the MFIE is examined to explain why these surface current-iterative methods have been successfully iterated to convergence.

In previous work Kaye *et al.* [1] found that iterative solutions to the MFIE for the surface current would always yield convergence for Perfectly Electrically Conducting (PEC) bodies which where divided into two parts: a side illuminated by the incident field, and a shadowed side. Coupled integral equations were written for each side. The iterative process started on the illuminated side by iterating from the Physical Optics (PO) [9] current to an improved value. The process then went to the shadowed side where the improved current on the illuminated side was used with an initial estimate (*most often zero*) for the shadowed side current to obtain an improved shadowed side current. The process continued by returning to the illuminated side to obtain further improvement for the illuminated side current and then returned to the shadowed side to obtain further improvement to the shadowed current. The process was halted when the delta change in the solution fell below some pre-set limit.

Reuster & Thiele [2] found that the same iterative procedure could be used for PEC cavities where the aperture of the cavity was treated as the illuminated side and the cavity walls were treated as the shadowed side. The iterative process began by taking the aperture field to be that produced by an external plane wave illumination. The aperture field was then used to find the total magnetic field, via iteration, along the cavity walls. The field along the cavity walls was then used to update the total field at the aperture via iteration. The improved knowledge of the aperture field was then used to obtain a further update of the field along the cavity walls, which in turn was used to update the aperture field. Again, the process was halted when the delta change in the solution fell below some pre-set limit.

Obelleiro-Basteiro *et al.* [3] demonstrated a method similar to the iterative method proposed in [2] where the PO approximation was used to simplify the iterative procedure. Numerical results are presented which demonstrate the convergence and accuracy of the method, but no mathematical analysis is provided as to why the method converges. Collins & Skinner [4] demonstrated an iterative method for calculating the scattering from perturbed circular dielectric cylinders by using equivalent currents along the perimeter of the cylinder. Their paper alludes to the mathematical properties of the method's convergence, but no mathematical analysis is presented. Reuster, *et al.* [5] showed by numerical example that convergence could be obtained by directly iterating the

entire currents on a PEC body if the PO approximation was used as an initial condition; however, little mathematical analysis was provided. Finally, Hodges & Rahmat-Samii [6] present an advanced iterative method for large PEC bodies consisting of both wires and closed surfaces. Their iterative method involves the Electric Field Integral Equation (EFIE) as well as the MFIE and the PO approximation. Again, no mathematical analysis is provided as to why the method converges, and convergence is determined when the delta change in the solution falls below some pre-set limit.

Essentially, all of these surface current-iterative methods are fixed-point iterative problems [10-12] where the MFIE or a related integral equation is manipulated (*usually by observing physical characteristics associated with the particular problem*) to develop an iterative scheme which is "hopefully" a contraction mapping. The establishment of a contraction mapping is the unique feature that guarantees that the iterative method will converge in a monotonic mean-square sense. In the work that follows, two formulations of the magnetic field integral equation (*Maue's formulation and the Total Field formulation*) are analyzed for their potential contraction mapping characteristics. The effect of the discrete form operator size on the contraction mapping properties of each formulation is studied, and a mathematical check is presented for the existence of spurious modes and the existence of internal resonance. Finally, a general iterative scheme, which involves subdividing the integral operator for the creation/insurance of contraction mappings, is presented. This general iterative scheme is related to the surface current-iterative methods [1-6] that were discussed earlier.

2. Contraction Mapping Analysis of the MFIE

For simplicity a 2D Transverse Electric (TE) PEC scattering problem, as shown in Figure 1, is chosen as a baseline model for analysis. This particular scattering problem allows the normally complex 3-dimensional vector integral equation to be reduced to a 2-dimensional scalar integral equation which still maintains all of the properties associated with the general vector integral equation. Hence, no loss in generality is experienced in working with the reduced integral equation. The derivation of both Maue's equation and the Total Field equation proceeds as follows.

For 2D electromagnetic radiation and scattering problems, where the magnetic field is parallel to the geometry of interest, the MFIE may be stated as [1,13]:

$$-H_z^I(\bar{r}) = \frac{j\beta}{4}\int_C H_z^T(\bar{r}')H_1^{(2)}(\beta|\bar{r}-\bar{r}'|)\cos\phi dl + \frac{1}{2}H_z^T(\bar{r}) \quad (1)$$

Where C is the simple closed curve (*in the x-y plane*) describing the PEC body of interest,

$$\lim_{\bar{r}'\to\bar{r}^-}\frac{j\beta}{4}\int_C H_z^T(\bar{r}')H_1^{(2)}(\beta|\bar{r}-\bar{r}'|)\cos\phi dl = 0$$

, and $\frac{1}{2}H_z^T(\bar{r})$ is the principle value of the integral. From (1), both Maue's formulation and the Total Field formulation for the MFIE may be obtained as follows.

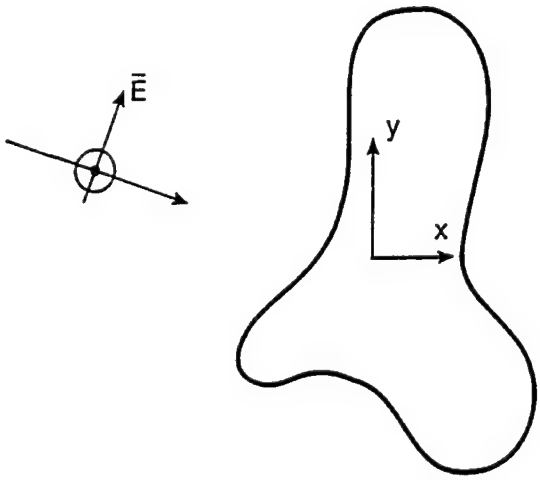

Figure 1 – 2D TE PEC Scattering Problem

Maue's Formulation. Maue's formulation is obtained from (1) by subtracting the integral operator from both sides of (1) and then scaling (1) by a factor of two.

$$H_z^T(\bar{r}) = -2H_z^I(\bar{r}) + \frac{-j\beta}{2}\int_C H_z^T(\bar{r}')H_1^{(2)}(\beta|\bar{r}-\bar{r}'|)\cos\phi dl \quad (2)$$

Total Field Formulation. The Total Field formulation is obtained from (1) by subtracting the integral operator from both sides of (1) and then adding the principle value to both sides of (1).

$$H_z^T(\bar{r}) = -H_z^I(\bar{r}) + \frac{-j\beta}{4}\int_C H_z^T(\bar{r}')H_1^{(2)}(\beta|\bar{r}-\bar{r}'|)\cos\phi dl + \frac{1}{2}H_z^T(\bar{r}) \quad (3)$$

Note that the only significant difference between Maue's formulation and the Total Field formulation is the location of the principle value of the integral. It will be shown that the location of the principle value has a major effect on the contraction mapping properties of the MFIE.

Integral equations (2) and (3) may be solved using fixed-point iteration, provided that these integral formulations are contraction mappings. By definition, contraction mappings may be iterated directly to a unique solution with a guarantee of mean squared-monotonic convergence [10-12]. This convergence is independent of the initial guess used to initiate the iterative process. The general test for a contraction mapping proceeds as follows.

Let ψ_1 and ψ_2 represent two approximations for ψ in an equation of the following form, where L is any linear operator and F is a constant forcing function

$$\psi = L(\psi) + F \,. \tag{4}$$

Then (4) is a contraction mapping and may be solved directly using fixed-point iteration (*with the guarantee of mean squared monotonic convergence*) if and only if

$$|L(\psi_2 - \psi_1)| \le \kappa |\psi_2 - \psi_1| \,, \qquad 0 \le \kappa < 1 \,. \tag{5}$$

Applying the above test to Maue's formulation yields (6).

$$|H_z^T(\bar{r})_2 - H_z^T(\bar{r})_1| \ge \left| \frac{\beta}{2} \int_C \left[H_z^T(\bar{r}')_2 - H_z^T(\bar{r}')_1 \right] h_1^{(2)}(\beta |\bar{r} - \bar{r}'|) \cos\phi \, dl \right| \tag{6}$$

After simplification, using the triangle inequality theorem, the contraction-mapping test can be obtained for Maue's formulation (7).

$$\int_C |h_1^{(2)}(\beta |\bar{r} - \bar{r}'|) \cos\phi| \, dl \le \frac{2}{\beta} \tag{7}$$

Similarly, the contraction-mapping test can be obtained for the Total Field formulation (8).

$$\int_C |h_1^{(2)}(\beta |\bar{r} - \bar{r}'|) \cos\phi| \, dl \le \frac{4}{\beta} \tag{8}$$

Note that (7) and (8) are purely functions of the problem's geometry and the wavelength of interest ($\beta = 2\pi/\lambda$). The requirements for convergence are independent of the initial conditions used in the iterative process. Also note that the convergence condition for Maue's equation is more difficult to satisfy than the convergence condition for the Total Field equation. This is a direct result of the removal of the principle value from the integral operator in Maue's formulation. While both (7) and (8) may be shown true for a particular geometry, there does not exist a general proof for arbitrary PEC scattering bodies. Hence, further investigation into the contraction mapping properties of both Maue's formulation and the Total Field formulation is continued on a discretized/numerical level.

3. Contraction Mapping Analysis of the Discretized MFIE

The inability to work with (7) and (8) results in the need to approximate the integral operators in (2) and (3) with systems of linear equations. Applying a pulse-basis point-patching MoM expansion [7] to (2) and (3) results in the following approximate expansions for Maue's formulation and the Total Field formulation. Similar analysis can be performed for more advanced MoM expansions [8].

$$H_z^T(\bar{r}_m) = -2 H_z^I(\bar{r}_m) + \frac{-j\beta}{2} \sum_{m \ne n} \Delta_n H_z^T(\bar{r}_n) h_1^{(2)}(\beta |\bar{r}_m - \bar{r}_n|) \cos\phi_{mn} \tag{9}$$

$$H_z^T(\bar{r}_m) = -H_z^I(\bar{r}_m) + \frac{-j\beta}{4} \sum_{m \ne n} \Delta_n H_z^T(\bar{r}_n) h_1^{(2)}(\beta |\bar{r}_m - \bar{r}_n|) \cos\phi_{mn} + \frac{1}{2} H_z^T(\bar{r}_m) \tag{10}$$

Expressing (9) and (10) in matrix from yields (11) and (12), respectively.

$$\begin{bmatrix} H_z^T(\bar{r}_m) \end{bmatrix} = \begin{bmatrix} 0 & \frac{-j\beta}{2} \Delta_n h_1^{(2)}(\beta |\bar{r}_m - \bar{r}_n|) \cos\phi_{mn} \\ & 0 \\ & & 0 \\ & & & 0 \\ \frac{-j\beta}{2} \Delta_n h_1^{(2)}(\beta |\bar{r}_m - \bar{r}_n|) \cos\phi_{mn} & & & 0 \end{bmatrix} \begin{bmatrix} H_z^T(\bar{r}_n) \end{bmatrix} - \begin{bmatrix} 2 H_z^I(\bar{r}_m) \end{bmatrix} \tag{11}$$

$$\begin{bmatrix} H_z^T(\bar{r}_m) \end{bmatrix} = \begin{bmatrix} 1/2 & \frac{-j\beta}{4} \Delta_n h_1^{(2)}(\beta |\bar{r}_m - \bar{r}_n|) \cos\phi_{mn} \\ & 1/2 \\ & & 1/2 \\ & & & 1/2 \\ \frac{-j\beta}{4} \Delta_n h_1^{(2)}(\beta |\bar{r}_m - \bar{r}_n|) \cos\phi_{mn} & & & 1/2 \end{bmatrix} \begin{bmatrix} H_z^T(\bar{r}_n) \end{bmatrix} - \begin{bmatrix} H_z^I(\bar{r}_m) \end{bmatrix} \tag{12}$$

Note that the principle value of the integral appears as the diagonal elements of the matrix equation associated with the Total Field formulation (12) while the principle value of the integral is incorporated into the forcing function of the matrix equation associated with Maue's formulation (11). This is a direct result of the removal of the principle value from the integral operator in Maue's formulation.

It is now possible to analyze (11) and (12) for their contraction mapping properties in a fashion similar to the analysis performed in Section 2.0. For matrix equations in the form of (11) and (12), the matrix equation represents a contraction mapping if and only if the spectral radius of the matrix operator ρ is less than one [10,11]. The spectral radius of a matrix is defined as the magnitude of the largest eigenvalue of the matrix. In general, eigenvalues are the most difficult of all matrix characteristics to compute, and for this reason an advanced matrix analysis package was utilized to perform the following study. The matrix analysis package is LAPACK, and was developed for Linear Operator analysis. This software package is in the public domain, and may be obtained via the Internet.

While the magnitudes of the eigenvalues associated with a given MoM expansion are typically functions of the number of elements used in the expansion, it may be shown that the

eigenfunctions of a given MoM expansion converge in a fashion similar to the convergence of the MoM solution. Figures 2a and 2b show the magnitude of the complex eigenvalues for a 0.5 λ radius PEC circular cylinder using 20, 30, and 40 basis functions.

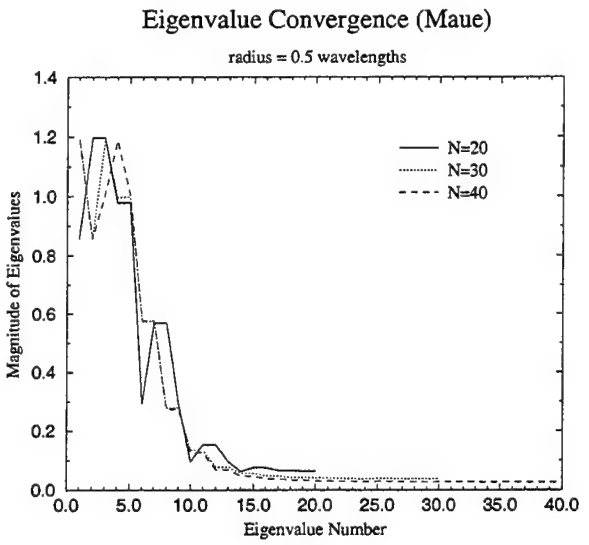

(a)

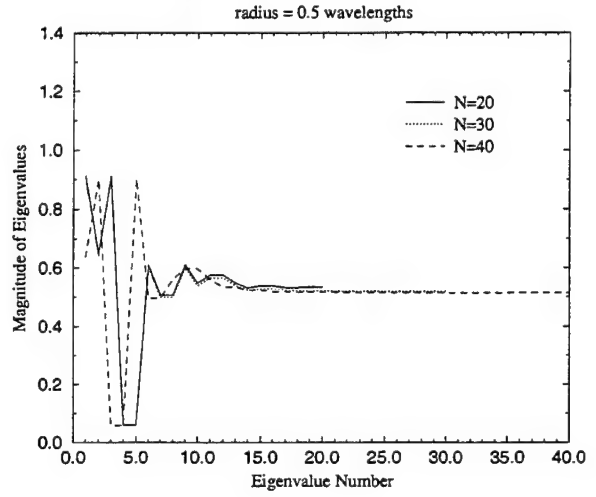

(b)

Figure 2 – Eigenvalue Convergence

For both Maue's formulation and the Total field formulation, convergence occurs at approximately 30 basis functions *(which is approximately 8 basis functions per wavelength)*. This is consistent with MoM expansions for a smooth surface [7]. It should be noted that no new eigenvalues occur above 30 basis functions, which equates to no new information being gained by increasing the number of basis functions being used. Also, note that the eigenvalues for the Total field equation tend toward 0.5 (*for large eigenvalue numbers*) and the eigenvalues for Maue's formulation tend toward 0.0 (*for large eigenvalue numbers*). These two limiting eigenvalues directly correspond to the diagonal values of their respective integral expansion (11) and (12).

Figures 3a-3d show plots of the complex eigenvalue versus the eigenvalue number for 2-dimensional circular cylinders with radii of 0.60985 λ and 0.38275 λ, respectively. These radii were chosen because they correspond to the TE01 and TM01 cutoff frequencies for circular waveguides [13]. Circular cylinders with these radii are historically difficult to solve numerically because of internal resonance problems. It should be noted that in both cases Maue's equation has eigenvalues with magnitudes greater than one, and the Total Field equation has eigenvalues with magnitudes less than or equal to one. This implies, for these particular cases, direct iteration of Maue's equation will not yield convergence and direct iteration of the Total Field equation may yield convergence (*the largest eigenvalue has to be strictly less than one to guarantee convergence*). In addition, for radii that correspond to the cutoff frequencies of the TE0n and TM0n circular waveguide modes, both the Total Field equation and Maue's equation will have eigenvalues of value one. It is these eigenvalues (*of value one*) which are responsible for the historically documented resonance problems. It also should be noted that Total Field equation has a zero eigenvalue for the 0.60985 λ case (*figure 3b*). This zero eigenvalue can cause a spurious mode to appear in the solution. While eigenvalues of value zero are not generally problems for direct iterative solutions, eigenvalues of values one or greater are problems, and lead to divergent solutions. It is this problem of eigenvalues of value one or greater that the previous surface current-iterative methods [1-6] are indirectly solving. Section 4 presents a general method for directly dealing with the problem of eigenvalues of value one or greater. Furthermore, it may be shown that the eigenvalues for Maue's equation and those for the Total Field equation are simply related.

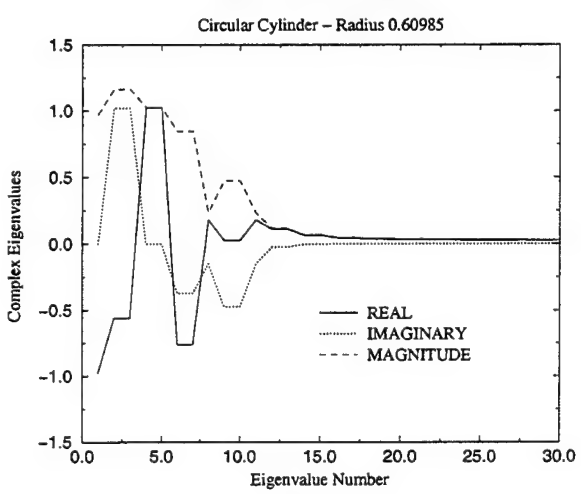

(a)

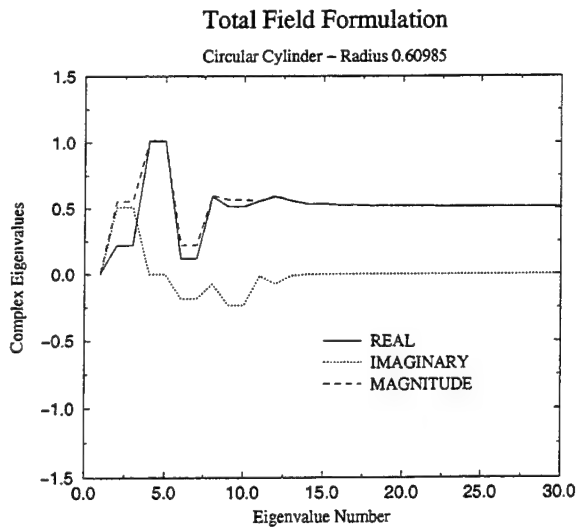

(b)

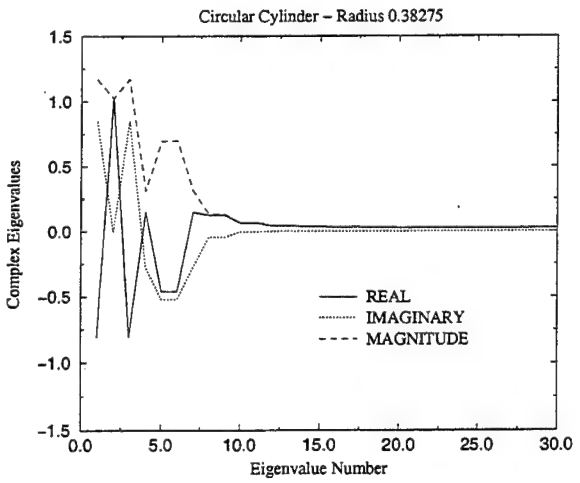

(c)

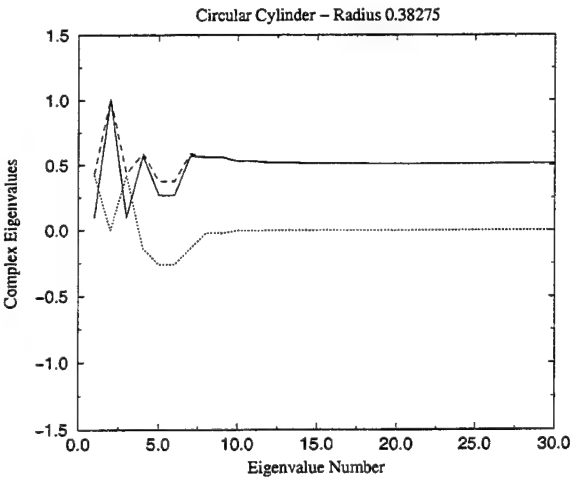

(d)

Figure 3 – Complex Eigenvalue Analysis

Write Maue's equation from (2) in operator form as

$$H_z^T = L^m(H) - 2H_z^I \tag{13}$$

and the Total Field equation from (4) as

$$H_z^T = L^T(H) - H_z^I, \tag{14}$$

where the operators L^T *and* L^m are related by

$$L^T = \frac{1}{2}I + \frac{1}{2}L^m \tag{15}$$

and [I] is the identity matrix.

Let λ^m, v^m be an eigenvalue and eigenvector pair for L^m, then v^m is an eigenvector for L^T corresponding to an eigenvalue $\lambda^T = \frac{1}{2}[1+\lambda^m]$. To see this, assume

$$L^m(v^m) = \lambda^m v^m. \tag{16}$$

It follows that

$$L^T(v^m) = \frac{1}{2}[I + L^m]v^m$$
$$= \frac{1}{2}[v^m + L^m(v^m)] = \frac{1}{2}[1+\lambda^m]v^m = \lambda^T v^m \tag{17}$$

By inspection of the curves in Figures 2 and 3, it may be seen that the above relationship is true for large eigenvalue numbers. By noting the complex nature of the eigenvalues in Figure 3 it may also be seen that the above relationship is true for the small eigenvalue numbers.

4. Methods of Insuring a Contraction Mapping

As can be seen from Figures 2 and 3, not all of the 2D TE PEC scattering problems contain a spectral radius that is less than one. In general, the spectral radius of the matrix associated with the Total Field formulation is less the spectral radius of the matrix associated with Maue's formulation. However, geometrical cases still exist where the spectral radius of the matrix associated with the Total Field formulation is greater than or equal to one (*figure 3b and 3d*). For these situations, the resulting system of linear equations can not be solved using a direct implementation of the fixed-point iterative method, and attempts to do so will result in a rapid divergence in the solution vector. For this case, where the spectral radius of the matrix associated with the particular magnetic field formulation is greater than one, a modified version of the fixed-point iterative method must be applied if a contraction mapping like-iterative solution is to be obtained.

In their work [1,14-16] Thiele *et al.* showed that it was possible to apply the method of fixed-point iteration to a 2D TE PEC scattering problem by subdividing the scattering body into two pieces which they defined as the illuminated side and the shadow side. While their work was restricted to a single subdivision of Maue's formulation, their method is shown here

to be completely general and may be applied to any of the magnetic field formulations for any number of arbitrary subdivisions provided the largest eigenvalue of each subdivision is less than unity.

We can express the hybrid iterative method (HIM) [1] as (18) where the sub-matrix $[L_{11}]$ is associated with the illuminated side, the sub-matrix $[L_{22}]$ is associated with the shadowed side, and the sub-matrices $[L_{12}]$ and $[L_{21}]$ are associated with the coupling between the illuminated and shadowed sides. The iterative method used in [1] to solve (18) is represent in (19).

$$\begin{bmatrix} H_z^T(\bar{r}_m) \end{bmatrix} = \begin{bmatrix} [L_{11}] & [L_{12}] \\ [L_{21}] & [L_{22}] \end{bmatrix} \begin{bmatrix} H_z^T(\bar{r}_m) \end{bmatrix} - \begin{bmatrix} 2H_z^I(\bar{r}_m) \end{bmatrix} \tag{18}$$

$$\begin{bmatrix} H_z^T(\bar{r}_m)^1 \end{bmatrix} = \begin{bmatrix} [L_{11}] & [0] \\ [0] & [I] \end{bmatrix} \begin{bmatrix} H_z^T(\bar{r}_m)^0 \end{bmatrix} - \begin{bmatrix} 2H_z^I(\bar{r}_m) \\ [0] \end{bmatrix},$$

$$\begin{bmatrix} H_z^T(\bar{r}_m)^2 \end{bmatrix} = \begin{bmatrix} [I] & [0] \\ [L_{21}] & [I] \end{bmatrix} \begin{bmatrix} H_z^T(\bar{r}_m)^1 \end{bmatrix} - \begin{bmatrix} [0] \\ 2H_z^I(\bar{r}_m) \end{bmatrix},$$

$$\begin{bmatrix} H_z^T(\bar{r}_m)^3 \end{bmatrix} = \begin{bmatrix} [I] & [0] \\ [0] & [L_{22}] \end{bmatrix} \begin{bmatrix} H_z^T(\bar{r}_m)^2 \end{bmatrix} - \begin{bmatrix} [0] \\ 2H_z^I(\bar{r}_m) \end{bmatrix},$$

$$\begin{bmatrix} H_z^T(\bar{r}_m)^4 \end{bmatrix} = \begin{bmatrix} [I] & [L_{12}] \\ [0] & [I] \end{bmatrix} \begin{bmatrix} H_z^T(\bar{r}_m)^3 \end{bmatrix} - \begin{bmatrix} 2H_z^I(\bar{r}_m) \\ [0] \end{bmatrix},$$

$$\begin{bmatrix} H_z^T(\bar{r}_m)^0 \end{bmatrix} = \begin{bmatrix} H_z^T(\bar{r}_m)^4 \end{bmatrix}. \tag{19}$$

This four step iterative method was found to always converge without internal resonance problems, although a formal proof was never given [1]. If we examine the eigenvalues of the resulting sub-matrices, it is apparent why the method converged and why it had no internal resonance problems. Figures 4a-d show the eigenvalues for the HIM matrices $[L_{11}]$, $[L_{12}]$, $[L_{21}]$ and $[L_{22}]$ of a circular cylinder with radius 0.5 wavelengths. The eigenvalues for each of the four matrices are all less than one; hence, each of the four sub-iterations is itself a contraction mapping. Since the four sub-iterations are nested in a linear fashion, then by the triangle inequality theorem the total iterative procedure is itself a contraction mapping. Thus, the system of linear equations may be iterated directly to a unique solution with a guarantee of mean squared-monotonic convergence [10-12]. It is extremely important to note that while the four sub-matrices in [1] were originally defined in terms of the system's excitation (*illuminated and shadowed sides*), the contraction mapping characteristics of the system are independent of the system's excitation. All that is important is that the matrix is partitioned such that the largest eigenvalue of each sub-matrix is less than one. If this case is true, then by the definition of a contraction mapping, the system of linear equations may be iterated directly to a unique solution with a guarantee of mean squared-monotonic convergence.

Maue's Formulation L11

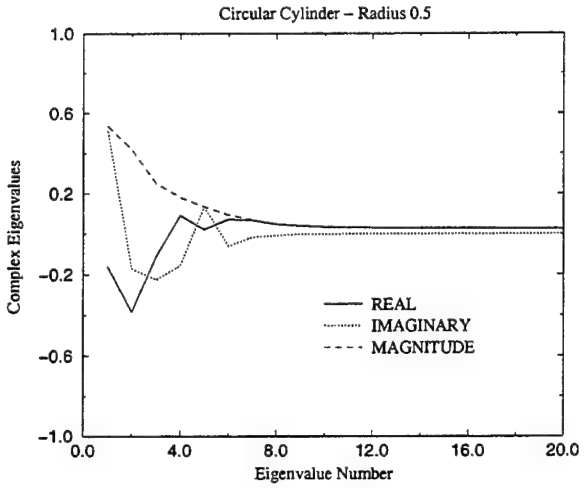

(a)

Maue's Formulation L12

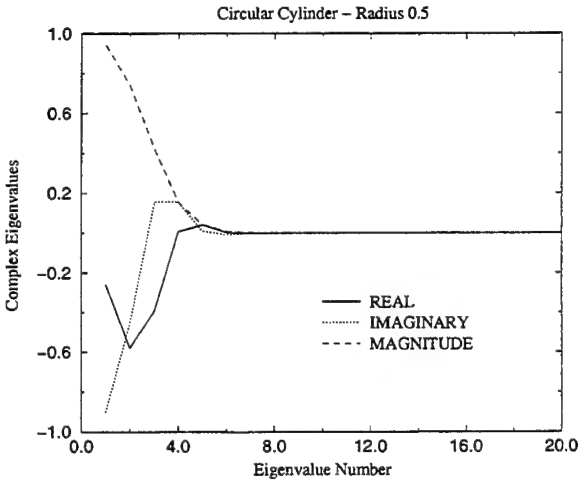

(b)

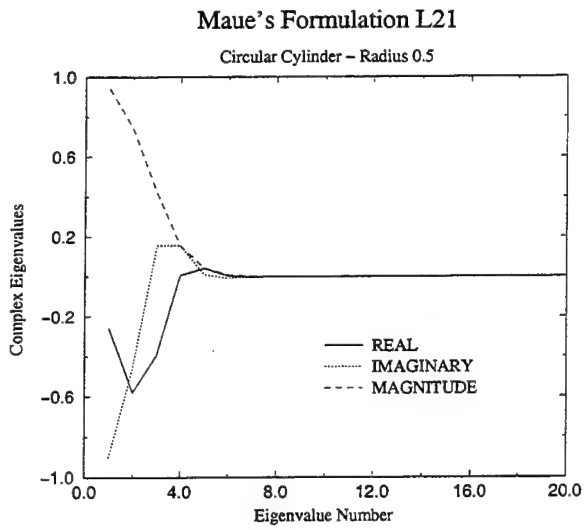

(c)

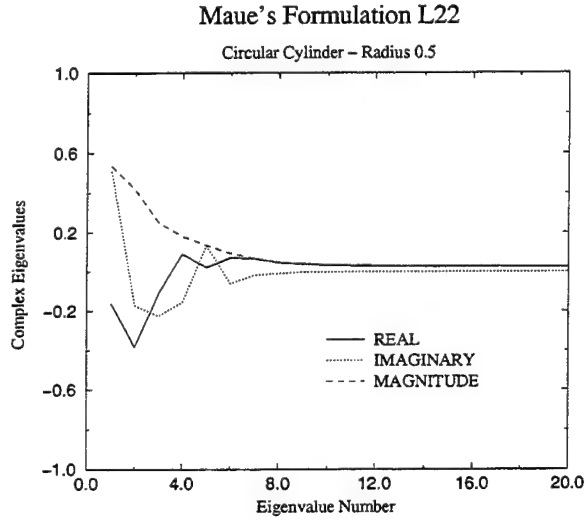

(d)

Figure 4 – Eigenvalue Analysis the Hybrid Iterative Method

While the guaranty of convergence is independent of excitation function and the initial guess used to start the iteration procedure, the rate of convergence is not. In fact the rate of convergence is heavily dependent upon the initial guess used to start the iteration procedure. To illustrate this point, the current distribution on a 0.5λ radius circular cylinder is solved for an incident plane wave using two different initial guesses. For this particular example, the Total Field formulation was utilized directly since all of its eigenvalues are less than one. The first initial guess used was the traditional PO approximation used in [1-6], and the second initial guess used was the negated reflection of the PO approximation. The PO approximation is considered to be a very good initial guess, while the negated reflection of the PO approximation is considered to be a very poor initial guess. In both cases, the exact solution was obtained directly using MoM. Figures 5a and 5b show the converging currents for each case.

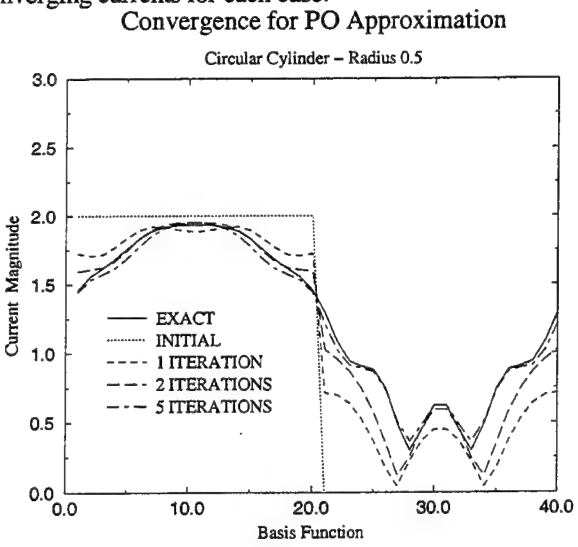

(a)

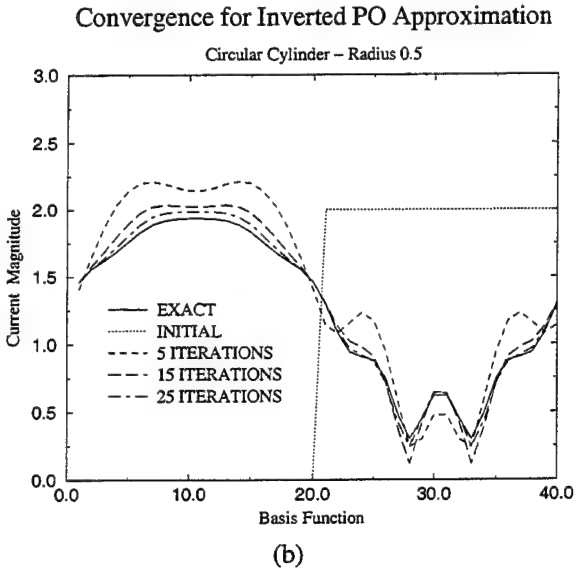

(b)

Figure 5 – Effects of Initial Guess on Convergence Rate

Figure 5a shows these currents for an initial guess that is the usual physical optics estimate of the current; twice the incident field on the illuminated side and zero on the shadow side. Note the vast improvement in the solution after one iteration, and the nearly converged result after five iterations. Figure 5b shows the currents for an initial guess of zero on the illuminated side and minus twice the incident field on the shadowed side; the "opposite" of the physical optics estimate. Note while the contraction mapping nature of the iteration procedure overcomes the poor initial guess, the rate of convergence is significantly slower, approximately five times slower than for the previous guess.

5. Summary and Conclusions

Maue's formulation and the Total Field formulation of the MFIE have been analyzed as to their suitability for iterative solutions. It was shown that both formulations could be directly iterated to a unique solution with a guarantee of mean squared-monotonic convergence provided the eigenvalues of their corresponding matrix expansions were less than one. This convergence is independent of the initial guess used to initiate the iterative process. The guarantee of monotonic mean square convergence is a direct result of the contraction mapping properties of Maue's formulation and Total Field formulation. The conditions under which these formulations have contraction mapping properties were developed in Section 2 for the integral forms and in Section 3 for the discrete forms.

Section 3 showed how the eigenvalues of the matrix representation could be used to determine the convergence characteristics of a matrix used in the iterative solution process. For the cases presented, the eigenvalue plots showed a preference for the Total Field formulation over Maue's formulation since the latter tended to have larger eigenvalues than the former. Eigenvalues of value greater than unity indicate that the solution will not have contraction mapping properties. Eigenvalues of value equal to one correspond to internally resonant cases. Eigenvalues of value equal to zero can allow the existence of spurious modes. In Section 4, it was noted that the previously published Hybrid Iterative Method [1] converged because the division of the geometry into two parts produced (for the cases examined) sub-matrices whose eigenvalues were less than unity, thereby creating a series of contraction mappings. The authors believe that the convergence obtained in the other direct surface current-iterative methods [2-6] discussed occurred because of a similar phenomenon.

Lastly, the material in this paper shows how to use either formulation of the MFIE successfully to obtain an iterative solution. Also, iterative solutions to the MFIE have the potential to substantially reduce the required computational time for large PEC bodies provided that the iterative process is initiated with a "good" initial guess, such as the PO approximation. Finally, additional computational speed can be obtained for extremely large PEC bodies by the direct parallelization of the iterative methods discussed in Sections 3 and 4.

ACKNOWLEDGEMENT

The authors would like to thank Richard Mead and James Reuster for their help in preparing the manuscript.

REFERENCES

[1] Kaye, M., Murthy, P.K., and Thiele, G.A., "An Iterative Method for Solving Scattering Problems," IEEE Trans. Ant. Prop., AP-33, No. 11, Nov. 1985.

[2] Reuster, D.D., and Thiele, G.A., "A Field Iterative Techniques for Computing the Scattered Electric Fields at the Apertures of Large Perfectly Conducting Cavities," IEEE Trans. Ant. Prop., AP-43, No. 3, March 1995.

[3] Obelleiro-Basteiro, F., Rodriguez, J.L., and Burkholder, R.J., "An Iterative Physical Optics Approach for Analyzing the Electromagnetic Scattering by Large Open-Ended Cavities," IEEE Trans. Ant. Prop., AP-43, No. 4, April 1995.

[4] Collins, P.J., and Skinner, J.P., "An Iterative Solution for the TM Scattering from Perturbed Circular Dielectric Cylinders," IEEE Trans. Ant. Prop., AP-44, No. 6, June 1996.

[5] Reuster, D.D., Thiele, G.A., and Eloe, W.P., "A Hybrid Magnetic Field Iterative Technique," Applied Computational Electromagnetics Society Journal (ACES), Vol. 11, No. 3, July 1996.

[6] Hodges, R.E., and Rahmat-Samii, Y., "An Iterative Current-Based Hybrid Method for Complex Structures," IEEE Trans. Ant. Prop., AP-45, No. 2, Feb.1997.

[7] Harrington, R.F., Field Computation by Moment Methods, Macmillan, New York, 1991.

[8] Wang, J.H., Generalized Moment Methods in Electromagnetics, Wiley, New York, 1991.

[9] Stutzman, W.L. and Thiele, G.A., Antenna Theory and Design, Wiley, New York, 1981. pp. 454-458.

[10] Burden, R.L., and Faires, J.D., Numerical Analysis, PWS-KENT, Boston, 1989. pp. 528-536.

[11] Varga, R.S., Matrix Iterative Analysis, Prentice-Hall, New Jersey, 1962.

[12] Brauer, F., and Nohel, J.A., The Qualitative Theory of Ordinary Differential Equation An Introduction, Dover, New York, 1989. Chapter 3.

[13] Balanis, C.A., Advanced Engineering Electromagnetics, Wiley, New York, 1989. pp. 707-716.

[14] Murthy, P.K., Hill, K.C., and Thiele, G.A., "A Hybrid-Iterative Method for Scattering Problems," IEEE Trans. on Antennas & Propagation, Vol. AP-34, Oct. 1986.

[15] Penno, R.P., Thiele, G.A., and Murthy, P.K., "Scattering from a perfectly Conducting Cube Using HIM," Special Issue of IEEE Proceedings on Radar Cross-Section, Vol. 77, May 1989.

[16] Thiele, G.A., "Hybrid Methods in Antenna Analysis," Special Issue of IEEE Proceedings, Vol. 80, NO. 1, Jan. 1992. Invited.

Modeling of Low-Gain Antennas on Aircraft Using APATCH

James Calusdian
412 TW/EWEE
Edwards AFB, CA

David Jenn
Naval Postgraduate School
Monterey, CA

ABSTRACT

Radiation patterns for low-gain antennas such as those used for telemetry and collision avoidance systems were computed using the APATCH program. APATCH uses shooting and bouncing rays (SBR) to compute the radiation pattern for the antenna installed on a scattering geometry. A built-in antenna model was used to represent a telemetry antenna and its accuracy verified by comparison with measurements and results from a method of moments patch code. Antenna patterns were computed for various locations on a Cessna 172 and an F-18 Hornet.

I. INTRODUCTION

When an antenna is installed on an aircraft, its radiation pattern will change due to the interaction between the radiating element and the aircraft surface. Scattering mechanisms, such as single and multiple reflections, surface waves, and edge diffraction, are responsible for altering the overall radiation pattern of the installed antenna [1]. The installation of new systems or physically reconfiguring an aircraft can affect the pattern performance of antennas already on the aircraft. This occurs frequently in flight testing, when instrumentation systems are temporarily installed on an aircraft. A performance analysis must be conducted to assure that the antennas provide adequate coverage for the anticipated aircraft maneuvers. Lost data may cause a test to be rescheduled, leading to cost overruns and schedule delays.

This paper demonstrates that a simple current source is an accurate model for low-gain wire antennas of the type commonly used for telemetry. The ensuing analysis presents the performance of two examples of low-gain antennas. The first is a telemetry antenna, which is used with an airborne instrumentation system, and the second is an antenna being considered for a traffic alert/collision avoidance system.

APATCH, a computer program developed by DEMACO Inc. [2], uses shooting and bouncing rays (SBR) to compute the radiation pattern of an antenna installed on an aircraft or any other electrically-large electromagnetic scatterer [3]. APATCH uses the same SBR model as the radar cross section prediction code XPATCH, which has been validated and used extensively [4,5,6]. Rays are shot from the antenna with a weighting determined by its pattern. APATCH has the capability to model several simple radiating elements, arrays of elements, or pattern data can be provided in tabular format. The Advanced Computer Aided Design (ACAD) program was used to generate a triangular facet model of the aircraft [7].

II. VALIDATION OF THE ANTENNA MODEL

To evaluate the low-gain antenna modeled in APATCH, a test case was run for a telemetry antenna located on a cylinder. The antenna's construction is a quarter-wavelength wire that is excited from one end. The wire is inclined at a 45° angle with respect to the horizontal, and the assembly is encased in an aerodynamically shaped radome as shown in Figure 1.

Measured data for the antenna mounted on an 8-inch (20.3 cm) diameter by 30-inch (76.2 cm) length cylinder was available from Haigh-Farr. This data was used to evaluate several approaches to modeling the antenna in APATCH. The faceted cylinder model referenced in the APATCH input file is also shown in Figure 1. The telemetry antenna is situated halfway along the length of the cylinder as indicated in the figure.

The telemetry antenna was modeled as a current source, which is one of the built-in antenna classes available in the APATCH program. It is a point source that launches rays with a dipole weighting [2]. Since this antenna class makes no provision for the control of the length and radius of the radiating element, the height of the current source (h) was varied until a good match was achieved between the computed results and the measured data. This provides a limited means by which the effects of element length, radius, and radome properties can be included.

Figure 2 compares measured data with the APATCH results for two heights. The agreement between measured and computed data is generally better in both the upper and lower hemispheres for a height of h=17 mm as compared to a height of h=2 mm.

The x-y plane pattern computed by APATCH closely resembles the measured data as shown in Figure 2b. The two curves have been shifted from the normalized value for clarity. The symmetric behavior of the scattered field about the scatterer is exhibited in these plots.

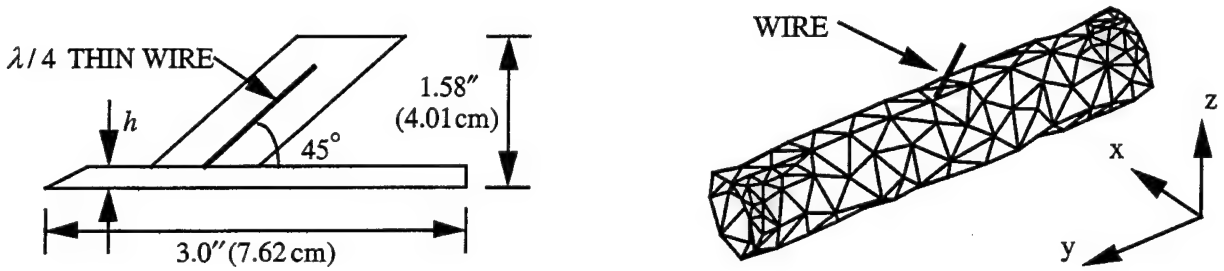

Figure 1: Telemetry antenna and ACAD model of cylinder used in the preliminary study.

The field due to edge diffraction can be computed by APATCH if an edge file is provided. The edge file is a sequential list containing edge length, orientation, and wedge angle for all edges in the ACAD model. This APATCH utility was implemented, but it did not significantly improve the agreement between the computed and measured results. This may have been due to the relatively coarse mesh of the cylinder.

The method of moments code PATCH [8] was also used to verify the antenna and cylinder model. PATCH uses the triangular surface subdomains with overlapping rooftop basis functions [9]. Unlike APATCH, where the antenna pattern is decoupled from the scatterer, PATCH includes interactions between the cylinder and antenna. Figure 3 shows a detail of the region where the antenna is attached to the cylinder in the ACAD model. One of the edges of the facets comprising the antenna is excited with a voltage source, and PATCH computes the resulting surface currents and scattered field.

Figure 3 also shows the elevation plane pattern. PATCH computed the gain to be 4.1 dB (compared with 4.9 dB from APATCH). Because PATCH is a method-of-moments code, from a practical perspective, it cannot be used to compute the radiation patterns of antennas on electrically large aircraft. Computation times for problems involving large scattering geometries can be quite high. Furthermore, the demand for computer memory rises very quickly as the electrical size of the scattering geometry increases. The close agreement between PATCH, APATCH, and the measured data indicates that the APATCH current source antenna model is a good representation of the actual stub.

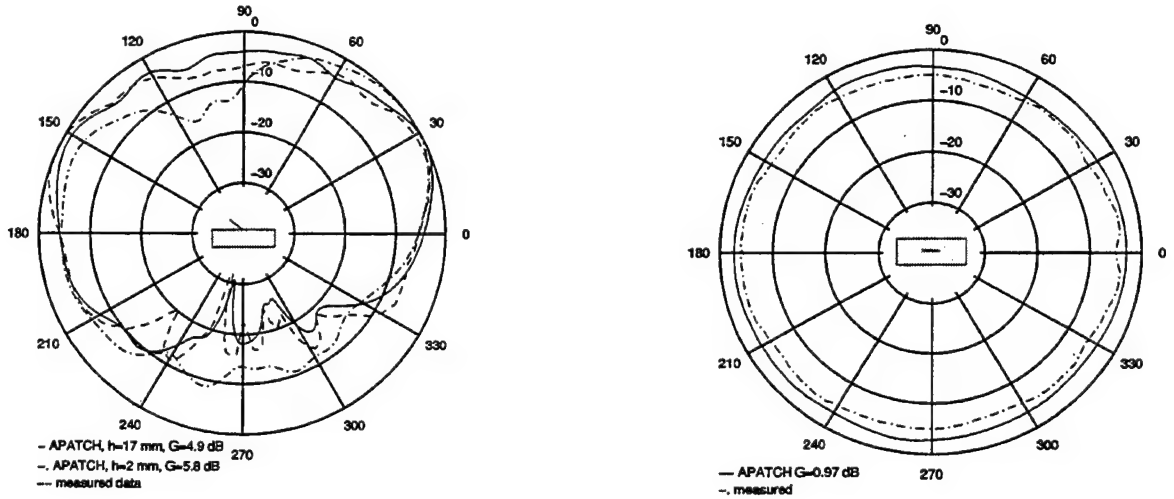

(a) (b)

Figure 2: APATCH results compared with measured data for the cylinder and telemetry antenna. E_θ polarization shown. (a) y-z plane (b) x-y plane

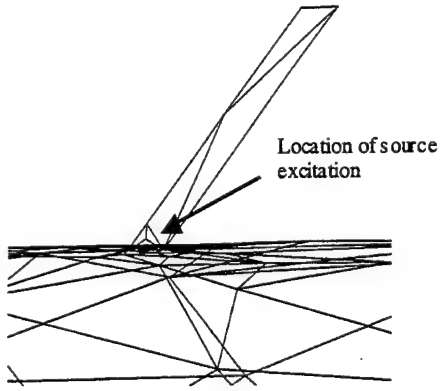

(a)

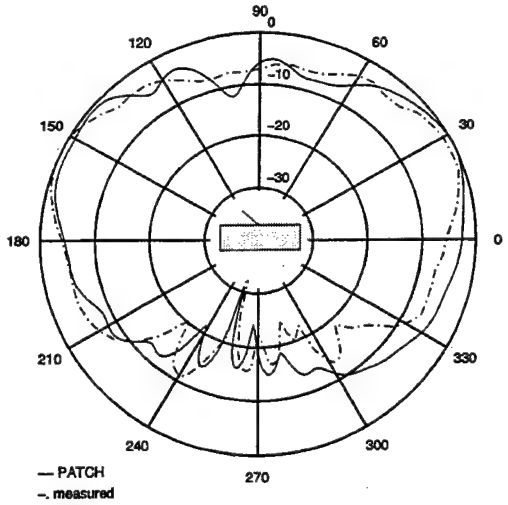

(b)

Figure 3: PATCH model and results for cylinder with telemetry antenna. (a) detail of ACAD model used in PATCH computation. (b) elevation plane pattern

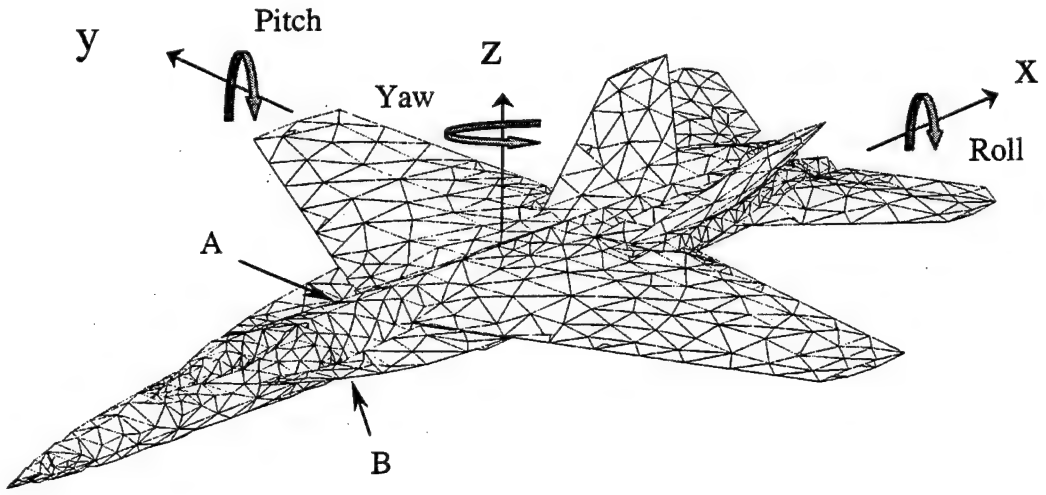

Figure 4: ACAD model of F-18 Hornet (2620 facets). Locations where the telemetry antenna was considered are designated as A and B.

III. F-18 HORNET WITH TELEMETRY ANTENNA

The antenna model discussed in Section II was simulated installed on the F-18 aircraft shown in Figure 4. With a highly dynamic aircraft such as the F-18, it is likely that two antennas would be used in a telemetry link: one on the bottom and one on top. This approach ensures that there is adequate reception at the test mission control facility as the aircraft executes the maneuvers required for a particular test. The two antennas are connected to the transmitter by a microwave coupler. Usually a 3 dB coupler is used which equally divides the signal power into the two antennas. However, there are situations where the majority of the time the lower antenna is visible to the control facility. In these cases it may be more efficient to use a 10 dB coupler so that 10% of the input power is

directed to the upper antenna and 90% to the lower antenna. The upper antenna is supplied so that the telemetry link is maintained during the brief time that a maneuver is executed, albeit the power from this antenna is significantly reduced.

APATCH results are shown in Figure 5 for the 10 dB coupler. The E_θ and E_ϕ polarizations are shown for the roll, pitch, and yaw planes. The reference gain values (i.e., the 0 dB levels) are listed for each plot. (Note that insignificant cross-polarized values were not plotted. For example, there is no significant E_ϕ in the pitch plane.) It can be seen that there is good coverage in the lower region. The region above the aircraft exhibits lower radiation levels than the region below the aircraft; this is expected when the 10 dB coupler is used. Finally, the yaw plane pattern is shown in Figure 5c. It displays the interference between the upper and lower antennas characterized by its oscillatory shape.

When a 3 dB coupler is used with the instrumentation system, the effective radiation patterns from the upper and lower telemetry antennas are shown in Figure 6. The roll and pitch plane patterns indicate that there is adequate radiation into the regions above and below the aircraft. This is the type of coverage desired when the aircraft is performing test missions requiring frequent maneuvers and unusual attitudes like those encountered in tests of performance and flying qualities.

The yaw plane pattern shown in Figure 6c displays large variations in the E_θ and E_ϕ polarizations in the horizontal plane. The peaks and nulls of the two polarizations occur in an alternating fashion due to the interferometer effect of two widely separated elements. This effect is more pronounced for the 3 dB coupler than for the 10 dB coupler because the equal power weighting provides nearly complete cancellation.

IV. CESSNA 172 WITH TCAS ANTENNA

An antenna suitable for use with the Traffic Alert and Collision Avoidance System (TCAS) was simulated on the Cessna 172 (C-172) aircraft. The US Federal Aviation Administration (FAA) mandates the use of TCAS on all passenger and cargo aircraft with 10 seats or more. TCAS aids pilots in detecting the presence of nearby aircraft. The system operates by interrogating the transponder of an approaching aircraft. Range is determined from the time required to receive the reply, and altitude is extracted from the information encoded within the reply [10]. Mode C is the term used to describe a transponder that reports its altitude when interrogated. In a complete TCAS system, a pair of directional antennas is used to establish the bearing of the approaching aircraft. This version is not explored here. Instead, only an omni-directional antenna is considered, which only yields the range and altitude of an intruding aircraft. It is proposed that bearing be determined from a position reporting feature of a transponder similar to Mode C operation. TCAS operates on two frequencies. It interrogates (transmits) on 1030 MHz and receives transponder replies on 1090 MHz.

The aircraft model used in the following analysis is shown in Figure 7. Indicated in the figure is the location considered for antenna placement. A vertically polarized quarter-wavelength monopole antenna was used, which in free space produces an omni-directional radiation pattern. Figure 8 shows the radiation pattern for the quarter-wave element installed on the aircraft. The roll pattern, Figure 8a, shows good coverage in the region above the aircraft, except for directly above, where there exists a sharp null in the pattern which is typical of vertically polarized antennas. There is less coverage in the region from the horizon to approximately 30° below the horizon. This is the effect of the wings on the pattern since the antenna is masked by the large wing surfaces.

Referring to the pitch plane pattern, Figure 8b, the gain in the aft region is higher than that in the front. The yaw plane pattern shows uniform radiation in the horizontal plane surrounding the aircraft. Antenna gain in the forward direction is comparable to that found in the aft region. With the antenna mounted at this location, the interaction with the wings gives an increased gain that improves the detection range in the region above the wings where the pilot experiences obstructed visibility.

By incorporating an array antenna, the gain in the aft region can be reduced in exchange for greater coverage in the forward region; this would improve TCAS performance and aircraft safety even more. A simple array can be manufactured consisting of two vertical elements, each a quarter-wavelength long and separated by one-quarter wavelength. The aft element is fed 90° out of phase with respect to the forward element to obtain a cardioid shape. Figure 9 shows the performance of the array antenna installed on this aircraft.

The roll plane pattern (Figure 9a) shows that the coverage in the space above the aircraft is similar to the single antenna at the same location, but the gain has increased slightly from 8.14 dB to 8.56 dB for 1030 MHz.

When the plots of the pitch and yaw planes are examined, the benefit of the array becomes apparent

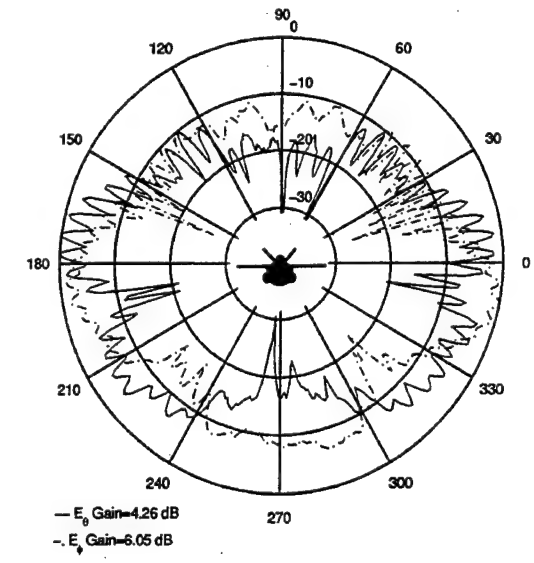

(a)

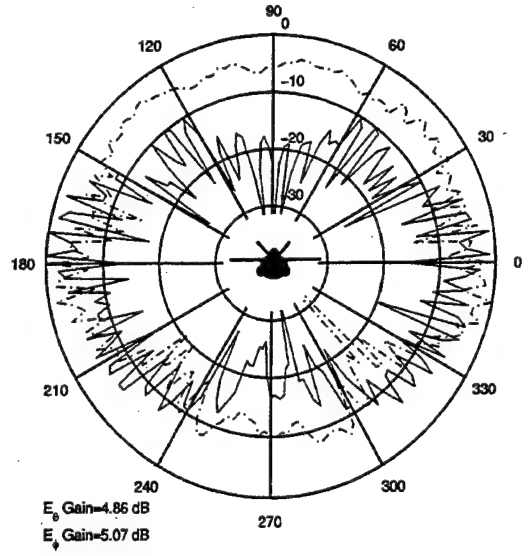

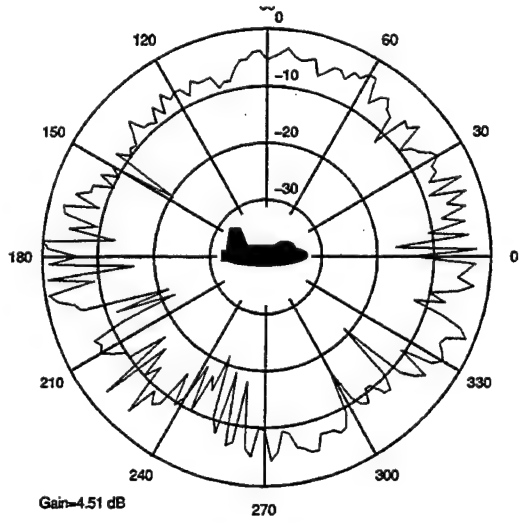

(b)

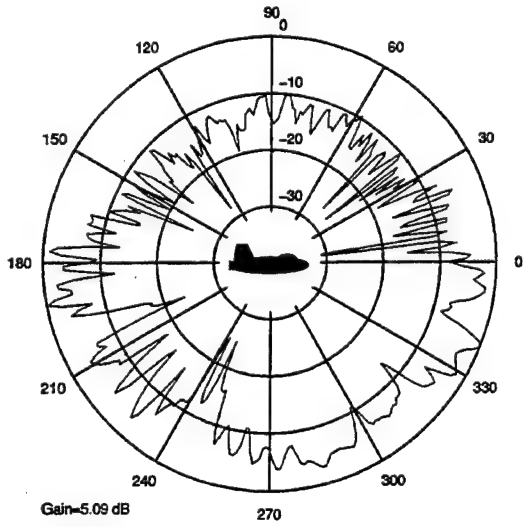

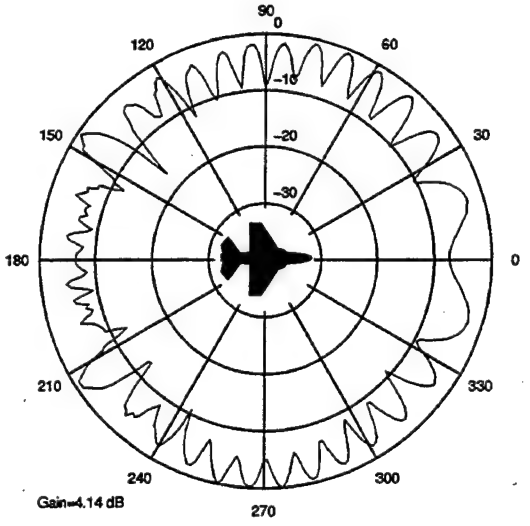

(c)

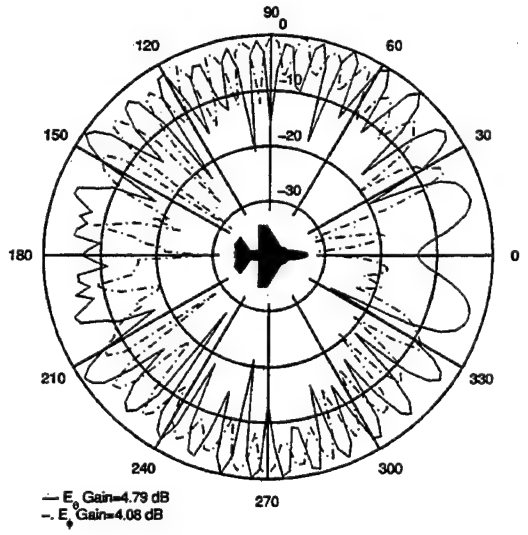

Figure 5: F-18 with two telemetry antennas and a 10 dB microwave coupler. (a) roll, (b) pitch, and (c) yaw

Figure 6: F-18 with two telemetry antennas and a 3 dB microwave coupler. (a) roll, (b) pitch, and (c) yaw

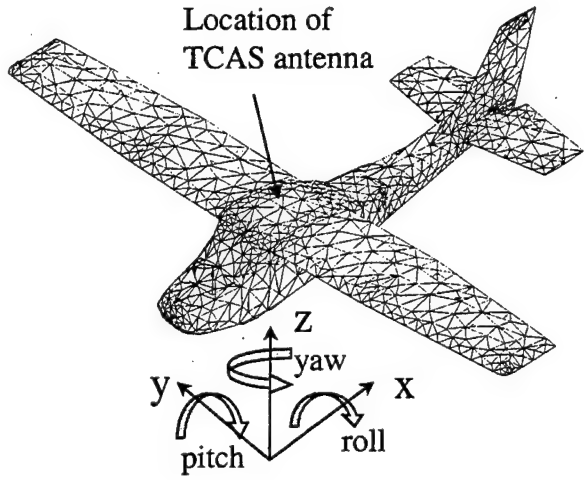

Figure 7: ACAD model of the C-172 aircraft (2790 facets).

(see Figures 9b and 9c). An increase in gain of approximately 3 dB in the forward direction is evident. Gain in this direction exceeds the gain in the aft region. Additionally, when compared with the single element antenna, a net gain of 0.8 dB is achieved in the horizontal plane.

IV. SUMMARY AND CONCLUSIONS

APATCH is a code used to compute the radiation patterns of antennas installed on complex objects. It is based on the SBR technique, which is applicable to electrically large structures. The built-in current element was used to model an antenna on a cylindrical test fixture and the C-172 and F-18 aircraft. Comparison of the APATCH results with measured data and the results from a method of moments patch code shows that the built-in current source is an accurate model for low-gain wire antennas of the type commonly used for telemetry. The run times for the F-18 and C-172 were approximately 17 and 5 minutes, respectively, on a SGI Indigo2. CPU times can vary widely depending on the number of facets, ray density, and number of bounces.

On a maneuvering F-18, good telemetry link performance can be expected from a pair of antennas mounted on the top and bottom of the aircraft. When a 3 dB coupler is used to split the telemetry signal, an interferometer pattern results in the yaw plane. This behavior can lead to telemetry drop-outs when a linearly polarized antenna is used in the receiving ground station.

This paper also presented a performance analysis of an antenna considered for a type of TCAS system on the C-172 aircraft. Acceptable performance can be achieved when either a single quarter-wave element or a two-element array is used.

ACKNOWLEDGEMENT

The authors wish to thank Haigh-Farr for the measurement data used in this paper and Mr. David Lednicer of Analytical Methods, Inc. for providing the CAD model of the Cessna 172 aircraft.

REFERENCES

[1] J. Calusdian, "Radiation Patterns of Antennas Installed on Aircraft," Naval Postgraduate School, Masters Thesis, December 1998.

[2] *APATCH Ver 2.1 Users Manual*, DEMACO Inc., 100 Trade Center Drive, Champaign, IL, 61820.

[3] H. Ling, R. Chou, and S. W. Lee, "Shooting and Bouncing Rays: Calculating the RCS of an Arbitrarily Shaped Cavity," *IEEE Trans. on Antennas and Propagation*, AP-37, No. 2, February 1989.

[4] J. Baldauf, S. W. Lee, L. Lin, S. K. Jeng, S. M. Scarborough, and C. L. Yu, "High Frequency Scattering From Trihedral Corner Reflectors and Other Benchmark Targets: SBR versus Experiment," *IEEE Trans. on Antennas and Propagation*, AP-39, No. 9, September 1991.

[5] D. Andersh, M. Hazlett, S. W. Lee, D. D. Reeves, D. P. Sullivan, and Y. Chu, "XPATCH: A High-Frequency Electromagnetic-Scattering Prediction Code and Environment for Complex Three Dimensional Objects, *IEEE Antennas and Propagation Magazine*, Vol. 36, No. 1, February 1994.

[6] T. Ozdemir, M. W. Nurnberger, J. L. Volakis, R. Kipp, J. Berrie, "A Hybridization of Finite-Element and High-Frequency Methods for Pattern Predictions for Antennas on Aircraft Structures," *IEEE Antennas and Propagation Magazine*, Vol. 38, No. 3, June 1996.

[7] *ACAD Users Manual*, Lockheed-Martin, Fort Worth, TX, 76108.

[8] W.A. Johnson, D. Wilton, and R. Sharpe, *PATCH Code User's Manual*, Sandia Report, SAND87-2991, May 1988.

[9] S. M. Rao, D. R. Wilton, and A. W. Glisson, "Electromagnetic Scattering by Surfaces of Arbitrary Shape," *IEEE Trans. on Antennas and Propagation*, AP-30, No. 3, May 1982.

[10] "TCAS–The Complete Heads Up," Product Support News, Winter 1998, [http://www.raytheon.com /rac/ uppnews /jet/tcas.htm].

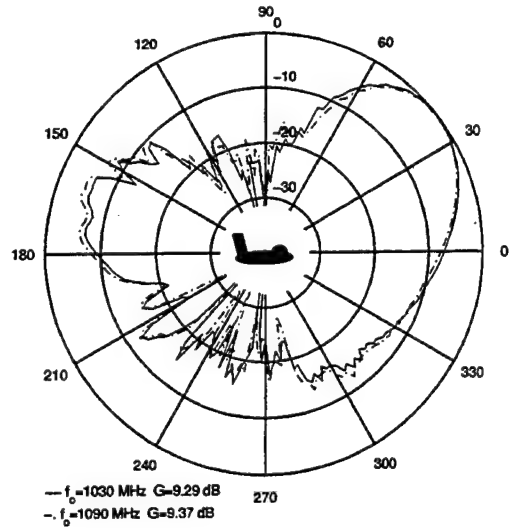

(a)

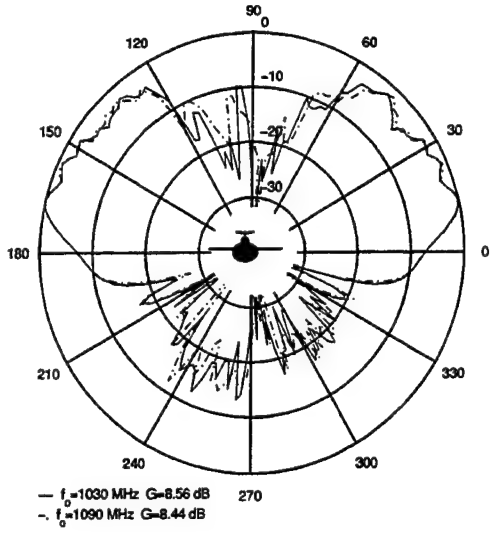

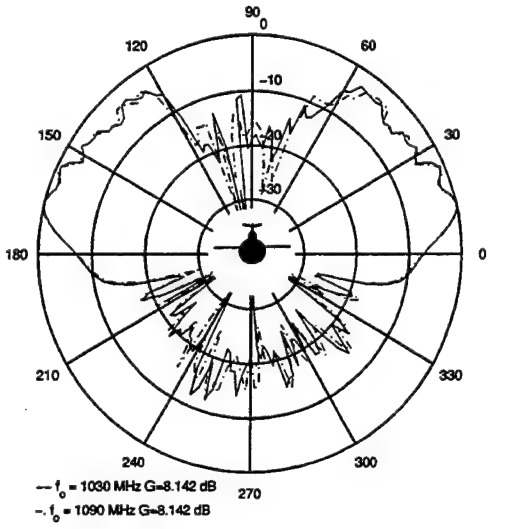

(b)

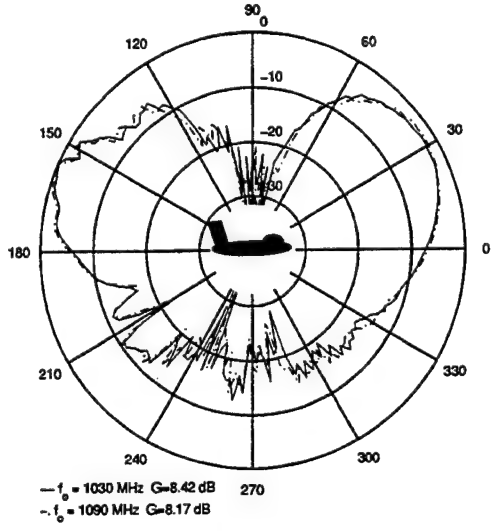

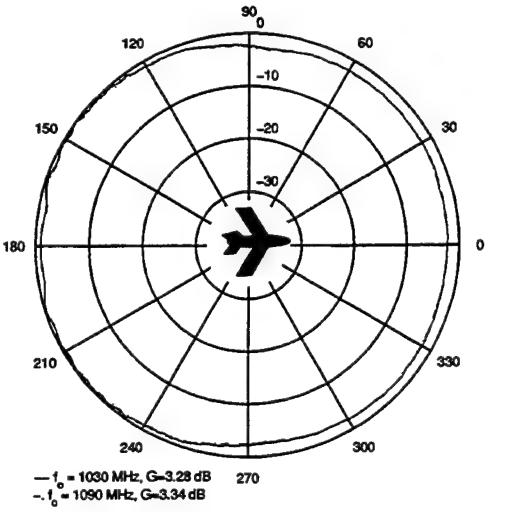

(c)

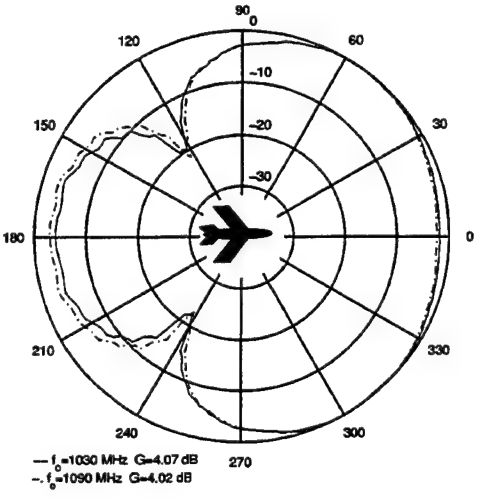

Figure 8: C-172 aircraft with TCAS antenna (a) roll, (b) pitch, and (c) yaw

Figure 9: C-172 aircraft with array antenna (a) roll, (b) pitch, and (c) yaw

A Novel Spatial Images Technique for the Analysis of Cavity Backed Antennas

A. Alvarez Melcón and Juan R. Mosig
Laboratoire d'Electromagnétisme et d'Acoustique (LEMA). EPFL, Lausanne, Switzerland

***Abstract*—This paper describes a new contribution to the analysis of arbitrary shielded circuits and antennas of complex shapes, in the frame of the integral equation (IE) and Method of Moments formulation (MoM). The technique is based on the spatial image approach and a new specially truncated set of images is developed to enhance the convergence behavior of the series involved. Results show that, with the new specially truncated series of images, convergence is achieved very fast. In this paper simulated results obtained with the new approach are compared with measurements.**

***Index terms*—Microwave circuits and antennas, shielding, Green function, spatial images, integral equation, method of moments.**

I. Introduction

The analysis of shielded microwave circuits and antennas is a subject that has always attracted much attention and several numerical models have been developed in the past. Among them, finite element techniques have been successfully used [1] but they usually lead to computer codes which are computationally heavy. Perhaps the most popular and efficient technique is the integral equation (IE) formulation combined with the Method of Moments (MoM) algorithm [2]. The main practical difficulty in this approach, however, is in the numerical evaluation of the associated Green's functions usually formulated as very slowly convergent modal series. For the efficient summation of these series the Fast Fourier Transform (FFT) has been successfully used in the past [2],[3], but it restricts the subsequent discretization of the circuits to uniform meshes. Other acceleration techniques, without the use of the FFT, have been recently reported, namely the use of the residue theorem [4] and the use of the Sommerfeld identity [5]. An alternative technique to the modal series approach is to formulate the Green's functions in the spatial domain using the image theory. In this context we can mention the work in [6] who used the Ewalt transformation to sum the spatial images series, but no dielectric layers are considered, and the work in [7] who formulated the spatial images series only to the quasi-static part of the kernel.

In the frame of IE-MoM, we provide in this paper a new contribution to the analysis of arbitrary shielded circuits and antennas of complex shapes. The technique is based on the spatial images approach and it formulates the complete Green's functions associated to a general multilayered medium as standard Sommerfeld integrals. Once Sommerfeld type Green's functions are computed, the effect of lateral walls is locally included by adding spatial images. Care is exercised to ascertain the convergence behavior of the resulting spatial images series. For those cases exhibiting slow convergence behavior, a specially truncated series of images is developed based on the imposition of the boundary conditions for the fields and potentials at specific points on the metallic walls. Results reveal that convergence with the specially truncated set of images is very fast and accurate results are obtained with only 10 spatial images. An interesting feature of the technique developed is that triangular-cell based MoM formulations can be easily used, thus allowing the analysis of arbitrary complex structures. In addition, with the proposed approach all the know-how in the field of Sommerfeld integrals evaluation can be directly put to work for the analysis of shielded structures.

II. Image theory

The key step in the analysis of planar multilayered printed circuits following the space IE approach, is the derivation of the spatial domain Green's functions formulated, in the case of a medium of infinite lateral transverse dimensions, as Sommerfeld integrals [8]. With ref-

A. Alvarez Melcón, 41-21-693-4637, fax 41-21-693-2673, Alejandro.Alvarez-Melcon@epfl.ch. Juan R. Mosig, 41-21-693-4628, fax 41-21-693-2673, Juan.Mosig@epfl.ch. web site: http://lemawww.epfl.ch.

This work was supported by ESA/ESTEC under Contract No. 11698/95/NL/SB, and it was developed in collaboration with the companies ALCATEL ESPACE, France and CASA, Spain.

erence to the shielded structure in Fig. 1, the corresponding Green's functions accounting for the presence of the lateral walls can be written using standard spatial image theory. The Green's functions are therefore again formu-

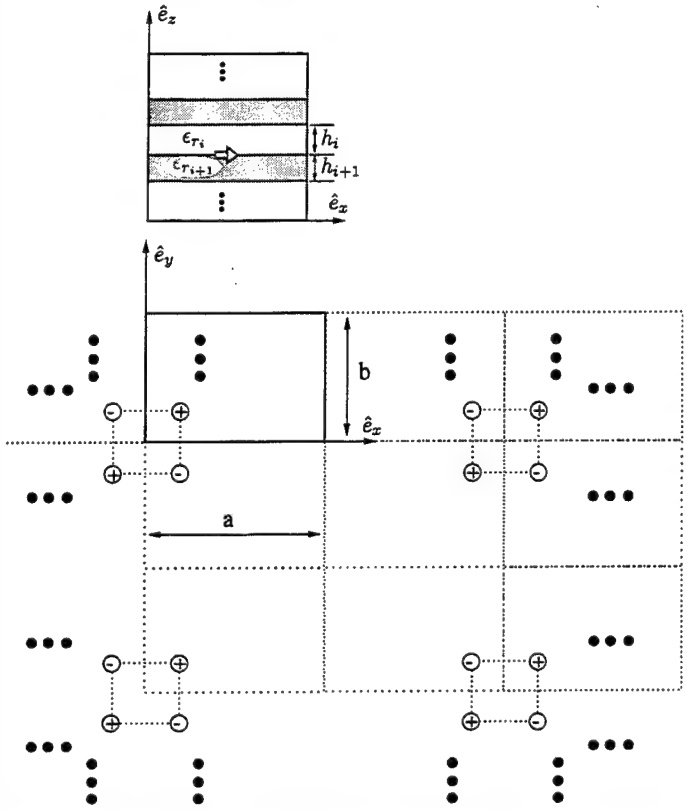

Fig. 1. Basic shielded multilayered structure analyzed in this paper and the associated spatial images for a unit point charge.

lated as Sommerfeld integrals, but they are computed for an extended range of source-observer distances to account for the interaction of all required spatial images. For this purpose asymptotic techniques specially efficient for large source-observer distances are best utilized as described in [9]. The boxed mixed potential Green's functions G_{Box} are then written as [8]

$$\begin{aligned} G_{\text{Box}}(x,y|x',y') = \\ \sum_{m=-\infty}^{\infty}\sum_{n=-\infty}^{\infty}\Big[& G(x,y|+x'+2ma,+y'+2nb) \\ & +s_x\, G(x,y|-x'+2ma,+y'+2nb) \\ & +s_y\, G(x,y|+x'+2ma,-y'+2nb) \\ & +s_x\, s_y\, G(x,y|-x'+2ma,-y'+2nb)\Big], \end{aligned} \tag{1}$$

where G is the corresponding Sommerfeld type Green's function and s_x, s_y are sign functions taking the values shown in Table I for the different types of mixed potential Green's functions components. As shown in (1) the total Green's functions are now expressed in terms of infinite series and the convergence behavior becomes therefore an issue. For instance, we have found convergence problems in the analysis of the microstrip line shown in Fig. 2, printed on a thick dielectric substrate ($\epsilon_r = 3.0$, $h/\lambda = 0.2$).

To illustrate this point, we present in Fig. 3(a) and 3(b) the computed S-parameters when, respectively, 22 and 102 spatial images are included in the analysis. As it can be observed, the ripple in the computed response indicates that convergence rapidly deteriorates with frequency. Moreover, the use of more images does not solve the problem and, as shown in Fig. 3(b), only the ripple is more compressed. This slowly convergence behavior can be explained as being due to the excitation of surface waves in the structure. To easily understand this fact we have computed the associated Green's functions using the imaginary axis decomposition reported in [9]. Following this technique, the total Green's functions are expressed as the sum of three main contributions, namely the quasi-static part, the spatial wave part and the contribution due to the surface waves excitation. Fig. 4 shows the computed electric scalar potential Green's function for two different frequencies. The first one (2 GHz) corresponds to a frequency where convergence is still good while the second one (10 GHz) corresponds to a frequency well inside the ripple region. We can clearly observe that at 2 GHz the surface wave is very weakly excited and it starts to dominate the global Green's function behavior for spatial distances (ρ) of order of ($k_0\,\rho = 100$). Moreover, for small source-observer distances the Green's function exhibit a strong decaying behavior of ($1/\rho^2$) type. On the contrary, at 10 GHz the surface wave is very strongly excited since it dominates the global Green's function behavior for spatial distances of about only ($k_0\,\rho = 1$). In addition, for small source-observer distances the decaying behavior is now inverse of the distance ($1/\rho$), instead of ($1/\rho^2$) as before. Consequently, we can conclude that the convergence properties of the spatial images series are related to the amount of electromagnetic energy coupled to the surface wave modes. To try to overcome this problem, a specially truncated set of images has been developed and it is described in the next section.

TABLE I

Value of the sign functions for all different mixed potential Green's functions components. G_{BA} denotes boxed magnetic vector potential Green's function while G_{BV} is the boxed electric scalar potential.

–	s_x	s_y
G_{BA}^{xx}	+1	−1
G_{BA}^{yy}	−1	+1
G_{BV}	−1	−1

III. Specially Truncated Set of Images

The problem of the slow convergence behavior of the series developed in the previous section can be overcome by noticing that there are two main features in any boxed Green's function that must be preserved in order to obtain accurate results, namely:

1. The singular behavior when $\rho \to 0$.
2. The boundary conditions at all lateral cavity walls.

The singular behavior is naturally preserved in the developed series of images, because they have been constructed using standard Green's functions. What remains then, is the accurate imposition of the boundary conditions at the metallic walls. This can be done by simply adding the first few images of the series as before, and then computing the needed strength of the last remaining images so that the boundary conditions for the fields are strictly satisfied at the projections of the observer points at the metallic walls. To simplify the analytical exposition of the problem we now show the procedure for the case of the electric scalar potential inside a parallel plate waveguide, being formally analogous for the rectangular cavity case. From (1) and Table I we write the electric scalar potential Green's function in the parallel plate waveguide structure shown in Fig. 5, as

$$G_{BV}(x,y|x',y') = \sum_{m=-\infty}^{\infty} \Big[G_V(x,y|+x'+2ma,y') - G_V(x,y|-x'+2ma,y') \Big], \quad (2)$$

where G_V is the Sommerfeld type electric scalar potential Green's function in the layered structure considered. In

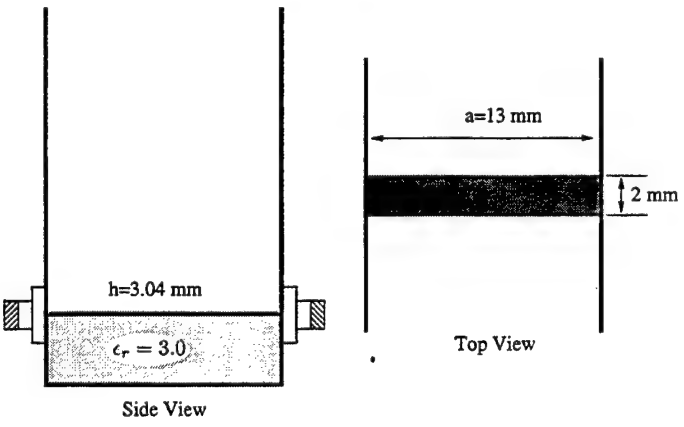

Fig. 2. Microstrip line printed on a thick substrate and backed by a parallel plate waveguide.

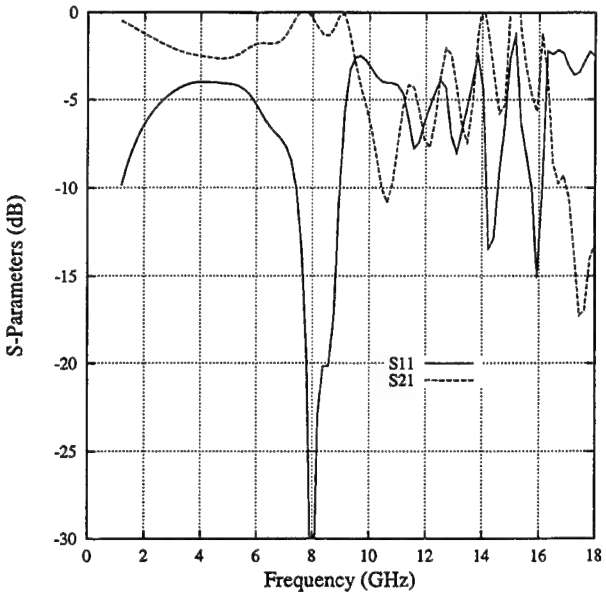

(a) Results with 22 spatial images.

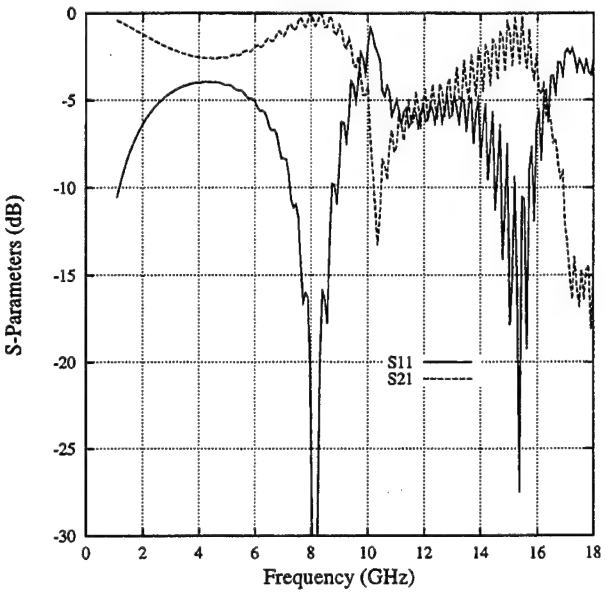

(b) Results with 102 spatial images.

Fig. 3. Scattering parameters of the structure in Fig. 2 when 22 and 102 spatial images are included in the analysis

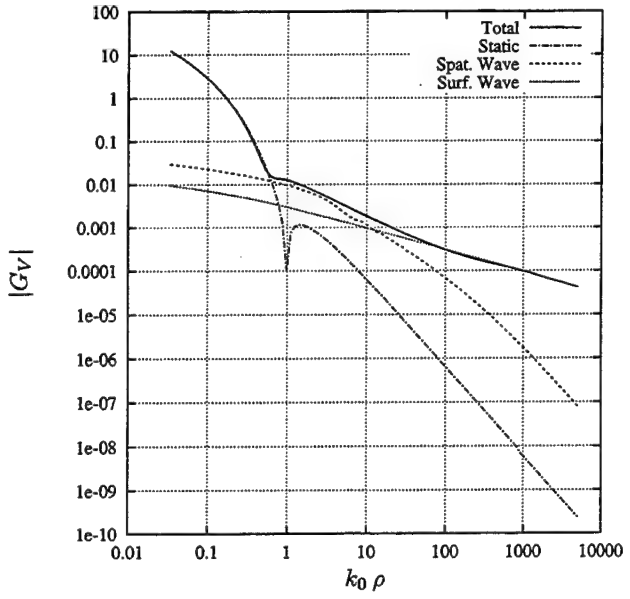

(a) Frequency 2 GHz.

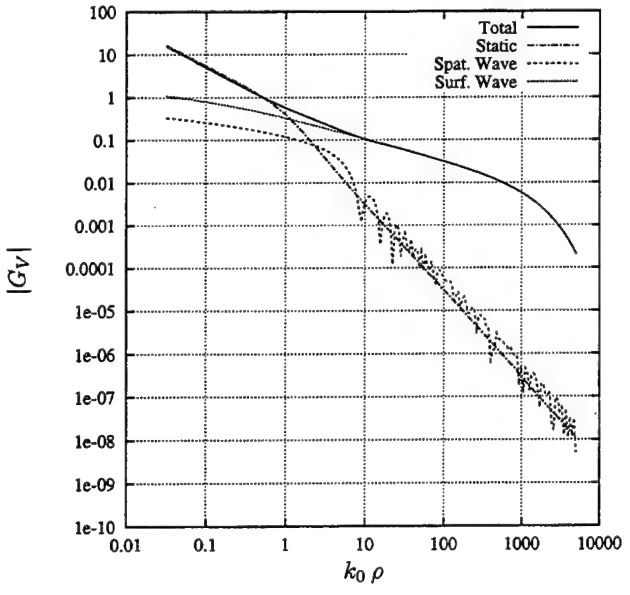

(b) Frequency 10 GHz.

Fig. 4. Imaginary axis decomposition for the electric scalar potential associated to the problem in Fig. 2. Source-observer distance is ρ.

the above equation, it is convenient to define an intermediate Green's function representing the potential created by a basic image couple (basic image set) as (Fig. 5)

$$G^{\text{BIS}}_{V_m}(x,y|x',y') = G_V(x,y|+x'+2ma,y') - G_V(x,y|-x'+2ma,y'), \quad (3)$$

and obviously, this intermediate Green's function matches the boundary conditions at the $x = 0$ wall. To serve our purposes, it is convenient to truncate the infinite spatial series with (M) and rewrite equation (2) using the definition in (3) as

$$G_{\text{BV}}(x,y|x',y') \approx \sum_{m=-M+1}^{+M-1} G^{\text{BIS}}_{V_m}(x,y|x',y') + G^{\text{BIS}}_{V_{+M}}(x,y|x',y') + G^{\text{BIS}}_{V_{-M}}(x,y|x',y'). \quad (4)$$

It is interesting to observe that the spatial images in (4) is balanced with respect the first metallic wall at $(x = 0)$, that is the boundary conditions are already rigorously imposed at this wall. On the contrary, the series is unbalanced with respect the second metallic wall at $(x = a)$. The key idea in this technique is to introduce an unknown constant (q) so that the strength of the two last basic image sets in the series are adjusted to enforce the right boundary condition for the potential also at the second metallic wall. We then introduce the unknown constant (q) and rewrite (4) as

$$G_{\text{BV}}(x,y|x',y') \approx \sum_{m=-M+1}^{+M-1} G^{\text{BIS}}_{V_m}(x,y|x',y') + q\left[G^{\text{BIS}}_{V_{+M}}(x,y|x',y') + G^{\text{BIS}}_{V_{-M}}(x,y|x',y')\right]. \quad (5)$$

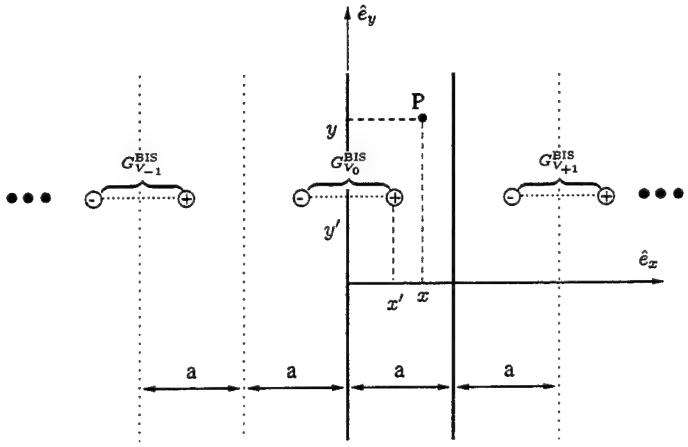

Fig. 5. Spatial images arrangement for a parallel plate waveguide structure.

In (5) the potential created by the first $(2M-1)$ basic image sets can now be defined as

$$\hat{G}_{\mathrm{BV}}(x,y|x',y') = \sum_{m=-M+1}^{+M-1} G^{\mathrm{BIS}}_{V_m}(x,y|x',y'), \qquad (6)$$

and the potential created by the two last basic image sets as

$$G^{l}_{\mathrm{BV}}(x,y|x',y') = q\left[G^{\mathrm{BIS}}_{V_{+M}}(x,y|x',y') + G^{\mathrm{BIS}}_{V_{-M}}(x,y|x',y')\right]. \qquad (7)$$

Next, the potential created by the first $(2M-1)$ basic image sets at the projection of the observer point at the second metallic wall is computed from (6) as

$$w = \hat{G}_{\mathrm{BV}}(a,y|x',y') = \sum_{m=-M+1}^{+M-1} G^{\mathrm{BIS}}_{V_m}(a,y|x',y'). \qquad (8)$$

Since the total potential must be zero also at the second metallic wall, the potential created by the two last basic image sets must compensate (8), and thus the following relation can be written

$$-w = q\left[G^{\mathrm{BIS}}_{V_{+M}}(a,y|x',y') + G^{\mathrm{BIS}}_{V_{-M}}(a,y|x',y')\right], \qquad (9)$$

from where the unknown constant required to annihilate the total potential also at the second metallic wall is easily found as

$$q = \frac{-w}{\gamma_1+\gamma_2}, \qquad (10)$$

with the redefinitions of the following coefficients

$$\gamma_1 = G^{\mathrm{BIS}}_{V_{+M}}(a,y|x',y'), \qquad \gamma_2 = G^{\mathrm{BIS}}_{V_{-M}}(a,y|x',y'). \qquad (11)$$

It is important to point out that a similar procedure as the one described here for the electric scalar potential is also applied for those components of the magnetic vector potential satisfying Newman boundary conditions at the metallic walls, and the only difference is that numerical differentiation is used in order to annihilate the total derivative.

To show the effectiveness of the approach developed, we have computed the electric scalar potential Green's function for the structure in Fig. 2 when the direct sum in (4) is used and when the new specially truncated set of images is used. In Fig. 6 we show the results obtained as a function of the observer point position for two different frequencies (10 GHz and 30 GHz), fixed position of the source ($x'/a = 0.107$) and when a total number of 3 and 60 pairs of basic image sets are included in the direct sum, and only 3 pairs of basic image sets in the specially

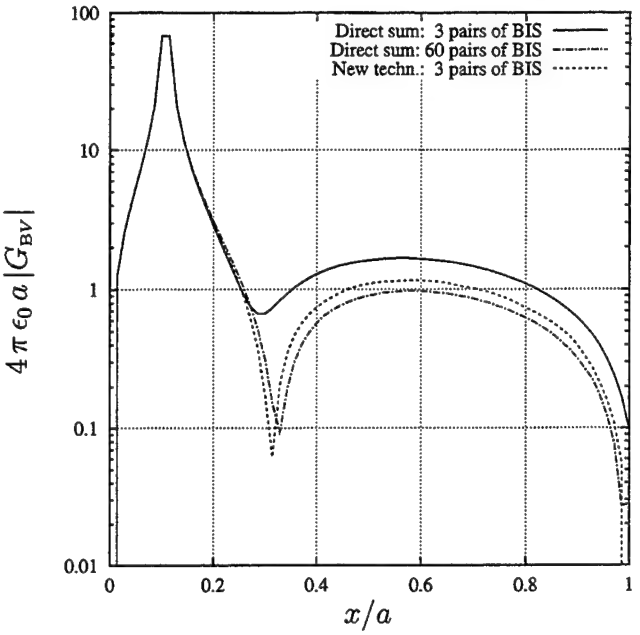

(a) Frequency 10 GHz.

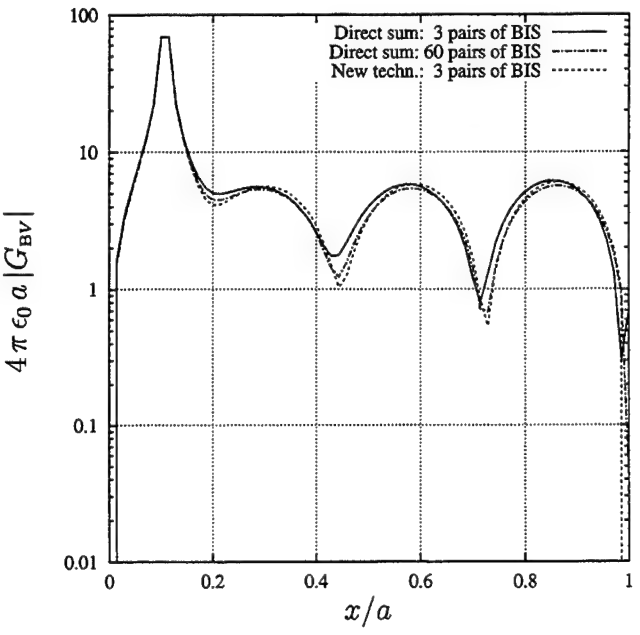

(b) Frequency 30 GHz.

Fig. 6. Shielded electric scalar potential Green's function associated to the problem in Fig. 2 when direct sum is used and when the new specially truncated set of images is used.

truncated series. As we can observe, close to singularity both approaches give similar results, but boundary conditions at the second lateral wall are only satisfied when the specially truncated set of images is used. Also we observe that the oscillations due to the standing wave created by the presence of the lateral walls are slightly readjusted when the specially truncated set of images is used. This readjustment appears to be necessary to allow the potential to be zero at the lateral metallic walls. Finally, it can be observed that when 60 pairs of basic image sets (242 images) are used in the direct sum, the boxed electric scalar potential converges to the results obtained with just 3 specially truncated pairs of basic image sets (14 images), thus indicating the huge saving in computational effort obtained with the new approach.

When the newly developed Green's functions are used in the analysis of the structure in Fig. 2 we observe fast convergence properties in the results. In Fig. 7 we present the computed S-parameters showing very smooth behavior and that the ripple has been effectively canceled out, even with only 3 specially truncated pairs of basic image sets (14 images). By contrast, convergence is not achieved even after 25 pairs of basic image sets (102 images) without truncation as shown in Fig. 3.

To further validate the theory presented, a breadboard of the structure in Fig. 2 has been manufactured and tested. In Fig. 8 we present measured versus simulated results showing good agreement for both S_{11} and S_{21} scattering parameters and with only 3 specially truncated pairs of basic image sets in the calculations.

Finally, it is important to point out that with the proposed approach all additional computations are performed analytically and that the reduction in the number of images required to obtain good convergence is considerable, so that the implementation of efficient software codes is possible.

IV. Results and Discussions

A software code based on the proposed approach has been written for the analysis of complex cavity backed antennas. The asymptotic technique described in [9] has been used for the evaluation of the basic Sommerfeld integrals for large values of source-observer distances and a MoM technique based on triangular cells has been implemented.

To show the usefulness of the technique, we present the analysis of a circular-polarized cavity-backed antenna containing two stacked patches of complex shapes (note in particular the narrow slits existing in both patches). In

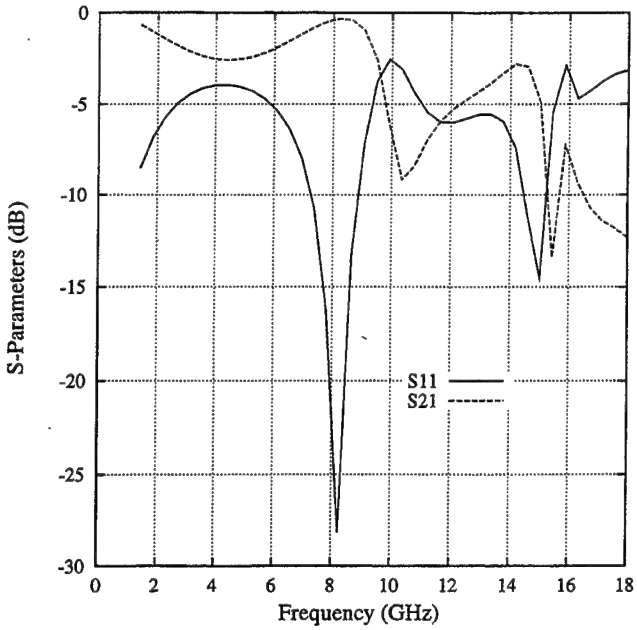

(a) Results with 2 truncated pairs of basic image sets.

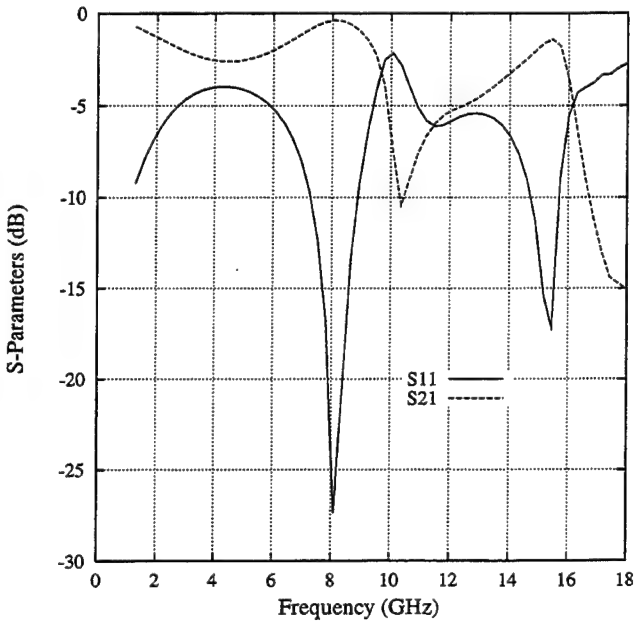

(b) Results with 3 truncated pairs of basic image sets.

Fig. 7. Scattering parameters of the structure in Fig. 2 when 2 and 3 specially truncated pairs of basic image sets are included in the analysis.

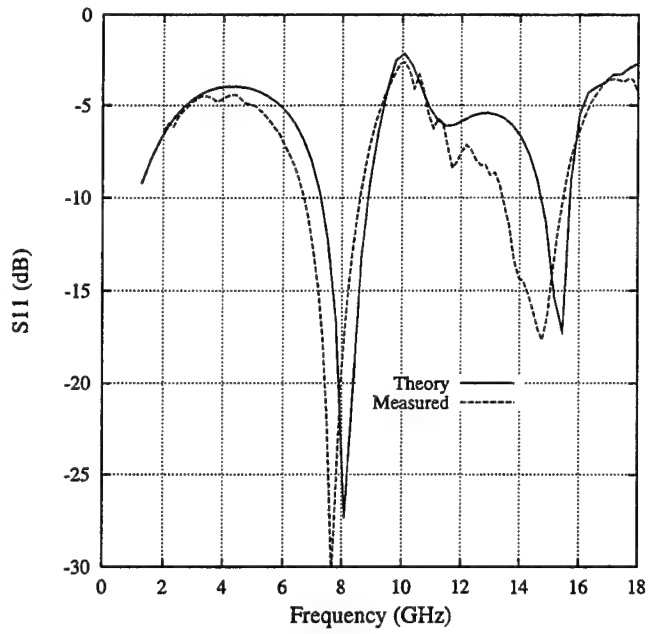

(a) S_{11} parameter.

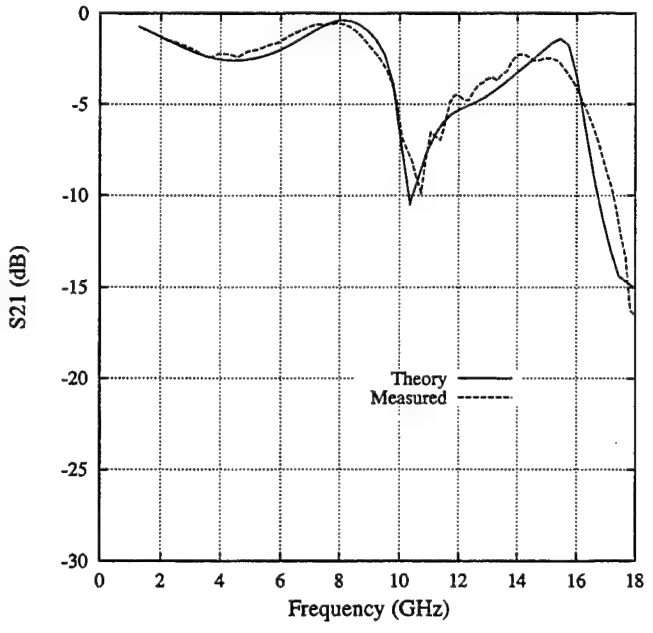

(b) S_{21} parameter.

Fig. 8. Measured versus simulated results for the scattering parameters of the structure in Fig. 2. Only 3 truncated pairs of basic image sets (14 images) are used in the theoretical prediction.

Fig. 9 we show the basic geometry of the antenna and the triangular meshes used in conjunction with the developed algorithms. For the analysis of this structure, adequate magnetic currents are defined at the cavity's top aperture and a set of coupled integral equations is defined and solved in the fashion described in [10]. In these equations, all electromagnetic interactions are computed with the specially truncated set of images derived in this paper. Fig. 10 presents measured versus simulated results for the S-parameters of the antenna when the upper patch is removed, and Fig. 11 for the complete antenna structure, with the upper patch on top, showing in all cases good agreement. An interesting feature of the technique derived is the rate of convergence of the numerical results when the number of specially truncated images is increased. For this last example no significance numerical difference is observed with 10 and 14 images, thus indicating good and fast convergence of the developed series.

V. Conclusions

In the frame of IE-MoM, a new contribution to the analysis of arbitrary shielded microwave circuits and cavity backed antennas has been presented. Following the proposed approach, Green's functions are formulated with well known Sommerfeld integrals and the know-how already available in this field is reused. The presence of lateral metallic walls is taken into account by using standard image theory and the convergence conditions of the resulting image series have been investigated. When slow convergence occurs, a specially truncated set of images has been derived, based on the rigorous imposition of the boundary conditions for the fields and potentials at the metallic walls. Results reveal that convergence using the specially truncated set of images is very fast and that with only 10-14 images accurate results are obtained. Moreover, the use of the technique described simply adds few analytical operations to the basic Sommerfeld formalism so that efficient computer codes can still be developed. In this paper measured and simulated results are compared for a stacked patch antenna with both patches exhibiting a complicated shape.

References

[1] J. Ching Cheng, H. I. Dib, and L. P. B. Katehi, "Theoretical modeling of cavity-backed patch antennas using a hybrid technique," *IEEE Transactions on Antennas and Propagation*, vol. 43, pp. 1003–1013, September 1995.

[2] J. C. Rautio and R. F. Harrington, "An electromagnetic time-harmonic analysis of shielded microstrip circuits," *IEEE Transactions on Microwave Theory and Techniques*, vol. 35, pp. 726–730, November 1987.

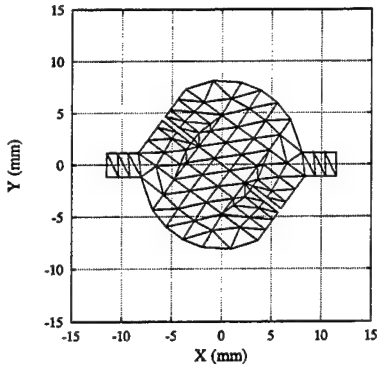

(a) Mesh lower patch.

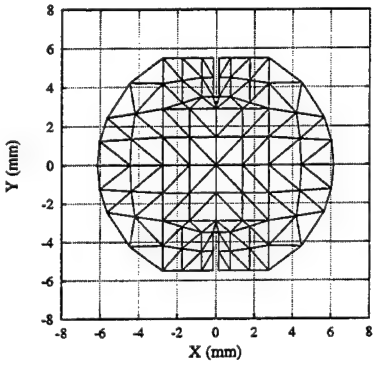

(b) Mesh upper patch.

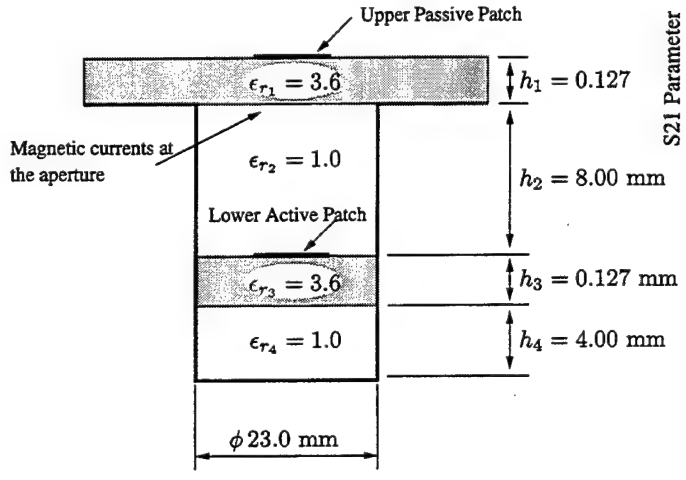

(c) Layered structure.

Fig. 9. Geometry of the double patch cavity-backed antenna analyzed in this paper.

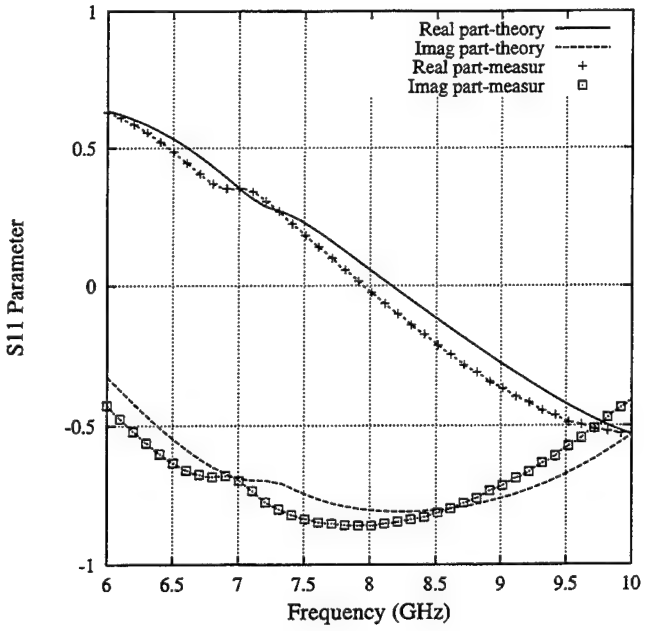

(a) S_{11} parameter.

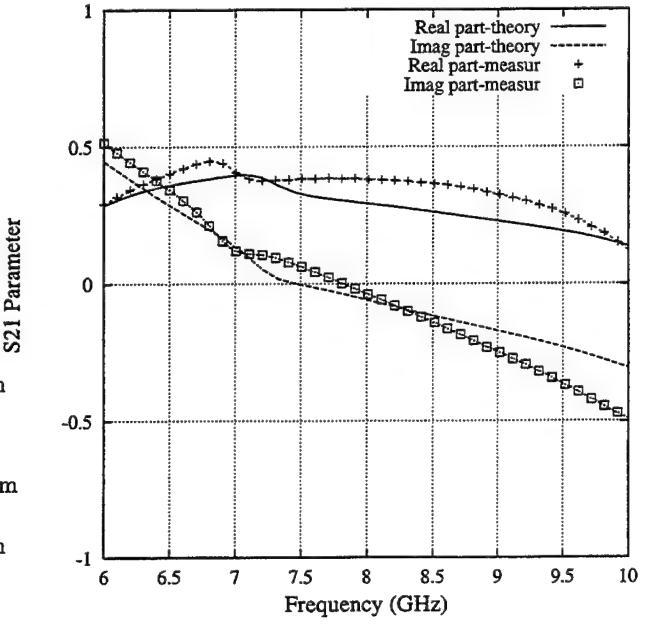

(b) S_{21} parameter.

Fig. 10. Measured versus simulated results for the antenna in Fig. 9 when the upper patch is removed. Real and imaginary part of the S-parameters are given.

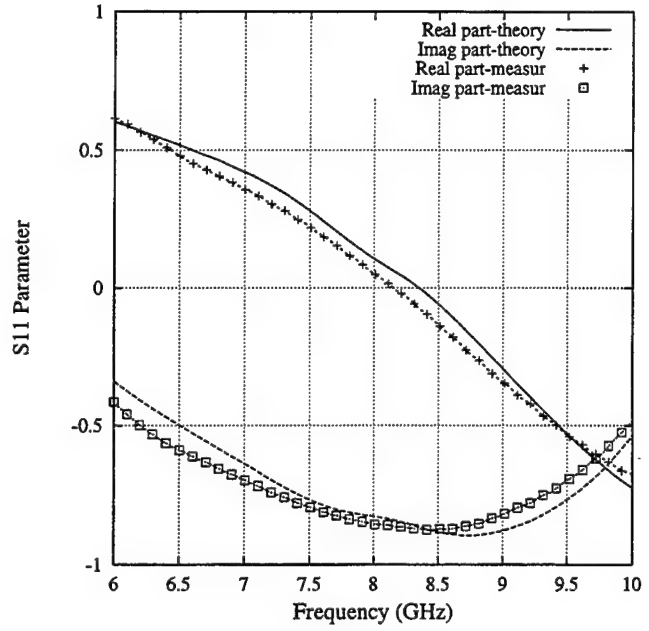

(a) S_{11} parameter.

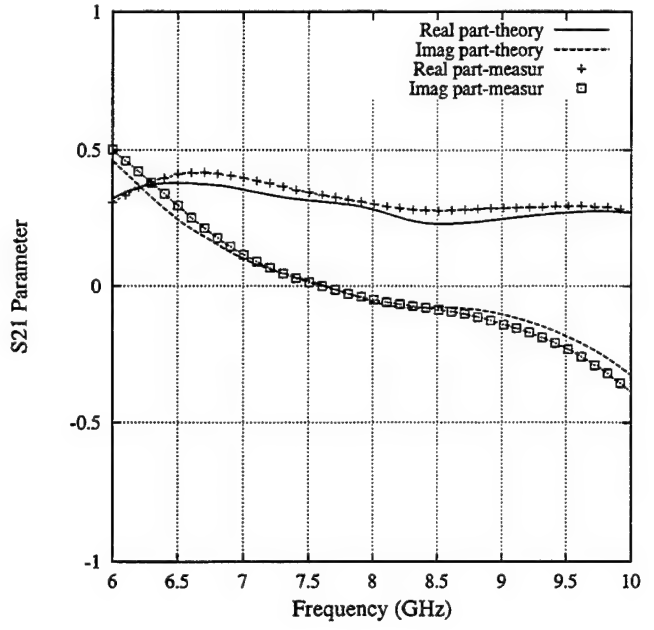

(b) S_{21} parameter.

Fig. 11. Measured versus simulated results for the antenna in Fig. 9 when the upper patch is placed on top. Real and imaginary part of the S-parameters are given.

[3] A. Hill and V. K. Tripathi, "An efficient algorithm for the three-dimensional analysis of passive microstrip components and discontinuities for microwave and millimeter-wave integrated circuits," *IEEE Transactions on Microwave Theory and Techniques*, vol. 39, pp. 83–91, January 1991.

[4] S. Hashemi-Yeganeh, "On the summation of double infinite series field computations inside rectangular cavities," *IEEE Transactions on Microwave Theory and Techniques*, vol. 43, pp. 641–646, March 1995.

[5] G. V. Eleftheriades, J. R. Mosig, and M. Guglielmi, "A fast integral equation technique for shielded planar circuits defined on nonuniform meshes," *IEEE Transactions on Microwave Theory and Techniques*, vol. 44, pp. 2293–2296, December 1996.

[6] M. Joo Park and S. Nam, "Efficient calculation of the green's function in rectangular waveguides," in *Proc. of the AP-S Symposium*, (Montreal, Canada), pp. 2354–2357, IEEE AP-S, 13-18 July 1997.

[7] G. G. Gentili, L. E. Garcia-Castillo, M. Salazar Palma, and F. Perez-Martinez, "Green's function analysis of single and stacked rectangular microstrip patch antennas enclosed in a cavity," *IEEE Transactions on Antennas and Propagation*, vol. 45, pp. 573–579, April 1997.

[8] K. A. Michalski and J. R. Mosig, "Multilayered media green's functions in integral equation formulations," *IEEE Transactions on Antennas and Propagation*, vol. 45, pp. 508–519, March 1997.

[9] J. R. Mosig and A. Alvarez Melcón, "Green's functions in layered media: imaginary axis integration and asymptotic behavior," in *Proc. of the AP-S Symposium*, (Baltimore, Maryland, USA), pp. 416–419, IEEE AP-S, 21-26 July 1996.

[10] J. R. Mosig, *Integral equation techniques for three-dimensional microstrip structures*, ch. 6: in The Review of Radio Science, pp. 127–152. Oxford University Press, 1990-1992. Ed. by Ross Stone.

Efficient Solution of Linear Systems in Microwave Numerical Methods

L. Tarricone, F. Malucelli*, A. Esposito**

D.I.E.I., Via G. Duranti,93, 06131, Perugia, Italy
*Dip. Elettronica ed Informazione, Politecnico di Milano. Via Ponzio 34/5, 20133, Milano, Italy.
**EDSI, Via del Coppetta, 46, 06124, Perugia, Italy.

Abstract— **A common bottle-neck, limiting the performance of many electromagnetic numerical methods, is the solution of sparse linear systems. Until now, this task has been typically solved by using iterative sparse solvers, whose require heavy computational efforts, especially when the problem is not well-conditioned.**

An alternative strategy is based on the use of banded solvers, which numerical complexity is quadratical with respect to the matrix bandwidth. Of course, these methods are efficient provided that the matrix bandwidth is sufficiently small. In this paper, a method (called WBRA) for the bandwidth reduction of a sparse matrix is presented: it is here specifically customized to typical electromagnetic matrices. The approach is superior to all the previous algorithms, also with respect to commercial well-known packages, and is suitable also for non-symmetric problems.

As demonstrated by results, the use of WBRA, in conjunction with common banded solvers, substantially improves (up to one order of magnitude) the solution times in several electromagnetic approaches, such as Mode-matching, FEM, and MoM analysis of microwave circuits. In conclusion, it is proved that the high efficiency and effectiveness of WBRA turns the strategy of bandwidth reduction combined with a banded solver into the most profitable way of solving linear systems in electromagnetic numerical methods.

I. Introduction

The use of numerical methods is nowadays commonly accepted as the most effective and efficient way to attack and solve electromagnetic (EM) problems. Many numerical codes are routinely used in the CAD of EM circuits, in complex scattering analyses, and in electromagnetic compatibility evaluations, just to mention some possible industrial and research tasks which are currently mainly performed via numerical approaches.

The obvious consequence of the continuous growth of numerical methods in daily work is an increasing demand for numerical efficiency and performance. As the problems get more complex, the issue of optimum memory exploitation and CPU-time reduction is crucial, provided that suitable numerical accuracy be guaranteed.

A common bottle-neck limiting the performance of many numerical approaches is represented by the solution of linear systems, usually sparse, which is very often one of the strongest numerical tasks for many EM methods. Mode-matching (MM), Method of Moments (MoM), both in its standard formulation and when using wavelet expansions, and Finite Element Methods (FEM) are just some examples demonstrating this.

In previous papers [17], [3] it was demonstrated that a very efficient strategy to improve the performance of many EM codes is the enhancement of the linear system solution time by an appropriate transformation of the system matrix. The matrix, generally sparse, is transformed into a banded one, with reduced bandwidth, this paving the way for a very effective use of high-performing banded solvers. The performance of the algorithm to reduce the bandwidth of a sparse matrix is, in this perspective, a key-point. In this paper, a new method is proposed to accomplish this task. It is suited to every kind of sparse matrix, but specifically tuned to achieve maximum performance on typical matrix patterns of EM problems. It is proved to outperform all the previous approaches, including commercial packages, on several real EM cases. The availability of such an efficient bandwidth reducer turns its use, in conjunction with a banded solver, into the most effective solution strategy, differently from before, when the bandwidth minimization effort was not so profitable, and the use of a sparse solver without matrix preprocessing was sometimes the winning approach.

The paper is structured as follows. In section 1 an overview of the problem is proposed. In section 2 the new algorithm for bandwidth reduction is proposed. In section 3 results are given. Finally, conclusions are drawn.

II. Bandwidth reduction used in conjunction with direct solvers vs. iterative sparse methods

Let

$$\mathbf{Ax} = \mathbf{B} \tag{1}$$

1054-4887 © 1999 ACES

be a sparse system.

We know from very basic matrix algebra that, considered a permutation matrix $\mathbf{P}$ so that $\mathbf{P} \cdot \mathbf{P^T} = \mathbf{I}$ (where $\mathbf{I}$ is the identity matrix), the system

$$\mathbf{PAP^T x'} = \mathbf{PB} \tag{2}$$

has the same numerical stability as (1), as its condition number is not changed. Moreover, the solution $\mathbf{x}$ of (1) is easily found from the solution $\mathbf{x'}$ of (2), as

$$\mathbf{x} = \mathbf{P^{-1} x'} \tag{3}$$

Therefore, if the permutation matrix is appropriately chosen, so that the transformed system matrix $\mathbf{A'} = \mathbf{PAP^T}$ is banded, with small bandwidth, banded solvers can be used with very high performance, as their complexity depends quadratically on the matrix bandwidth [5]. Unfortunately, the task of finding the transformation $\mathbf{P}$ that gives the minimum possible bandwidth is a very difficult problem; in [12] it is shown to be an NP-hard problem.

Many efforts have been made until now in order to solve this problem both in an exact way providing the optimal permutation, and in an approximated way, so that good permutations that sensibly reduce the bandwidth can be found with a much smaller computational effort. A very thorough review of approaches is proposed in [5], which must be integrated with more recent contributions [4], [7], [2].

Due to this difficulty, instead of looking for an optimum transformation, alternative approximated but faster strategies are usually followed in practical applications, as illustrated in the next section where the method for bandwidth reduction proposed in [6] referred as WBRA will be reviewed, putting forward its peculiar features with respect to other previous approaches.

Of course, the development of an effective bandwidth reduction algorithm does not guarantee an a-priori enhancement of performance whatever the EM numerical method might be. Its impact must be benchmarked by comparing it with respect to the current existing approaches. Among them, a usual approach is the use of iterative sparse solvers, which are generally applied directly to the original matrix, without any previous preprocessing. Iterative solvers are not very efficient, and require large numbers of iterations especially on non-well-conditioned problems. Nonetheless, they are largely used, due to their easy availability and to their strong stability. In fact, direct sparse solvers, which could be in principle more performing, are often prone to the risk of dense LU factors [5], highly degrading memory and computing-time requirements, and are therefore not considered a viable solution.

Therefore, on the basis of the previous considerations, when presenting results, we generally propose a comparison between a strategy using a bandwidth reduction, and a more standard one, using an iterative sparse solver.

III. The WBRA Approach for Bandwidth Reduction

One of the most effective classes of algorithms specifically devoted to bandwidth reduction is the one derived from the Cuthill-McKee (CM) method [8]. The main idea of this class of algorithms is related to the graph representation of the matrix (see Fig. 1). Consider a symmetrically structured matrix $\mathbf{A}$ of order n, let $G = (N, E)$ be the undirected adjacency graph related to $\mathbf{A}$, where each node $i \in N = \{1, \ldots, n\}$ represents the i-th row/column of the matrix, and there is an edge (i, j) between two nodes i and j $(i \neq j)$ if and only if the element of matrix $\mathbf{A}$ $a_{ij} \neq 0$. The basic idea of the computation can be summarized by the following steps:

1) *partitioning phase*: select a root node r, and partition N into subsets called *levels* $\{L_0, L_1, \ldots, L_p\}$ with $r \in L_0$, so that there are edges only between nodes belonging to the same level or to two adjacent levels; a partition into levels is called *level structure*. In Fig. 2, the level structure obtained with root equal to 6 is shown.

2) *numbering phase*: sort the nodes by increasing level index, and inside each level number them according to a particular criterion.

As the other algorithms in the CM class, WBRA follows this general scheme, but in the two phases exploits the structure of the combinatorial optimization problem underneath.

In the partitioning phase a partition into levels, whose larger subset has minimum cardinality, is sought. In fact the bandwidth is directly affected by the size of the largest subset. However, as this problem is as difficult as finding the minimum bandwidth, an approximated algorithm is applied. In Fig. 3 a possible redistribution of nodes between levels is provided. In this case the width of the largest level in the new structure is reduced to 2.

Now consider the numbering phase. WBRA applies the numbering to a set of "promising" level structures determined during the partitioning phase, that is to a set of level structures whose largest level is small.

Let $\{L_0, L_1, \ldots, L_p\}$ be the partition under consideration during the generic iteration:

Numbering the nodes, we assign the first numbers (i.e. the first positions in the permuted matrix) to the nodes in L_0, then the other positions are assigned following the precedence between levels, that is any element of level L_{h-1} always has a smaller number with respect to any other element

of level $L_h, h = 1, \ldots, p$. Thus the numbering phase is carried out by a sequence of steps, one for each level.

Determining the optimal numbering of level L_h WBRA considers:

- (i) the numbers assigned to the elements of L_{h-1}, but in addition it considers also
- (ii) the possible effects of the numbering in level L_{h+1}.

These two criteria give rise to a well characterized combinatorial optimization problem whose particular structure allows us to determine the numbering of a level in almost linear time. The numbering obtained by applying the algorithm to the level structure of Fig. 3 is shown in Fig 4. A detailed discussion of the combinatorial structure of the problem, and of the numbering algorithm can be found in [6].

The rearranged matrix according to the permutation found by the algorithm is shown in Fig. 5.

A. The unsymmetric case

The method proposed until now, based on a matrix representation through an adjacency graph, is devoted to matrices with symmetrical patterns. On the contrary, as described in the result section, a method working also on matrices with an unsymmetric zero-non zero structure is needed quite often. One of the key-points of WBRA is its amenability to cope with this problem, without degradating the performance of the algorithm. This is achieved by symmetrizing the matrix structure in a cumbersome way.

Generally, the matrix pattern could be symmetrized in two possible fashions:

i) consider a matrix $\mathbf{A}^*$ where $a^*_{ij} = \max\{a_{ij}, a_{ji}\}$;

ii) symmetrize the matrix, that is consider $\mathbf{A}^* = \frac{1}{2}\mathbf{A}\mathbf{A}^{\mathbf{T}}$.

The latter approach is avoided as it may introduce some ill conditioning. In the former case, any symmetric bandwidth reduction algorithm can be applied to $\mathbf{A}^*$, then matrix $\mathbf{A}$ is permuted according to the obtained reordering. The drawback of this approach is evident when $\mathbf{A}$ is highly unsymmetric: many zero elements are dealt as they would be non zero. This is why devising ad hoc algorithms that can take advantage of the unsymmetry becomes important.

By contrast to the symmetric case, in the bandwidth minimization of unsymmetric matrices, we are not obliged to apply the same permutation to rows and columns. Thanks to this observation, we propose an algorithm divided into two phases. In the former phase a permutation is applied to rows only. Then the matrix is symmetrized according to method i). In the latter phase the bandwidth is reduced by applying the same permutation to rows and columns. Finally the matrix is "desymmetrized" by removing the nonzero elements introduced by the symmetrization step.

We adopted two methods for the first phase. The former method applies the row permutation that maximizes the number of non zero elements on the diagonal. This problem is known as the *transversal maximization* [5]. An alternative method (*symmetry maximization*) tries to maximize the number of symmetric elements, that is tries to permute the matrix rows so that in the final matrix the number of elements $a_{ij} \neq 0$ having the corresponding $a_{ji} \neq 0$ are as many as possible.

After the first phase (either transversal maximization or symmetry maximization), the WBRA is applied. The final performance (as demonstrated by results) is quite attractive. The algorithm is publically available through Internet at the web site `http://dvorak.istel.ing.unipg.it`.

IV. Results

Four main areas of applications are proposed: the MM analysis of rectangular waveguide circuits, the FEM analysis of planar circuits with metalic boxes, the MoM analysis of planar circuits with a Mixed-Potential Integral Equation (MPIE) approach, and a MoM using wavelet expansions. In the case of MM and MoM, the use of a bandwidth reduction in couple with a banded solver is compared with a standard iterative biconjugate-gradient sparse solver with preconditioning. For FEM, the performance of a standard package is compared with an implementation taking advantage from bandwidth reduction.

A. MM Analysis of MW Circuits

The MM analysis of MW circuits is an efficient and rigorous method, often used in CAD packages. Among its several attractive issues, the amenability to MW circuit optimization, via the Adjoint Network Method is one of the most interesting, as well as a paramount impulse to improve its performance.

As already discussed and demonstrated in [17], the solution of a sequence of linear systems, with different right-hand-sides and same matrix, is the numerical core of the approach. The pattern of the sparse system matrix $\mathbf{A}$ depends on the numbering adopted for the physical and electrical ports, as well as on the number of modes selected in every section of the circuit.

In this paper, we compare the performance of WBRA with other methods to reduce the bandwidth of the system matrix, and show the corresponding performance of the MM analysis. More specifically, we compare WBRA with a proprietary routine performing the Modified- Reversed-Cuthill-McKee (MRCM) approach (one of the most efficient implementation of the CM method [8]), with

a commercial routine for bandwidth reduction proposed by MATLAB, and with a previous novel technique proposed by the authors in [3], called Tabu Search (TS). In Tab. I results are given on three matrices coming from the MM analysis of a complex 4x4 Butler matrix (Fig. 6), with different spatial resolutions. In Tab. I the reader can note: the system size N, the bandwidth of the original matrix $\mathbf{A}$ (IB), the final bandwidth achieved by the different algorithms and, in brackets, the time necessary to evaluate the permutation matrix. Times are given in seconds, on an IBM RS6000 250 T.

N	IB	MRCM	MATLAB	TS	WBRA
116	75	6 (0.039)	6 (0.062)	6 (91.1)	6 (0.051)
245	115	83 (0.24)	55 (0.36)	25 (242)	27 (0.229)
503	452	78 (1.572)	61 (1.97)	64 (1000)	51 (1.234)

Tab. I: The effectiveness of different bandwidth reduction methods and (times in brackets) their efficiency.

As inferred from the table, TS is too slow to be used on serial platforms, and is therefore omitted. The WBRA is superior to both MATLAB and MRCM, as it is more effective and its time performance is better as the size of the problem increases. In Tab. II, for the same cases of Tab. I, the solution times are shown using: 1) a standard iterative sparse solver (BCG) with the original $\mathbf{A}$ matrix 2) a banded solver on the original $\mathbf{A}$ matrix (BNT) 3) a banded solver on the transformed $\mathbf{PAP^T}$ matrix ($\mathbf{P}$ evaluated with MATLAB (BTM)) 4) a banded solver on the transformed $\mathbf{PAP^T}$ matrix ($\mathbf{P}$ evaluated with WBRA (BTW)).

N	BCG	BNT	BTM	BTW
116	9.5	27.1	0.46	0.46
245	101.1	198	36.3	8.2
503	521	longer than 1000	442	296

Tab. II: Different simulation times for a MM code on a 4x4 Butler's matrix. A standard iterative solution (BCG) is compared with a banded solution (BNT), a banded solution with bandwidth minimization by MATLAB (BTM), and a banded solution with bandwidth minimization by WBRA (BTW).

As shown in Tab. I, the WBRA method outperforms the other approaches. Its use (as evidenced by Tab. II if you compare BTW with respect to BCG), allows a speed-up in the system solution of up to one order of magnitude with respect to the use of a standard iterative sparse solver, and (as evidenced by comparing BTW and BTM) of up to 4 times with respect to the use of previous bandwidth reduction methods.

B. FEM Analysis of Boxed Microstrip Lines

The analysis of microstrip lines surrounded by a metallic box is a common problem for the MW and EMC community. This problem has been attacked by using a public domain FEM package called EMAP [10]. In EMAP, a key-point in the analysis of the circuit is the repeated solution of a linear system. In FEM, the system is generally reduced to a banded structure. Therefore, EMAP uses a banded solver, and is quite amenable to be interfaced with the above mentioned modules for bandwidth reduction.

Several tests have been performed on circuits such as the one in Fig. 7, for different substrates and dimensions of both the box and microstrip. Some of the results are shown in two tables, with the same scheme as for the MM section: in Tab. III data report the efficiency of the different bandwidth reduction methods, whilst Tab. IV shows the effects of different bandwidth reductions (Matlab (BTM), and WBRA (BTW)) on the system solution time using the standard banded solver used in EMAP (BNT).

N	IB	MRCM	MATLAB	WBRA
291	107	106 (0.32)	106 (0.48)	62 (0.29)
615	156	165 (3.75)	163 (8.9)	88 (1.56)
1180	297	245 (24.8)	237 (142)	184 (5.9)

Tab. III: A comparison of performance for different bandwidth reduction methods for a FEM linear system.

N	BNT	BTM	BTW
291	34.1	33.8	8.8
615	243	289	59.6
1180	2048	1621	973

Tab. IV: Solution times for the FEM problem using a standard EMAP banded solver (BNT), with respect to 1) standard EMAP solver and Matlab bandwidth reduction (BTM) and 2) standard EMAP solver and WBRA bandwidth reduction (BTW).

It can be noted from Tabs. III and IV that the superior performance of WBRA, both for effectiveness, and for computing times, allows a speed-up in the system solution time of up to 4 times with respect to standard EMAP code.

C. MoM Analysis of Microstrip Circuits

Recent enhancements in the analysis of planar circuits with an MPIE approach using a closed-form spatial-domain Green's function [11] allow a very efficient implementation of CAD tools. The MPIE can be discretized by using the MoM, thus generating a linear system whose solution allows the evaluation of the scattering parameters of the circuit. The system is generally dense, but very recently it has been demonstrated that it can be

reduced to a sparse one, without affecting the accuracy of the simulation [1]. Therefore, also in this case the core of the numerical effort is a sparse linear system, and a bandwidth reduction is worth to be performed.

In Tabs. V and VI results are shown for two circuits reported in Fig. 8. As usual, Tab. V gives results concerning the effectiveness and efficiency of the WBRA with respect to other methods for bandwidth reduction. Tab. VI compares the solution time using a standard iterative sparse solver (BCG) with respect to using a banded solver, invoked straightly (BNT) or after performing a bandwidth reduction (using MATLAB (BTM) or WBRA (BTW)).

N	IB	MRCM	MATLAB	WBRA
220	208	120 (0.34)	119 (0.51)	72 (0.3)
401	310	141 (1.23)	136 (1.5)	82 (0.98)

Tab. V: A comparison of performance for different bandwidth reduction methods for a MPIE/MoM linear system.

N	BCG	BTM	BTW
220	71	14.8	6.4
401	214	49.6	18.8

Tab. VI: Solution times for the MPIE/MoM problem using standard sparse iterative solver (BCG), with respect to 1) banded solver and Matlab bandwidth reduction (BTM) and 2) banded solver and WBRA bandwidth reduction (BTW).

From Tabs. V and VI it can be noted that the use of WBRA enhances the efficiency of the system solution by up to 12 times with respect to a standard sparse iterative solver, and up to 3 times with respect to using a commercial bandwidth reducer before invoking a banded solver.

D. MoM using Wavelet expansions

In the past few years, the use of wavelet expansions in the solution of electromagnetic problems has become more and more frequent. Wavelet expansions have been introduced, for instance, in conjunction with the Method of Moments (MoM) discretization of integral equations [9], [20], in order to solve scattering problems with large-scale scatterers (thus containing a variety of length scales with respect to wavelength) [15]-[18], or to analize slot-apertures [19], microstrip floating line structures [21], as well as to study 2D and 3D dielectric structures [13], [14]. A common key-issue for all the above mentioned applications is the derivation of very sparse and well-conditioned linear systems, representing the numerical core of MoM approaches [1], [13], [14]. The moment matrix sparsity allows the use of very efficient iterative sparse solvers, and the good condition number guarantees a low number of iterations to converge, with a consequent dramatic improvement of performance.

Up to now, once the moment matrix has been sparsified using wavelet expansions, it has been assumed that iterative solvers are the best way to attack the linear system solution. We demonstrate here that, by means of appropriate matrix transformations, the use of a banded direct solver in conjunction with WBRA outperforms the iterative approach, especially when non-symmetric moment matrices are attained after split testing procedures in presence of compact-support functions [15], [16], [13], [14]. It must be put forward that the capability of dealing with non-symmetrical cases, without lost of effciency, is one of the most attractive features of WBRA. In fact, for previous bandwidth reduction approaches, the only way to face non-symmetric problems was represented by the matrix pattern symmetrization, with an obvious dramatic reduction of performance.

We refer, for the proposed results, to a MoM discretization of a Mixed-Potential Integral-Equation formulation for the analysis of planar microstrip circuits, as described in [1]. The MoM matrices are transformed in accordance with the use of Battle-Lemarie multiresolution expansions, as described in [15], [16], [13], [14], thus attaining non-symmetric matrices when splitting and truncations are performed to comply with boundary conditions. A double-layer microstrip waveguide has been studied, with different basis expansions, and different threshold values v_t have been applied onto the moment matrices, so that values having magnitude less than v_t per cent of the largest entry are considered as zeros. Of course, different approximations are attained on varying v_t, and errors have been estimated by comparing approximate results with the correct result attained without any thresholding. Table VII and VIII present results from two different cases of analysis of a double-layer microstrip (see Fig. 9), using different numbers of Battle-Lemarie wavelet functions. Different matrix sizes, respectively N=250 and N=478, have been attained. For different thresholds, the matrix sparsity S, the approximation error, and the results are reported, from two different strategies: i) a banded solver with WBRA (BTW), ii) an iterative sparse BCG solver (BCG) (the number of iterations to converge is also reported).

			Sol. time (s.)	
v_t	S	Error	BTW	BCG (n.iterations)
2%	99%	5.4%	0.08	0.09 (8)
1%	96%	2.4%	0.12	0.23 (17)
0.5%	91%	0.7%	0.21	0.48 (31)

Tab. VII : Results for a matrix of dimension

N=250. Computing times for a banded solver and WBRA strategy versus BCG strategy are shown, for different threshold values, and the corresponding matrix sparsity S and solution error due to thresholding effects. For BCG the number of iterations needed to converge is shown in the brackets.

			Sol. time (s.)	
v_t	S	Error	BTW	BCG (n.iterations)
2%	98%	4.8%	0.30	0.1 (11)
1%	94%	2.1%	0.64	1.4 (14)
0.5%	88%	0.6%	0.80	6.0 (28)

Tab. VIII : Results for a matrix of dimension N=478. Computing times for a banded solver and WBRA strategy versus BCG strategy are shown, for different threshold values, and the corresponding matrix sparsity S and solution error due to thresholding effects. For BCG the number of iterations needed to converge is shown in the brackets.

As apparent from Tab. VII and VIII, an appropriate value for thresholding is 0.5%, so that the approximation error is smaller than 1%. In this case, for N=250, a speed-up of nearly 2.3 is achieved, when using the BTW strategy with respect to BCG, whilst for N=478 a speed-up of nearly 7.5 is observed.

V. Conclusions

In this paper a new method, called WBRA, to perform the bandwidth reduction of a sparse matrix has been presented. It generally works for every kind of sparse matrix, but it is specifically tuned to achieve maximum performance on typical matrix patterns encountered in electromagnetic numerical problems, as well as to manage also with non-symmetric zero-non-zero-pattern matrices (this being crucial when attacking some wavelet problems).

The efficiency and effectiveness of the method is superior to all the other commercial and public domain packages available on the market, as demonstrated on matrices generated by the mode-matching, FEM, MoM/MPIE, and MoM/wavelet analysis of rectangular waveguide and planar circuits.

The huge advantages of the WBRA's use in the analysis of MW circuits is also proved for the above mentioned problems. It is demonstrated that enhancements of one order of magnitude can be achieved, with respect to the use of classical iterative sparse solvers, by using WBRA in conjunction with banded solvers. This is attained thanks to the high efficiency of WBRA, which reduces the bandwidth reduction times, improves the effectiveness of bandwidth reduction, and substantially decreases the numerical complexity of the banded solution.

References

[1] A. Caproni, F. Cervelli, M. Mongiardo, L. Tarricone, F. Malucelli, "Bandwidth Reduced Full-Wave Simulation of Planar Microstrip Circuits", Int. Journal of Appl. Comp. Electromagnetics Society, 13, 2, pp.197-204, 1998.

[2] G. M. Del Corso, G. Manzini, "Finding exact solutions to the bandwidth minimization problem", Computing (forthcoming).

[3] M. Dionigi, A. Esposito, R. Sorrentino and L. Tarricone, "A Tabu Search Approach for the Solution of Linear Systems in Electromagnetic Problems", to appear in *Int. Journal of Numerical Modelling*, 1998.

[4] Dueck, G. and J. Jeffs, "A heuristic bandwidth reduction algorithm", Journal of Combinatorial Mathematics and Combinatorial Computing, 1995. 18: p. 97-108.

[5] Duff I. S., A. M. Erisman and J. K. Reid (1986). Direct methods for sparse matrices. Oxford University Press.

[6] A. Esposito, S. Fiorenzo Catalano, F. Malucelli and L. Tarricone, "A new bandwidth matrix reduction algorithm", *Operations Research Letters*, 23/5, pp. 99-107, 1999.

[7] A. Esposito, S. Fiorenzo Catalano, F. Malucelli and L. Tarricone, "Sparse Matrix Bandwidth Reduction: Algorithms, Applications And Real Industrial Cases In Electromagnetics", in "High Performance Algorithms for Structured Matrix problems", series "Advances in Computation: Theory and Practice", Nova Science, New York, 1999

[8] Gibbs, N. E., W. G. Poole and P. K. Stockmeier, An algorithm for reducing the bandwidth and profile of sparse matrix. SIAM Journal of Numerical Analysis, 1976. 13(2): p. 236-250.

[9] G. C. Goswami, A. K. Chan, C. K. Chui, "On Solving First-kind Integral Equations Using Wavelets on a Bounded Interval", IEEE Trans. Ant. Prop., 43, 6, pp. 614-622, June 1995.

[10] Hubing, T. H., M. V. Ali and G. K. Bat, EMAP: A 3D finite element modeling code. Journal of Applied Comp. Electromagnetics Soc., 1993. 8(1).

[11] N. Kynaiman and M. I. Aksun, "Efficient and Accurate EM Simulation Technique for Analysis and Design of MMICs", Int. J. MW and MM Wave Comp. Aided Eng., vol. 37: pp. 344–358, Sept. 1997.

[12] C. Papadimitriou, "The NP-completeness of the bandwidth minimization problem", Computing, 16, pp. 263-270, 1976.

[13] K. Sabet, L. P. B. Katehi, "Analysis of Integrated Millimeter-Wave and Submillimeter-wave Waveguides using Orthonormal Wavelet Expansions", IEEE Trans. Microwave Th. Techn., 42, 12, pp. 2412-2422, Dec. 1994.

[14] K. Sabet, L. P. B. Katehi, "An Integral Formulation of Two- and Three-Dimensional Dielectric Structures Using Orthonormal Multiresolution Expansions", Int. Journal Num. Modelling, 11, pp. 3-19, 1998.

[15] B. Z. Steinberg, Y. Leviathan, "On the use of Wavelet Expansions in the Method of Moments", IEEE Trans. Ant. Prop., 41, 5, pp. 610-619, May 1993.

[16] B. Z. Steinberg, Y. Leviathan, "A multiresolution Study of 2-D Scattering by Metallic Cylinders", IEEE Trans. Ant. Prop., 44, 4, pp. 572-579, Apr. 1996.

[17] L. Tarricone, M. Dionigi, R. Sorrentino, "A strategy for the efficient fullwave description of complex waveguide networks",Int. Journal Microwave and MM-Wave Computer Aided Engineering, 6, 3, 1996, pp. 183–198

[18] G. Wang, "Analysis of EM Scattering from Conducting Bodies of Revolution Using Orthogonal Wavelet Expansions", IEEE Trans. EM Comp., 40, 1, pp. 1-11, Feb. 1998.

[19] G. Wang, "On the Utilization of Periodic Wavelets Expansions in the Moment Methods", IEEE Trans. Microwave Th. Techn., 43, 10, pp. 2495-2497, Oct. 1995.

[20] R. L. Wagner, W. C. Chew, "A Study of Wavelets for the Solution of Electromagnetic Integral Equations", IEEE Trans. Ant. Prop., 43, 8, pp. 802-810, Aug. 1995.

[21] G. Wang, G. Pan, "Full-wave Analysis of microstrip floating line structures by Wavelet Expansion Method", IEEE Trans. Microwave Th. Techn., 43, 10, pp. 131-142, Jan. 1995.

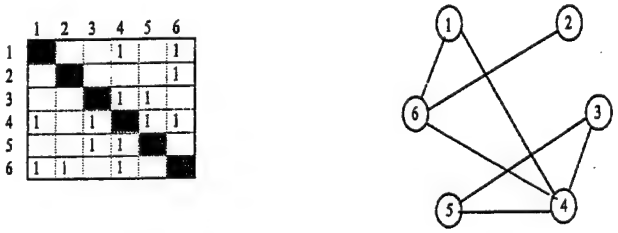

Fig. 1. The input matrix (bandwidth=5) and the relative adiacency graph.

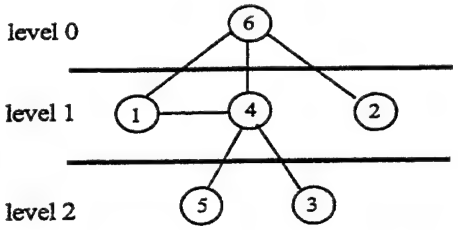

Fig. 2. The adiacency graph partitioned into levels.

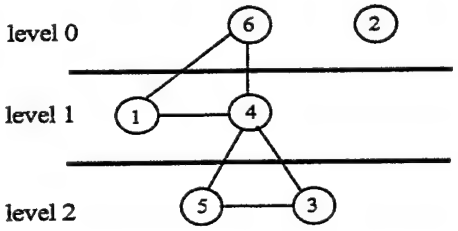

Fig. 3. The level structure after the enhancement phase.

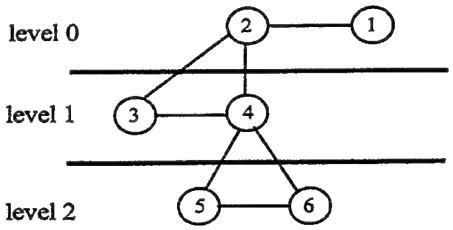

Fig. 4. The level structure after the renumbering phase.

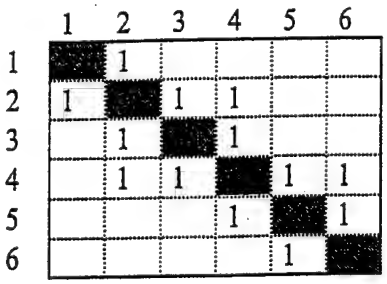

Fig. 5. The renumbered matrix (bandwidth=2).

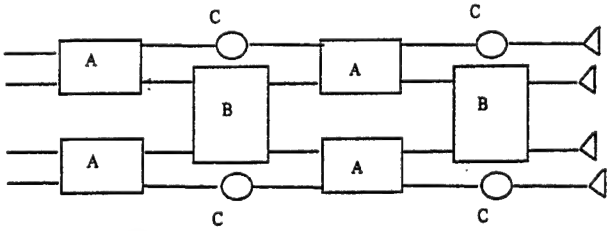

A: 3 dB Coupler

B: 0 dB Coupler

C: Phase shifter

Fig. 6. The 4x4 Butler matrix simulated with the MM approach.

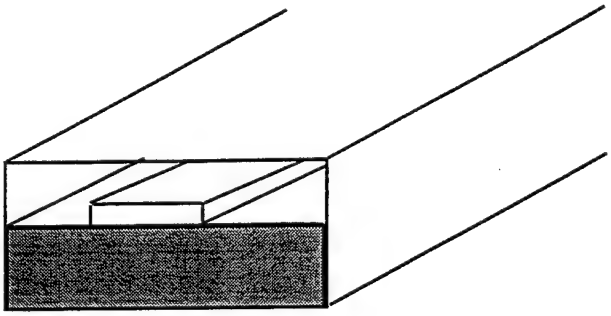

Fig. 7. The boxed microstrip waveguide simulated with the FEM approach.

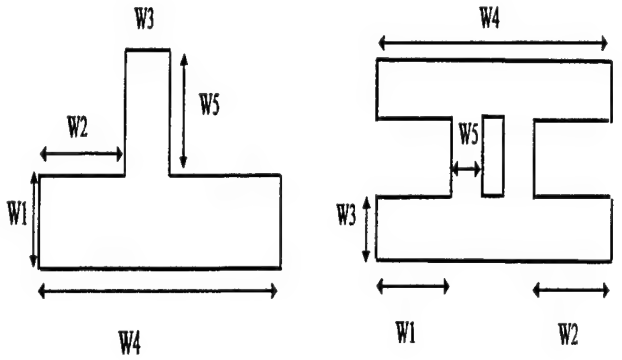

Fig. 8. The circuit simulated, with different values for w1, w2, w3, w4 and w5, with the MoM approach.

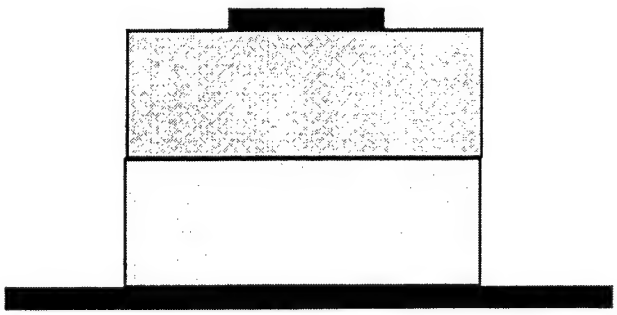

Fig. 9. The circuit simulated, with different wavelet basis functions, with the MoM approach.

PARALLEL IMPLEMENTATION OF GALERKIN TECHNIQUE IN LARGE-SCALE ELECTROMAGNETIC PROBLEMS

Dimitra I. Kaklamani, Konstantina S. Nikita and Andy Marsh
Department of Electrical and Computer Engineering
Institute of Communication and Computer Systems
National Technical University of Athens
9 Iroon Polytechniou, Zografos 15780, Athens, Greece

ABSTRACT. An integral equation formulation in conjunction with a parallelised Galerkin technique is employed to solve large-scale electromagnetic (EM) problems. The proposed technique is applicable to EM structures consisting of similar conducting or dielectric parts, defined as "elements". Coupled integral equations are derived in the frequency domain, written in terms of the conductivity currents or the electric fields developed on the conducting or dielectric "elements" surfaces, respectively. The system of integral equations is numerically solved via the parallel computed Galerkin technique, with convenient entire domain basis functions. Even for electrically large structures, the use of entire domain basis functions leads to relatively small order linear systems and the main computational cost refers to the matrix fill rather than the matrix solution. The parallelisation introduced to the computation of the matrix elements overcomes the limitation of using Method of Moments at lower and resonant frequencies. The inherent parallelism of the introduced technique allows for the results to be obtained with minimal additional to the sequential code programming effort. Two indicative electromagnetic compatibility applications are presented, concerning the coupling of incident waves with multiple conducting rectangular plates and the coupling phenomena occurring in a multi-element waveguide array looking into a layered lossy cylinder. Numerical results are presented, while the applicability/suitability of diverse High Performance Computing platforms is judged, based on both performance obtained and ease of code portation.

Keywords: Method of Moments, Code Parallelisation, Electrically Large Structures.

1. INTRODUCTION

The analysis and design of complex realistic electromagnetic (EM) structures is limited by the relatively restricted computational power of the conventional sequential computers -even those of "main frame" or "vector processing" type- as well as by the vector nature of the EM radiation and the extended power radiation in the environment. The introduction of massively parallel computer architectures has opened new research horizons in this area (Davidson 1990). Indeed, the major advantage of applying High Performance Computing (HPC) to EM problems (Calalo et al. 1989, Davidson 1993, Fijany et al. 1995, Cwik et al. 1997, Lu et al. 1997) is the reduction of execution times of a given size of problem from days/hours to minutes/seconds, enabling the investigation of problems, that were so computationally expense, that they were practically "unsolvable". Pioneering research work in such areas becomes an arduous tedious endeavour. To fully exploit the computing power offered by available parallel platforms, the existing algorithms based on diverse numerical techniques must be re-examined with emphasis on their efficiency for parallel implementation.

Focusing on Method of Moments (MoM) algorithms (Harrington 1983), their use in solving large-scale EM problems is mainly restricted by the extensive computational cost in calculating the kernel elements and solving the resulting matrix equation. Aiming at reducing the storage requirements and speeding-up the solution algorithms on either von Neumann or parallel computers, a variety of basis functions, discretisation schemes and solvers have been employed (Davidson 1993, Aksun and Mittra 1993, Alanen 1991, Coen et al. 1994, Bornholdt and Medgyesi-Mitschang 1988). Subdomain, entire domain and mixed domain or hybrid Galerkin expansions have been used in the literature (Aksun and Mittra 1993, Alanen 1991, Coen et al. 1994, Bornholdt and Medgyesi-Mitschang 1988). Subdomain basis functions have been favored, due to their geometric flexibility and ability to handle localised surface features, apertures or feed-point distributions. Although the arising multiple integrals of the kernel matrix are relatively easily evaluated, the kernel matrix becomes of very large order for problems even slightly outside the resonance region, since at least ten basis functions are approximately required per wavelength. Therefore, when employing subdomain Galerkin technique, the main computational cost refers to the matrix solution and the choice of the proper discretisation scheme and solver is of major importance. Alternatively, smooth entire domain basis functions can be employed and, when successfully selected for a specific geometry, can lead to relatively small matrix dimensions even for electrically large structures. In this case, the main computational cost refers to the matrix fill and the efficient computation of its elements is very crucial.

In this context, a drastic reduction of the computation time is achieved in (Park and Ballanis 1997), by introducing an analytical technique to evaluate the asymptotic part of the kernel elements. Furthermore, taking advantage of the fact that any EM scattering solution can be analysed into high and low frequency components, a multilevel formulation of MoM has been presented in (Kalbasi and Demarest 1993), while in (Kaklamani and Marsh 1995), a parallel computed MoM technique is used to analyse fundamental electrically large planar conducting structures, both allowing substantial computational savings and therefore use of MoM to higher frequencies.

The present work also deals with the parallel implementation of Galerkin technique, providing an effective and accurate near-field solution to a system of frequency domain coupled integral equations modelling a class of canonical large-scale EM problems. Entire domain basis functions are used and emphasis is given on the efficient fill of the derived matrix. To this end, a parallel algorithm is developed, implementing a 12-point Gauss quadrature integration rule to compute the integrals of the kernel matrix, arising from the Galerkin technique procedure. In section 2, the parallelised Galerkin technique is presented and its applicability to different EM engineering areas is demonstrated. Two specific problems are solved, concerning the coupling of incident waves with multiple conducting rectangular plates and the coupling phenomena occurring in a multi-element waveguide array looking into a layered lossy cylinder. The former application also serves as a pilot problem, in order to demonstrate the inherent parallelism of the method that can be exploited. To this end, in section 3, different HPC platforms are utilised and their advantages are determined in terms of both performance obtained and ease of code portation. Finally, section 4 provides some concluding remarks.

2. PARALLEL COMPUTED ENTIRE DOMAIN GALERKIN TECHNIQUE

The technique presented in this section can be used to analyse a class of electrically large canonical structures consisting of similar dielectric or conducting parts, defined as "elements". In order to demonstrate its applicability, two specific electromagnetic compatibility (EMC) problems are treated.

The first problem deals with EM scattering from electrically large planar conductors. This is a subject of much research, since plates can be considered as building structures of more complex configurations (Alanen 1991, Peters and Volakis 1988, Kaklamani and Uzunuglu 1994, Ufimtsev 1996). Furthermore, employing Babinet's principle, the complementary problem of EM penetration through apertures "cut" on infinite planar conducting screens (Butler et al. 1978, Luebbers and Penney 1994) can also be considered, enlightening many EMC problems. The specific examined geometry is given in Fig. 1, where Q-number of perfectly conducting infinitesimal thickness rectangular plates, placed with identical orientation at arbitrary positions on planes parallel to the xy-plane, are presented.

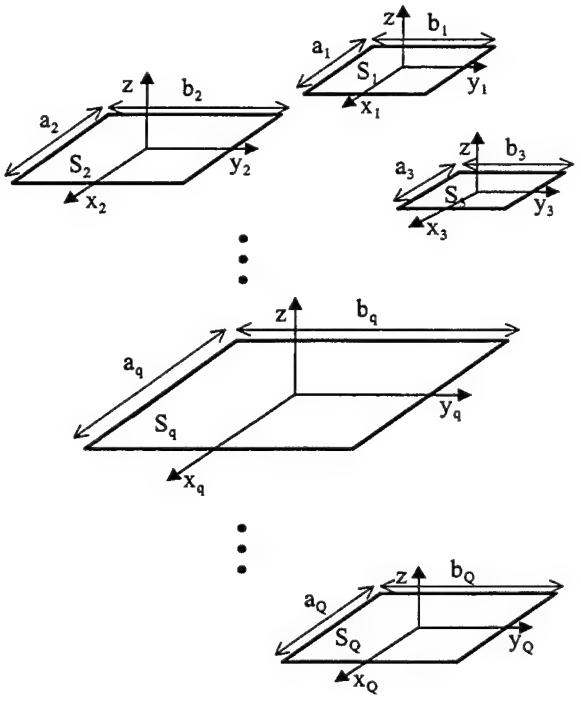

Fig. 1: Q-number of perfectly conducting infinitesimal thickness parallel rectangular plates.

The second problem deals with the analysis of coupling phenomena occurring in a concentric multi-waveguide array used to provide focusing inside a layered biological tissue model. Focusing of EM energy inside biological tissues is an important topic in many biomedical applications (Weiyian and Shoroung 1992, Arcangeli et al. 1984). For this purpose, until now, mainly the low microwave spectrum (100-1000 MHz) has been employed and continuous wave concepts have been applied, with limited success (Chen and Ghandhi 1992, Boag et al. 1993), while recently the use of a concentric multi-element waveguide array and pulsed signals of short pulse width with a high frequency (9.5 GHz) carrier has also been reported (Nikita and Uzunoglu 1996). However, in multi-element arrays significant interaction exists between system elements, resulting in non-predictable behaviour of this type of systems, as shown in (Nikita and Uzunuglu 1996) for concentric waveguide systems operating at low microwave frequencies. In the present paper, the investigation of coupling phenomena occurring in concentric waveguide arrays operating at higher frequencies is enabled by applying the parallelised Galerkin technique. The examined geometry consists of a three-layer cylindrical biological tissue model, irradiated by Q rectangular aperture waveguide applicators (Fig. 2).

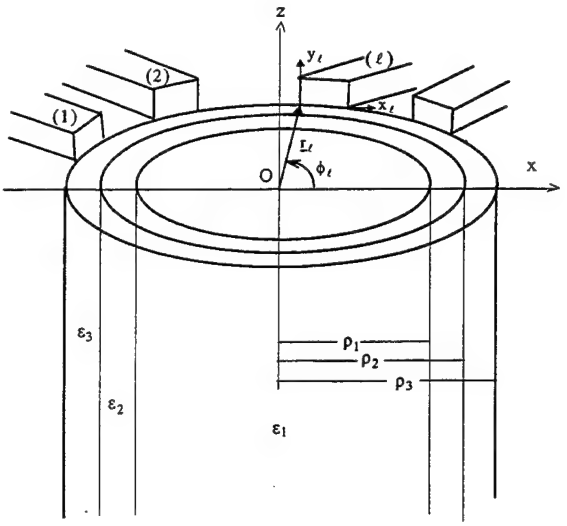

Fig. 2: Multi-waveguide array radiating into a three-layer biological tissue model.

In order to analyse the coupling of time harmonic EM fields with the structures shown in Figs. 1 and 2, a system of coupled integral equations is derived in terms of the unknown distribution on each "element" (conducting plate or waveguide aperture) surface, by using a Green's function approach or a phase space eigenwaves description approach. The operator form of the derived coupled system of integral equations is converted into a matrix equation by a Galerkin technique. Since structures of canonical shape are considered, entire domain basis functions are favored (see detailed formulations and analyses in (Kaklamani and Marsh 1995) and (Nikita and Uzunoglu 1996)). The order of the resulting kernel matrices depends upon the number of dielectric or conducting "elements" and mainly upon the frequency, increasing fast for problems even slightly outside the resonance region, since more basis functions are required to accurately describe the unknown tangential electric or magnetic field distribution on each "element" surface. It is important to emphasise that the "clever" choice of the entire domain basis functions results into relatively small order matrices and the main computational cost refers to the evaluation of the kernel matrix elements rather than the matrix solution. Working in the spectral domain, the arising integrals over the "elements" surfaces are analytically computed, while the infinite phase space integrals, associated to the Green's function Fourier transformation or to the eigenwave field description, are numerically evaluated, using a 12-point Gauss quadrature procedure (Abramowitz and Stegun 1970). The exact expressions of the arising integrals are given in the Appendix for both problems under investigation. Their computation constitutes the most time consuming part of the corresponding developed codes and is easily parallelised, by distributing the integration over 12 processors, without the need of inter-processor communication. If the integration path is divided into M independent Gauss calculations, it can be seen that, with minimal programming effort, the method has an inherent $12\times M$-fold parallelism. It is, therefore, envisaged that the computation times can be further reduced by a factor of M, if $12\times M$ processors are available. These characteristics allow for the algorithms to be ported to both shared and distributed memory machines without extensive programming effort. Nevertheless, since the contribution to the final value of the computed integrals is non-uniform along the integration path, special care has to be taken in distributing the corresponding calculations over the $12\times\ell$ processors, in order to avoid load imbalancing problems. A detailed examination of varying HPC platforms suitability is presented in section 3.

Indicative EM results obtained by applying the proposed parallel computed entire domain Galerkin technique are given in Figs. 3 and 4. The convergence and stability of the obtained solutions have been checked by increasing the number of basis functions used to describe the currents on the plates and the electric fields on the apertures. Considering the fact that the EM field expressions satisfy both the Maxwell's equations and the relevant boundary conditions, it is concluded that the derived results are self-consistent and accurate within the framework of the approximate solution of the system of coupled integral equations.

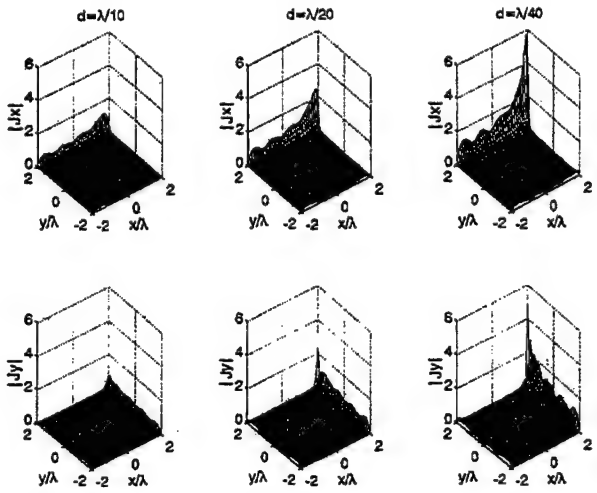

Fig. 3: Conductivity currents distribution induced on a $2\lambda\times2\lambda$ conducting plate lying in the xy-plane and excited by a y-oriented Hertzian dipole placed at a distance d above its right-back corner.

As far as the problem of EM scattering from electrically large conducting plates is concerned (see Fig. 1), the convergence rate of the conductivity currents induced precisely on the plates surfaces is the most important result concerning the accuracy of the proposed method, since it refers to near field quantities. Detailed convergence tests and comparison with published data concerning the single-plate problem are presented in (Kaklamani and Marsh 1995). Focusing on edge behaviour phenomena, in Fig. 3, it is shown how moving a y-oriented Hertzian dipole along the z

axis and towards the back-right corner of a $2\lambda \times 2\lambda$ rectangular plate, affects the conductivity currents distribution induced on the plate surface.

As far as the problem of a layered biological tissue model irradiated by a multi-waveguide array is concerned (see Fig. 2), the strength of coupling phenomena can be analysed, by exciting one element, and computing the TE_{10} mode coefficients coupled to the other elements (mutual coupling coefficients, S^c) and the coefficient of the reflected TE_{10} mode on the same aperture (self reflection coefficient, S^r). The parallelised Galerkin technique has been used to compute the coupling parameters in a 30-element TE_{10} waveguide (2×1 cm^2 aperture size) array placed symmetrically at the periphery of a cylindrical tissue model, 16 cm in diameter. The computations are carried out at the operation range ($1.1\,f_0$ - $1.8\,f_0$, f_0 being the cut-off frequency of the TE_{10} mode) of the system. The tissue model consists of two layers, simulating bone and brain tissues and it is surrounded by a 2 cm thick lossless dielectric layer. The thicknesses of the bone and the external dielectric layers are assumed to be $\rho_2 - \rho_1 = 0.5$ cm and $\rho_3 - \rho_2 = 2$ cm, respectively ($2\rho_3 = 20$ cm) (see Fig. 2). The dielectric constant of the external layer is taken to be $\varepsilon_3 = 2.1$. The numerical values of tissue complex permittivities used in the calculations are defined at the frequency range of interest by using the data compiled from the relevant literature (Gabriel et al. 1996). In Table 1, convergence patterns are presented at 9.5 GHz, in terms of the self reflection coefficient (S^r) and the mutual coupling coefficients with neighbouring (S^c_{ne}) and opposite (S^c_{op}) applicators, by increasing the number

Table 1. *Convergence of the self reflection coefficient S^r and mutual coupling coefficients (S^c_{ne}, S^c_{op}) for the configuration of Fig.2 at 9.5 GHz by increasing the number of aperture modes.*

Modes appearing on the excited aperture	S^r	S^c_{ne}	S^c_{op}
TE_{10}	0.61 ∠-14.35°	0.0091 ∠-44.9°	0.0027 ∠-126.6°
TE_{10} TE_{12} TM_{12}	0.612 ∠-15.2°	0.0123 ∠-41.7°	0.0024 ∠-130.3°
TE_{10} TE_{12} TE_{30} TE_{32} TM_{12} TM_{32}	0.6035 ∠-14.02°	0.011 ∠-42°	0.0025 ∠-128°

of modes appearing on the excited aperture. It can easily be observed that the subset of modes (TE_{10}, TE_{12}, TE_{30}, TE_{32}, TM_{12}, TM_{32}) appearing on applicator apertures is considered to be sufficient to assure convergence and accuracy. Numerical results for the strength of coupling between neighbouring (S^c_{ne}) and opposite (S^c_{op}) applicators in the examined 30-element waveguide array are presented in Fig. 4, at the operation range of the system. It is important to emphasise that in the obtained results, a detailed three-dimensional EM model is employed, which takes into account the modification of the field on each waveguide aperture resulted from the other radiating elements of the array, as well as from the presence of the lossy, layered, dielectric body standing at the near field region.

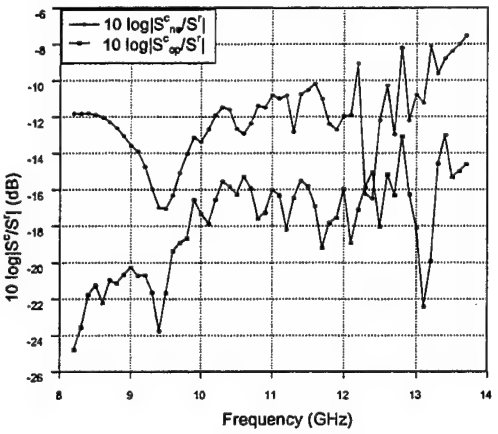

Fig. 4: *The ratio of the mutual coupling coefficient between neighbouring (S^c_{ne}) and opposite (S^c_{op}) applicators to the self reflection coefficient (S^r) in a symmetric configuration of 30 rectangular aperture (2×1 cm^2) waveguide applicators, placed at the periphery of a cylindrical body model of circular cross section, 20 cm in diameter, at the operation range of the system.*

3. IMPLEMENTATION ON VARIOUS HPC PLATFORMS

Due to the nature of the computation of the phase space integrals, which are the elements of the system kernel (see Appendix), the developed algorithm can be adapted for both shared-memory, distributed-memory and additionally vector processing HPC platforms. It has already been shown in (Kaklamani and Marsh 1995) that the code possesses a substantial amount of inherent parallelism, that can be exploited by a shared-memory architecture. Nevertheless, varying HPC platforms can exploit the different degrees of parallelism inherent in the algorithm.

The first application, shown in Fig.1, concerning the EM illumination of Q number of conducting rectangular plates lying on parallel planes, also serves as a pilot problem, in order to answer the emerging question, which HPC platform to use in solving more complex EM problems. For reasons of CPU time savings, the case Q=1 and a_1=b_1 (i.e. one square plate) is chosen for the benchmarking process. Small, intermediate and large size problems (N=8, N=98 and N=512 respectively, with N denoting the order of the derived linear system) are solved on each HPC plat-

form and the corresponding CPU times are compared. There are two crucial points that should be noted here. Firstly, the three orders of systems that have been selected (N=8, N=98, N=512) are only indicative, in order to demonstrate the scalability of the proposed method. That is, by filling and solving the same order system, other geometries (e.g. larger number of plates at a lower frequency) can be solved. Secondly, the characterisation of the three cases as small, intermediate and large size problems is not referred to the absolute value of the system order, but to the electrical size of the problem that can be treated. The system order is in any case small, due to the employment of entire domain basis functions. For example, by the N=512 system, the case of one square plate of 10λ side can be accurately solved.

The HPC platforms currently evaluated are the Silicon Graphics Power Challenge and Intel Paragon, both located at the NTUA, Greece and the CRAY C90 and CRAY T3D, both located at CINECA, Italy. The shared-memory Silicon Graphics Power Challenge has 14 TFP Processors (MIPS R8000 CPU & MIPS R8010 FPU), a 16K data cache, a 16K instruction cache and 8-way interleaved main memory of 1024 Mbytes, providing a peak performance of 4.2 Gflops, while the distributed-memory Intel Paragon XP/S has 48 processing nodes with i860 processors, providing a peak performance of 48 × 75 Mflops = 3.6 Gflops. The shared-memory CRAY vector processing C-90 has 2 × 1 Gflops vector processing CPU's providing a peak performance of 2 Gflops and the massively parallel distributed-memory CRAY T3D has 64 processing nodes providing a peak performance of 64 × 150 Mflops = 9.6 Gflops. Each of the HPC platforms is judged on both performance obtained and ease of code portation, which is directly related to the extent of extra needed code.

Before comparing these four computing platforms, some generalised assumptions need to be mad. Firstly, the platforms are aimed to be used only as computational tools. The main concern is related to the ease of code portation and the ability to solve the largest problem in a given tolerable period of time, without getting involved with the pragmatics and detailed code optimisations. Secondly, if a computational platform with a performance of 1 Gflop takes τ hours to solve a given problem, then the same platform with a 2 Gflops performance would need $\tau/2$ hours to solve the same problem. Thirdly, since the platforms are of different sizes and costs, two performance figures are of interest: the absolute time taken to solve a given problem ("absolute performance") and an estimated relative time taken to solve the same problem ("relative performance"). This relative time is calculated as the time taken if the platform had a 1 Gflop peak performance. These assumptions enable trans-architectural platforms to be composed at an abstract level, without getting involved with complex benchmarks etc., as discussed in detail in the following and summarised in Table 2.

As far as the shared-memory SGI Power Challenge platform is concerned, the 12-point quadrature Gauss algorithm is parallelised, by subdividing the integration path and splitting the corresponding calculations onto 12 processors. This is achieved, by the hand addition of a single line of code, containing the parallel directive C$DOACROSS. For brevity and ease of porting the code, only 12 of the possible 14 TFP processors are used. The peak performance used is therefore 12 × 300 Mflops = 3.6 Gflops. The consumed CPU time is 40 seconds for N=8, 23 minutes for N=98 and approximately 25 hours for N=512, resulting in relative performances of approximately 3.6 × 40 = 144 seconds, 3.6 × 1380 = 4968 seconds and 3.6 × 9000 = 32400 seconds respectively (see Table 2). The large size problem CPU time (25 hours) also includes a large overhead, due to page swapping, incurred by accessing huge data arrays. Fortunately, the porting from standard FORTRAN 77 to the SGI Power FORTRAN has only taken 30 minutes of programming and consultation effort. When employing more rigorous optimisation techniques, such as using the full potential of software pipelining and the SGI PFA (Parallel FORTRAN Accelerator), it is probable that these execution times will be considerably further reduced.

Table 2. *Performance comparison of diverse HPC machines.*

Machine		SGI Power Challenge	Intel Paragon XP/S	CRAY C-90	CRAY T3D
Peak Performance (Gflops)		3.6	2775	2.0	9.0
Absolute Perform. (sec)	N=8	40	47	255	26
	N=98	1380	2940	1960	2040
	N=512	9000	16920	12240	-
Relative Perform. (sec)	N=8	144	130	510	234
	N=98	4968	8158	3920	18360
	N=512	32400	46953	24480	-

Due to the fact that the algorithm can be divided to M independent Gauss calculations, as described in section 2, a greater number of processors can be used. Therefore, the parallelisation of the algorithm or the distributed-memory Intel Paragon XP/S consists in using 37, out of the possible 48, i860 processing nodes; 3 groups of 12 slave processing nodes (i.e. M=3 independent Gauss calculations) and a master controlling processing node, leading to a peak performance of 37 × 75 Mflops = 2.775 Gflops. Communication between processing nodes is accomplished via explicit message-passing. Each group of 12 processing nodes concentrates on the parallelisation of a single 12-point quadrature Gauss algorithm,

analogous to the SGI approach. It was seen, however, that this resulted in load imbalances, because of the fact that all the kernel integrands given by eq. (A.1) vary more rapidly with the increase of k; therefore, when integrating with respect to the φ_k-variable more subdivisions must be considered for large k values, leading to further computational cost with the k increase. After an explicit investigation, the optimum distribution was derived. To this end, the porting from standard FORTRAN 77 to the Paragon platform has taken about 2 hours involving about 15 modifications of the original code. These modifications involve the introduction of the message-passing constructs *irecv* and *isend* and the explicit subdivision of the total computation over the 36 slave processing elements. The consumed CPU time is 47 seconds for N=8, 49 minutes for N=98 and approximately 47 hours for N=512, resulting in relative performances of $2.775 \times 47 \approx 130$ seconds, $2.775 \times 2940 \approx 8158$ seconds and $2.775 \times 16920 = 46953$ seconds respectively (see Table 2). As it is expected, due to the peak performances offered, the Paragon performs slower than the SGI machine. However, what is more disappointing is the relative performances of the Paragon compared to the SGI machine. For example, when N=98, the relative performance of the Paragon machine is 81158 seconds compared with the SGI machine relative performance of 4968 seconds. In this case, for this example, a Paragon machine with 1.6 times the peak performance of the SGI machine would be required to solve the given problem in the same time. Clearly some work has to be done to optimise the data locality, when using the Paragon to solve problems with very large data arrays. It must be noted that, when N=98, the message-passing and system overheads represents about 2% of the total execution time, whereas, when N=512, this value increases to 25%. From these initial investigations, it can be seen that, the algorithm possesses an inherent coarse-grained parallelism that can be exploited by both architectural models.

The suitability of the CRAY C-90 architecture is also investigated, to see if the algorithm possesses a substantial fine-grain parallelism, that could be exploited by a vector processor. Each of the two CPUs of the CRAY C-90 is a vector processor with 128 banks, a clock of 4 ns and a memory speed of 88 ns. The exploitation of vectorisation and parallelisation is achieved by the CRAY cf77 compiler with default settings and with aggressive optimisation switched on. The addition of two vector processing directives (CDIR$ IVDEP) leads to further reduction of the execution times. The porting process required about 1 hour. It consisted mainly in examining the code listing for further vectorisable loops and introducing 2 line modifications. The consumed CPU time is 255 seconds for N=8, 33 minutes for N=98 and approximately 34 hours for N=512, resulting in relative performances of $2.0 \times 255 = 510$ seconds, $2.0 \times 1960 = 3920$ seconds and $2.0 \times 12240 = 24480$ seconds respectively (see Table 2). This indicates that the algorithm contains a significant amount of fine-grain parallelism that can be exploited by the vector processor. The relative performances are impressive, out performing the SGI platform. For example, from the relative performances for N=98, it can be seen that the CRAY C-90 with 2.0×1 Gflop = 2 Gflops peak performance would be equivalent to a SGI with $4968/(3920/2.0) = 2.53$ Gflops peak performance (9×300 Mflops processors). Considering the ease of portability and absolute performance of the CRAY C-90, it remains a realistic alternative shared-memory platform. However, both CRAY C-90 and SGI platforms have the memory access bottleneck, when considering larger problem sizes.

An alternative to the Intel Paragon distributed-memory platform is the CRAY T3D, a superscalar architecture with 64 processing nodes. Each node is based on the DEC α 21064 chip providing a peak performance of 150 Mflops, with a clock of 6.67ns. The limiting factor, however, is the 8 Kbytes data cache and the 8 Kbytes instruction cache. Although possessing facilities for PVM and message-passing, the work sharing on shared data paradigm was used. To this end, porting from standard FORTRAN 77 to the MPP FORTRAN has required about 30 minutes programming effort, involving definition of a global (shared) array to collect the results and explicit subdivision of the computation, similar to the Paragon approach. For brevity, 60 processing nodes are used, providing a peak performance of 60×150 Mflops = 9.0 Gflops, divided in 5 groups of 12 processing nodes. Each group of processing nodes is responsible for a Gauss calculation, similar to that implemented on the Paragon. Due to load balancing, one group of processors performs two Gauss calculations. The resulting performance is only 26 seconds for N=8 and 34 minutes for N=98, while the estimated performance for N=512 is 10 hours (see Table 2). The CRAY T3D could be used for benchmarking purposes only for up to 8 hours. Therefore, there are no available results for the absolute performance in solving the N=512 problem and the estimated performance of 10 hours is considered to be adequate for the current research. It must be noted that, these results are achieved without any optimisation and there exists a load imbalance. Taking these factors into consideration, the performances are impressive.

It can be concluded that, for both ease of portation and resulting performance the shared-memory Silicon Graphics (and to a lesser extent the CRAY C-90) and the distributed-memory CRAY T3D appear to be more suitable in solving problems in the domain of electrically large EM structures. However, the potential of the shared-memory platforms for solving even larger problem sizes is limited by the memory access, whereas the distributed-memory model is modularly extendible and, in the authors' opinion, more suitable in solving even larger problem sizes. It must also be noted that the work sharing paradigm adopted by the

CRAY T3D provides an appealing alternative to message-passing approaches, making programming large distributed-memory machines, to solve large problem sizes, a realistic possibility.

4. CONCLUSIONS

HPC has been employed in order to extent MoM for the treatment of a certain class of large-scale EM problems. Namely, a parallel computed Galerkin technique in conjunction with a frequency-domain coupled integral equation formulation has been adopted, applicable to electrically large structures consisted of similar conducting or dielectric parts.

The resulting algorithm parallelisation overcame the limitation of using MoM at lower and resonant frequencies, while the inherent parallelism of the introduced technique allowed for the results to be obtained with minimal additional to the sequential code programming effort. Namely, the phase space integrals, appearing in the system kernel have been computed numerically employing a 12-point quadrature Gauss algorithm, which has been parallelised, by subdividing the integration path and splitting the corresponding calculations over various HPC platforms. For both ease of portation and resulting performance the shared-memory Silicon Graphics and the distributed-memory CRAY T3D appear to be more suitable, though the potential of the shared-memory platforms for solving even larger problem sizes is limited by the memory access, whereas the distributed-memory model is modularly extendible and, therefore, more suitable in solving even larger problem sizes.

Two specific EMC applications were solved, concerning the coupling of incident waves with multiple conducting rectangular plates and the coupling phenomena occurring in a multi-element waveguide array looking into a layered lossy cylinder, while numerical results were computed for indicative cases. Due to the algorithm parallelisation, the computation times became tolerable, allowing the problems' size, hence the accuracy, to be increased. The convergence rate of near-field quantities excited on electrically large structures is the most important result concerning the accuracy of the proposed method, while following the same approach, more complex configurations can be constructed and analysed.

5. APPENDIX

In solving the Q number of conducting rectangular plates structure shown in Fig. 1, the analytical expressions of the system kernel sub-matrices are defined as

$$\overline{\underline{K}}^{\ell q}_{nmn'm'} = \frac{\omega\mu_0}{8\pi k_0^2}\iint_{\Omega_k} d\tilde{\underline{k}}\left(\frac{e^{-j[q_0\,\mathrm{sgn}(z_\ell^0-z_q^0)(z_\ell^0-z_q^0+\delta_\ell)]}}{q_0}\right.$$
$$\left.\times\frac{e^{-j[q_0\,\mathrm{sgn}(-k_x(x_\ell^0-x_q^0)-k_y(y_\ell^0-y_q^0))}}{q_0}\right.$$
$$\left.\times\overline{\underline{U}}_{\ell_{n'm'}}(-\tilde{\underline{k}})\cdot\overline{\underline{A}}(\tilde{\underline{k}})\cdot\overline{\underline{U}}_{q_{nm}}(\tilde{\underline{k}})\right), \qquad (A.1)$$

where (q=1,2,...,Q ; ℓ=1,2,...,Q),

$$\iint_{\Omega_k} d\tilde{\underline{k}} \equiv \int_{-\infty}^{+\infty} dk_x \int_{-\infty}^{+\infty} dk_y \equiv \int_0^{+\infty} dkk \int_0^{2\pi} d\varphi_k ,$$

$$\tilde{\underline{k}} = k_x\hat{x} + k_y\hat{y} = k(\cos\varphi_k\hat{x} + \sin\varphi_k\hat{y}) , \qquad (A.2)$$

$k_0 = \omega\sqrt{\varepsilon_0\mu_0}$ is the free space propagation constant, ω is the angular frequency, ε_0 and μ_0 are the free space dielectric permittivity and magnetic permeability respectively, $\underline{r}_q^0 = x_q^0\hat{x} + y_q^0\hat{y} + z_q^0\hat{z}$ denotes the position vector of the q-th plate centre of gravity with respect to a global system of coordinates (x,y,z), $\delta_\ell \to 0^+$,

$$q_0 = q_0(\tilde{\underline{k}}) = \sqrt{k_0^2 - k^2}$$
$$\text{with } \mathrm{Re}(q_0)>0 \;\&\; \mathrm{Im}(q_0)<0, \qquad (A.3)$$

as required by the exp($j\omega t$) time dependence and the satisfaction of the radiation condition at infinity,

$$\overline{\underline{A}}(\tilde{\underline{k}}) = \overline{\underline{A}}(k,\varphi_k) = (k_0^2 - k_x^2)\hat{x}\hat{x} - k_x k_y(\hat{x}\hat{y} + \hat{y}\hat{x}) + (k_0^2 - k_y^2)\hat{y}\hat{y} , \qquad (A.4)$$

and

$$\overline{\underline{U}}_{q_{nm}}(\tilde{\underline{k}}) = \frac{(n+1)J_{n+1}(-\frac{k_x a_q}{2})J_m(-\frac{k_y b_q}{2})}{2j^{(n+m)}k_x/(b_q\pi^2)}\hat{x}\hat{x} + \frac{(m+1)J_{m+1}(-\frac{k_y b_q}{2})J_n(-\frac{k_x a_q}{2})}{2j^{(n+m)}k_y/(a_q\pi^2)}\hat{y}\hat{y} , \qquad (A.5)$$

with $J_\nu(x)$ denoting the Bessel function of the first kind of ν-th order and S_q=a_q×b_q, (q=1,2,...,Q) denoting the finite zero-thickness q-th conducting plate surface. The kernel elements encountered in the problem of Fig. 2 are of the following type:

$$K_{pn}^{\ell q} = \iint_{S_\ell} dxdy \iint_{S_q} dx'dy' \underline{h}_{p,t}(x,y)\cdot\overline{\underline{K}}_{\ell q}(x,y/x',y')\cdot\underline{e}_{n,t}(x',y')$$

where S_ℓ is the aperture of the $\ell-$th waveguide, $\underline{e}_{n,t}$ and $\underline{h}_{n,t}$ are the transverse electric and magnetic

fields of the waveguide normal modes, respectively, being of TE or TM type and

$$\underline{\overline{K}}_{\ell q}(x,y/x',y') = \int_{-\infty}^{+\infty} dk \sum_{m=-\infty}^{+\infty} \left(e^{jm(\phi_\ell - \phi_q)} e^{jm\left(-\frac{x}{\rho_3}+\frac{x'}{\rho_3}\right)}\right) \times e^{jk(y-y')} \underline{\overline{N}}(m,k) - \delta_{\ell q}\,\underline{\overline{\Omega}}(x,y/x',y')\Big), \qquad (A.6)$$

In eq. (A.6), $(\ell = 1,2,...,Q; q = 1,2,...,Q)$, $\delta_{\ell q}$ is the Kronecker's delta,

$$\underline{\overline{N}}(m,k) = \frac{1}{(2\pi)^2} \frac{jk_3}{\omega\mu_0\mu_3\rho_3} \underline{\overline{L}}'(m,k;\rho_3)\left(\underline{\overline{L}}(m,k;\rho_3)\right)^{-1}$$

$$\underline{\overline{\Omega}}(x,y/x',y') = \sum_{n=1}^{\infty} \left\{ \left(-\frac{\gamma_n}{\omega\mu_0}\right) \underline{h}_{n,t}^{TE}\, \underline{e}_{n,t}^{TE} + \left(\frac{\omega\varepsilon_0}{\lambda_n}\right) \underline{h}_{n,t}^{TM}\, \underline{e}_{n,t}^{TM} \right\}, \qquad (A.7)$$

with γ_n, λ_n being the propagation constants of the TE and TM modal fields, respectively and $k_3 = k_0\sqrt{\varepsilon_3}$. The matrices involved in (A.7) are given by the following equations:

$$\underline{\overline{L}}'(m,k;\rho_3) = \underline{\overline{T}}_{3m}^{(1)}(k;\rho_3) + \frac{Z_m^{(2)}(\alpha_3\rho_3)}{Z_m^{(1)}(\alpha_3\rho_3)} \underline{\overline{T}}_{3m}^{(2)}(k;\rho_3)\underline{\overline{R}}_{3m},$$

$$\underline{\overline{L}}(m,k;\rho) = \underline{\overline{D}}_{3m}^{(1)} + \frac{Z_m^{(2)}(\alpha_3\rho)}{Z_m^{(1)}(\alpha_3\rho)} \underline{\overline{D}}_{3m}^{(2)} \underline{\overline{R}}_{3m}$$

where

$$\underline{\overline{D}}_{im}^{(q)}(k;\rho) = \begin{pmatrix} -\dfrac{\partial Z_m^{(q)}(\alpha_i\rho)/\partial\rho}{Z_m^{(q)}(\alpha_i\rho)} & -\dfrac{mk}{k_i\rho} \\ 0 & \dfrac{\alpha_i^2}{k_i} \end{pmatrix},$$

$$i = 3/q = 1,2 \qquad (A.8)$$

$$\underline{\overline{T}}_{im}^{(q)}(k;\rho) = \begin{pmatrix} -\dfrac{mk}{k_i\rho} & -\dfrac{\partial Z_m^{(q)}(\alpha_i\rho)/\partial\rho}{Z_m^{(q)}(\alpha_i\rho)} \\ \dfrac{\alpha_i^2}{k_i} & 0 \end{pmatrix},$$

$$i = 3/q = 1,2 \qquad (A.9)$$

with $Z_m^{(1)}(\alpha_i\rho) = J_m(\alpha_i\rho)$ and $Z_m^{(2)}(\alpha_i\rho) = Y_m(\alpha_i\rho)$, $k_i = k_0\sqrt{\varepsilon_i}$, $\alpha_i = \left(k_i^2 - k^2\right)^{1/2}$,

$$\underline{\overline{R}}_{3m} = \frac{Z_m^{(1)}(\alpha_3\rho)}{Z_m^{(2)}(\alpha_3\rho)} \left(\underline{\overline{T}}_{3m}^{(2)} - \frac{k_2}{k_3} \underline{\overline{G}}_{2m}\, \underline{\overline{F}}_{2m}\, \underline{\overline{D}}_{3m}^{(2)} \right)^{-1} \times \left(-\underline{\overline{T}}_{3m}^{(1)} + \frac{k_2}{k_3} \underline{\overline{G}}_{2m}\, \underline{\overline{F}}_{2m}\, \underline{\overline{D}}_{3m}^{(1)} \right) \text{ at } \rho = \rho_2 \qquad (A.10)$$

The matrices involved in (A.10) are

$$\underline{\overline{G}}_{2m}(k;\rho) = \underline{\overline{T}}_{2m}^{(1)} + \frac{Z_m^{(2)}(\alpha_2\rho)}{Z_m^{(1)}(\alpha_2\rho)} \underline{\overline{T}}_{2m}^{(2)} \underline{\overline{R}}_{2m},$$

$$\underline{\overline{F}}_{2m}(k;\rho) = \left[\underline{\overline{D}}_{2m}^{(1)} + \frac{Z_m^{(2)}(\alpha_2\rho)}{Z_m^{(1)}(\alpha_2\rho)} \underline{\overline{D}}_{2m}^{(2)} \underline{\overline{R}}_{2m} \right]^{-1},$$

$$\underline{\overline{R}}_{2m} = \frac{Z_m^{(1)}(\alpha_2\rho)}{Z_m^{(2)}(\alpha_2\rho)} \left(\underline{\overline{T}}_{2m}^{(2)} - \frac{k_1}{k_2} \underline{\overline{T}}_{1m}^{(1)} (\underline{\overline{D}}_{1m}^{(1)})^{-1} \underline{\overline{D}}_{2m}^{(2)} \right)^{-1} \times \left(\frac{k_1}{k_2} \underline{\overline{T}}_{1m}^{(1)} (\underline{\overline{D}}_{1m}^{(1)})^{-1} \underline{\overline{D}}_{2m}^{(1)} - \underline{\overline{T}}_{2m}^{(1)} \right) \text{ at } \rho = \rho_1 \qquad (A.11)$$

The matrices $\underline{\overline{D}}_{im}^{(q)}$, $\underline{\overline{T}}_{im}^{(q)}$, $i = 1,2$ and $q = 1,2$, appearing in (A.11), are obtained from eq. (A.8) and eq. (A.9), respectively, for i=1,2.

6. REFERENCES

Abramowitz M. and I.A. Stegun, ***Handbook of Mathematical Functions***, Dover Publications, Inc., New York, 875-924, (1970).

Aksun M.I. and R. Mittra, "Choices of Expansion and Testing Functions for the Method of Moments Applied to a Class of Electromagnetic Problems", ***IEEE Trans. Microwave Theory Tech.***, MTT-41, 503-509, (1993).

Alanen E., "Pyramidal and Entire Domain Basis Functions in the Method of Moments", ***J. Electro. Waves Applic.***, 5, 315-329, (1991).

Arcangeli G., P.P. Lombardini, G.A. Lovisolo, G. Marsiglia and M. Piatelli, "Focusing of 915 MHz Electromagnetic Power on Deep Human Tissues", ***IEEE Trans. Biomed. Eng.***, BME-31, 47-52, (1984).

Boag A., Y. Leviatan and A. Boag, "Analysis and Optimization of Waveguide Multiapplicator Hyperthermia Systems", ***IEEE Trans. Biomed. Eng.***, BME-40, 946-952, (1993).

Bornholdt J.M. and L.M. Medgyesi-Mitschang, "Mixed-Domain Galerkin Expansions in Scattering Problems", ***IEEE Trans. Antennas Propag.***, AP-36, 216-227, (1988).

Butler C.M., Y. Rahmat-Samii and R. Mittra, "Electromagnetic Penetration through Apertures in Conducting Surfaces", ***IEEE Trans. Antennas Propag.***, AP-26, 82-93, (1978).

Calalo R.H., T.A. Cwik, W.A. Imbriale, N. Jacobi, P.C. Liewer, T.G. Lockhart, G.A. Lyzenga and J.E. Patterson, "Hypercube Parallel Architecture Applied to Scattering Electromagnetic Problems", ***IEEE Trans. Magnetics***, 24, 4, 2888-2890, (1989).

Chen J. and O.P. Ghandhi, "Numerical Simulation of Annular Phased Arrays of Dipoles for Hyperthermia of Deep Seated Tumors", ***IEEE Trans. Biomed. Eng.***, BME-39, 209-216, (1992).

Coen G., N. Fache and D. De Zutter, "Comparison Between Two Sets of Basis Functions for the Current Modeling in the Galerkin Spectral Domain Solution for Microstrips", ***IEEE Trans. Microwave Theory Tech.***, MTT-42, 505-513, (1994).

Cwik T., D.S. Katz and J. Patterson, "Scalable Solutions to Integral Equation and Finite Element Simulations", ***IEEE Trans. Antennas Propag.***, AP-45, 544-555, (1997).

Davidson D.B., "Parallel Matrix Solvers for Moment Method Codes for MIMD Computers", ***ACES Journal***, 8, 2, 144-175, (1993).

Davidson, D.B., "A Parallel Processing Tutorial", ***IEEE Antennas and Propagation Mag.***, 32, 2, 6-19, (Apr. 1990).

Fijany A., M.A. Jensen, Y. Rahmat-Samii and J. Barhen, "A Massively Parallel Computation Strategy for FDTD: Time and Space Parallelism Applied to Electromagnetics Problems", ***IEEE Trans. Antennas Propag.***, AP-43, 1441-1449, (1995).

Gabriel C., S. Gabriel and E. Corthout, "The Dielectric Properties of Biological Tissues", ***Med. Phys.***, 41, 2231-2293, (1996).

Harrington R.F., ***Field Computation by Moment Methods***, New York: Macmillan, Florida: Krieger Publishing, (1983).

Kaklamani D.I. and A. Marsh, "Solution of Electrically Large Planar Scattering Problems Using Parallel Computed Method of Moments Technique", ***J. Electro. Waves Applic.***, 9, 10, 1313-1337, (1995).

Kaklamani D.I. and N.K. Uzunoglu, "Scattering from a Conductive Rectangular Plate Covered by a Thick Dielectric Layer and Excited from a Dipole or a Plane Wave", ***IEEE Trans. Antennas Propag.***, AP-42, 1065-1076, (1994).

Kalbasi K. and K.R. Demarest, "A Multilevel Formulation of the Method of Moments", ***IEEE Trans. Antennas Propag.***, AP-41, 589-599, (1993).

Lu Y., and C.Y. Shen, "A Domain Decomposition Finite Difference Method for Parallel Numerical Implementation of Time-Dependent Maxwell's Equations", ***IEEE Trans. Antennas Propag.***, AP-45, 556-562, (1997).

Luebbers R. and C. Penney, "Scattering from Apertures in Infinite Ground Planes Using FDTD", ***IEEE Trans. Antennas Propag.***, AP-42, 731-736, (1994).

Nikita K.S. and N.K. Uzunoglu, "Analysis of Focusing of Pulse Modulated Microwave Signals Inside a Tissue Medium", ***IEEE Trans. Microwave Theory Tech.***, MTT-44, 1788-1798, (1996).

Nikita K.S. and N.K. Uzunoglu, "Coupling Phenomena in Concentric Multi-Applicator Phased Array Hyperthermia Systems", ***IEEE Trans. Microwave Theory Tech.***, MTT-44, 65-74, (1996).

Park S.-O. and C.A. Balanis, "Analytical Technique to Evaluate the Asymptotic Part of the Impedance Matrix of Sommerfeld-Type Integrals", ***IEEE Trans. Antennas Propag.***, AP-45, 798-805, (1997).

Peters T.J. and J.L. Volakis, "Application of the Conjugate Gradient FFT Method to Scattering from Thin Planar Material Plates", ***IEEE Trans. Antennas Propag.***, AP-36, 518-526, (1988).

Ufimtsev P.Y., "Comments on Diffraction Principles and Limitations of RCS Reduction Techniques", ***Proc. IEEE***, 84, 1830-1851, (1996).

Weiyian W. and Z. Shoroung, "Unrelated Illumination Method for Electromagnetic Inverse Scattering of Inhomogeneous Lossy Dielectric Bodies", ***IEEE Trans. Antennas Propag.***, AP-40, 1292-1296, (1992).

CALL FOR PAPERS

THE APPLIED COMPUTATIONAL ELECTROMAGNETICS SOCIETY

ANNOUNCES A SPECIAL ISSUE OF THE ACES JOURNAL ON

EVOLUTIONARY METHODS IN COMPUTATIONAL ELECTROMAGNETICS

The Applied Computational Electromagnetics Society is pleased to announce the publication of a 2000 Special Issue of the ACES Journal on applications and advances in evolutionary computing methods applied to computational electromagnetics. The objectives of this special issue are to present applications and advances in evolutionary methods applied to antennas, scattering, EMC, microwave filters, and other relevant electromagnetic problems. Prospective authors are encouraged to submit papers of archival value that address these objectives and other suggested topics listed below.

SUGGESTED TOPICS

- genetic algorithms
- genetic programming
- evolutionary algorithms
- electromagnetic applications of computational evolutionary methods
- advances in GA operators and algorithms
- advances in EA and genetic programming

DEADLINE FOR PAPERS IS DECEMBER 20, 1999

Potential contributors wishing to discuss the suitability of their contribution to the special issue may contact one of the following two Guest Editors by email or phone:

Prof. Randy L. Haupt haupt@ieee.org **Tel: (435) 797-2841**
Prof. J. Michael Johnson jmjohnson@ieee.org **Tel: (775) 784-6485**

All submissions for this special issue should be addressed to:

Special Issue on Evolutionary Methods
Prof. Randy Haupt
Utah State University
Dept. of Electrical and Computer Engineering
4120 Old Main Hill
Logan, UT 84322-4120

CALL FOR PAPERS

THE APPLIED COMPUTATIONAL ELECTROMAGNETICS SOCIETY

ANNOUNCES A SPECIAL ISSUE OF THE ACES JOURNAL ON

COMPUTATIONAL ELECTROMAGNETIC TECHNIQUES IN MOBILE WIRELESS COMMUNICATIONS

The Applied Computational Electromagnetics Society is pleased to announce the publication of a Special Issue of the ACES Journal on the role that computational electromagnetics plays in the design and analysis of wireless communications components, subsystems, and systems. The complexity of present wireless mobile architectures and the future complexities of wideband wireless mobile systems has sparked an interest in computational electromagnetics (CEM) as one of the many tools needed for the design of third generation mobile wireless communications systems. The purpose of this special issue is to draw analysts, designers, and management from both industry and academia to outline their ideas and research on the role of CEM in present or future wireless designs. Applications oriented papers are highly encouraged.

SUGGESTED TOPICS

Applications of computational electromagnetic techniques on any of the following:

- Smart and adaptive antennas
- PCS, Mobile, Gateways, Satellite antennas
- Propagation Models
- Atmospheric Models
- Systems design
- Correlation of measurement techniques and models
- Electromagnetic Interference
- Bioelectromagnetics
- LEO, MEO, Satellites Communications
- Digital/Analog components design
- RF components design

DEADLINE FOR PAPERS IS MARCH 28, 2000

Expected Publication Date is Fall 2000 Issue of ACES Journal

Please submit 4 copies of papers to either of the Guest Editors listed below. The review process will commence as papers are received. Notification of accepted papers will be made immediately as papers are reviewed.

Ray Perez
c/o:Lockheed Martin Astronautics
MS: S8800 P.O Box 179
Denver, Colorado 80201, USA
phone: 303-977-5845
fax: 303-971-4306
email:ray.j.perez@lmco.com

Chris Holloway
NTIA/ITS.T
325 Broadway
Boulder, Colorado 80303, USA
phone: 303-497-6184
fax: 303-497-3680
email:cholloway@its.bldrdoc.gov

CALL FOR PAPERS

THE APPLIED COMPUTATIONAL ELECTROMAGNETICS SOCIETY

ANNOUNCES A SPECIAL ISSUE OF THE ACES JOURNAL ON

COMPUTATIONAL BIOELECTROMAGNETICS

The Applied Computational Electromagnetics Society is pleased to announce the publication of a Special Issue of the ACES Journal on applications and advances in methods and applications in computational bioelectromagnetics. The objectives of this special issue are to present advances in computational techniques, reviews and/or comparisons of methods, and applications of computational bioelectromagnetics. Prospective authors are encouraged to submit papers of archival value that address these objectives and other suggested topics listed below.

SUGGESTED TOPICS

- Applications of computational bioelectromagnetics
  - Cellular telephone analysis, design, etc.
  - Medical imaging
  - EM Safety analysis
  - Etc.
- Methods used for computational bioelectromagnetics
  - Finite-difference time-domain
  - Finite element method
  - Other methods
- Models for computational bioelectromagnetics
  - High resolution human body models
  - Electrical properties of human tissue
- Comparisons of methods, models, or techniques

DEADLINE FOR PAPERS IS AUGUST 25, 2000

Potential contributors wishing to discuss the suitability of their contribution to the special issue may contact one of the following three Guest Editors by email or phone:

Cynthia Furse	**furse@ece.usu.edu**	**Tel: (435) 797-2870**
Susan Hagness	**hagness@engr.wisc.edu**	**Tel: (608) 265-5739**
Ulrich Jakobus	**jakobus@ihf.uni-stuttgart.de**	**Tel: +49 (0)711 685-7420**

All submissions for this special issue should be addressed to:

Cynthia Furse -- Special Issue on Bioelectromagnetics
Dept. of Electrical and Computer Engineering
Utah State University
Logan, UT 84322-4120

CALL FOR PAPERS

MTT IMS' 00

SESSIONS ON HF/VHF/UHF TECHNOLOGY

Boston, Massachusetts – June 2000

The IEEE Microwave Theory and Techniques (MTT) Society has formed a new technical committee (MTT-17) for HF, VHF, and UHF Technology. Its purpose is to help MTT address the needs of the 26,000 RF engineers who work at frequencies below 1 GHz.

We have sponsored special sessions at IMS'97, and '98 and a regular session at IMS'99. We are looking forward to continuing these sessions on HF/VHF/UHF technology at IMS'00 in Boston (June 11-16, 2000). Papers can address any area of technology that is of particular interest to RF engineers, including:

- Receiver and associated DSP
- Transmitters and power amplifiers
- Applications such as plasma/laser drivers and MRI
- Filters and matching networks
- Components (transistors, diodes, mixers, etc.)

DEADLINE FOR PAPERS IS NOVEMBER 29, 1999 FOR PAPER FORM .
DEADLINE FOR PAPERS IS DECEMBER 6, 1999 FOR ELECTRONIC FORM

Proposals including a 30-50 word abstract and a 500-1000 word summary must be submitted by DECEMBER 6, 1999 in electronic form or by NOVEMBER 29, 1999 in paper form. For full information, see:http://www.mtt.org/ims2000. When submitting, please note that HF/VHF/UHF Technology is TOPIC CATEGORY 8 on the author's information form. To ensure that your submission is not accidentally routed to another committee, it is recommended that you send a copy of your proposal to F.H. Raab at the address shown below.

Please distribute this notice to your colleagues.

Questions about the HF/VHF/UHF committee or sessions should be directed to:
Dr. Frederick H. Raab
Green Mountain Radio Research
50 Vermont Avenue
Colchester, VT, 05446, USA
Fax: (802) 655-9670
E-mail: f.raab@ieee.org

EUROEM 2000, EDINBURGH, SCOTLAND

CALL FOR PAPERS

The Organising Committee has great pleasure in inviting you to submit papers for the EUROEM 2000 conference being held in Edinburgh, Scotland from 30 May - 2 June 2000.

EUROEM 2000 continues the tradition of the EUROEM/AMEREM Conference Series, drawing together the 12th High Power Electromagnetics Conference, the 5th Ultra-Wideband Short Pulse Electromagnetics Conference and the 5th Unexploded Ordnance Detection and Range Remediation Conference.

Papers are solicited which describe original work suitable for the three conferences comprising EUROEM 2000. The **deadline** for receipt of abstracts is **Friday, 14 January 2000.**

Authors are requested to submit a one page abstract, original plus 3 copies in **camera-ready format** by the deadline date to: EUROEM 2000, Concorde Services Ltd, Suite 325, Pentagon Business Centre, Washington Street, Glasgow G3 8AZ, Scotland, UK. You should specify at the time of submission whether your paper is for HPEM, UWB-SP or UXO and specify a topic (see the full list on the website).

The abstract must consist of at least 250 words and must be limited to one page, including figures. Since there will be a reduction of about 70% of the original linear dimensions, letters and symbols in all diagrams should be sufficiently large and clear. Do not include list of references; a few open-literature references may be included parenthetically, for example (R L Lewis & J R Johler, Radio Sci 2, 75-81, 1976). Acknowledgement of financial support is not deemed appropriate. **Please note that it is the authors' responsibility and not that of the Conference Committee, to see that their abstract and paper are cleared for public release.**

All abstracts must be written in English. The text should be typed single space on A4 (8.27" x 11.69" or 210 x 297 mm) white paper. Margins should be 1.5" on left and right and sides and 1" top and bottom of page. The title should be centred in capital letters 1 inch from the top of the page. Author's name and complete organisational affiliation should be two lines below the title. For multiple authors, the **expected presenter** should be indicated by an **asterisk**. The text should start three lines below the last name. Double space between paragraphs.

Alternatively, you may submit your abstract via the web. **NB: Web submissions should be plain text only, no graphics allowed. If using graphics please submit camera-ready copy by post.**

A camera-ready paper will be requested prior to the conference, for accepted UWB-SP presentations. Instructions will be sent to the relevant authors.

For additional information please contact the Conference Secretariat, Concorde Services at (Tel) +44 (0)141 221 5411 or (Fax) +44 (0)141 221 2411 or visit our web site at: http://www.mcs.dundee.ac.uk:8080/~euroem

CALL FOR PAPERS

THE APPLIED COMPUTATIONAL ELECTROMAGNETICS SOCIETY

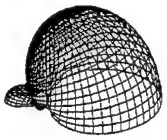

The 16th Annual Review of Progress in Applied Computational Electromagnetics
March 20 - 25, 2000
Naval Postgraduate School, Monterey, California
Share Your Knowledge and Expertise with Your Colleagues

The Annual ACES Symposium is a large gathering of engineers and scientists sharing information and experiences about the practical application of computational electromagnetics (CEM). The symposium offerings include technical presentations, demonstrations, vendor booths, short courses, and hands-on workshops. All aspects of CEM are represented. This Symposium is a highly influential outlet for promoting awareness of recent technical contributions to the advancement of CEM. Attendance and professional program paper participation from non-ACES members and from outside North America are encouraged and welcome. Papers may address general issues in applied computational electromagnetics, or may focus on specific applications, techniques, codes, or computational issues of potential interest to the ACES membership.

Areas and topics:

Code performance analysis	Computational studies of physics	Code validation
Computer hardware issues	Practical code application	New, fixed, and enhanced codes

Applications and Techniques:

Antennas	Bioelectromagnetics	Scattering
Visualization	Wave propagation	Radar cross section
Integral & Differential Equations	Finite Difference & Finite Element	Frequency-domain & Time-domain
Diffraction	Modal Expansion	Physical Optics

INSTRUCTIONS FOR AUTHORS AND TIMETABLE

Submission Deadline - November 1, 1999: Electronic submission preferred (Microsoft Word). Otherwise submit three copies of a full-length, camera-ready paper to the Technical Program Chairman. Specific format required; please request instructions via e-mail or see on-line instructions. **Authors notified of acceptance by December 1, 1999.**

For all questions regarding the ACES Symposium please contact **Douglas H. Werner**, Technical Program Chair
The Pennsylvania State University, 211A Electrical Engineering East, University Park, PA 16802
Tel: (814) 863-2946, Fax: (814) 865-7065, E-mail: **aces@engr.psu.edu**
or visit ACES on line at: **http://aces.ee.olemiss.edu**

EARLY REGISTRATION FEES

ACES MEMBERS $300	STUDENT/RETIRED/UNEMPLOYED	$130 (no proceedings)
NON-MEMBER $350	STUDENT/RETIRED/UNEMPLOYED	$165(includes proceedings)

$500 BEST-PAPER PRIZE

A $500 prize will be awarded to the authors of the best non-student paper accepted for the 16th Annual Review.

$200 BEST STUDENT PAPER CONTEST

This will be for the best student paper accepted for the 16th Annual Review. The prize will include: 1) free Annual Review registration for the following year; 2) one free short course; and 3) $200 cash for the paper.

2000 ACES Symposium Sponsored by: ACES, NPS, PSU, UNR, U OF NV, MSU, UWI, SWRI
In cooperation with: IEEE Antennas and Propagation Society, IEEE Electromagnetic Compatibility Society and USNC/URSI

Technical Program Chair	Symposium Co-Chair	Symposium Co-Chair	Vendor Chair	Symposium Administrator	Short Course Chair	Publicity Chair
Douglas H. Werner Penn State University	Randy Haupt Utah State University	Ping juan L. Werner Penn State DuBois Campus	Leo C. Kempel Michigan State University	Richard W. Adler Naval Postgraduate School	Susan C. Hagness University of Wisconsin	Keith A. Lysiak Southwest Research Institute

CALL FOR PAPERS

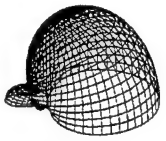

THE APPLIED COMPUTATIONAL ELECTROMAGNETICS SOCIETY

The 16th Annual Review of Progress in Applied Computational Electromagnetics
March 20 - 25, 2000
Naval Postgraduate School, Monterey, California
Share Your Knowledge and Expertise with Your Colleagues

The Annual ACES Symposium is an ideal opportunity to participate in a large gathering of EM analysis enthusiasts. The purpose of the Symposium is to bring analysts together to share information and experience about the practical application of EM analysis using computational methods. The symposium offerings include technical presentations, demonstrations, vendor booths, short courses, and hands-on workshops. All aspects of electromagnetic computational analysis are represented.

The ACES Symposium is a highly influential outlet for promoting awareness of recent technical contributions to the advancement of computational electromagnetics. Attendance and professional program paper participation from non-ACES members and from outside North America are encouraged and welcome.

Papers may address general issues in applied computational electromagnetics, or may focus on specific applications, techniques, codes, or computational issues of potential interest to the Applied Computational Electromagnetics Society membership.

Areas and topics

Computational studies of basic physics
Examples of practical code application
New codes, algorithms, code enhancements, and code fixes
Computer hardware issues
Code validation
Code performance analysis

Partial list of applications

Communications systems	Microwave components	Wireless	Radar Imaging
Remote sensing & geophysics	EMP EMI/EMC	Shielding Fiberoptics	Radar cross section
Dielectric & magnetic materials	MIMIC technology	Visualization	Fiberoptics
Non-destructive evaluation	Wave propagation	Eddy currents	Direction finding
Propagation through plasmas	Bioelectromagnetics	Inverse scattering	Antennas

Partial list of techniques

Diffraction theories	Moment methods	Physical optics
Frequency-domain & Time-domain techniques	Hybrid methods	Modal expansions
Finite difference & finite element analysis	Numerical optimization	
Integral equation & differential equation techniques	Perturbation methods	

INSTRUCTIONS FOR AUTHORS AND TIMETABLE

Submission Deadline - November 1, 1999: Electronic submission preferred (Microsoft Word). Otherwise submit three copies of a full-length, camera-ready paper to the Technical Program Chairman. Please supply the following data for the corresponding authors: name, address, email address, FAX, and phone numbers. **Authors notified of acceptance by December 1, 1999.**

PAPER FORMATTING REQUIREMENTS

The recommended paper length is 6 pages, with 8 pages as a maximum, including figures. The paper should be camera-ready (good resolution, clearly readable when reduced to the final print of 6x9 inch paper). The paper should be printed on 8-1/2x11 inch papers with 13/16 side margins, 1-1/16 inch top margin, and 1 inch on the bottom. On the first page, place title 1-1/2 inches from top with authors, affiliations, and e-mail addresses beneath the title. Single spaced type using 10 or 12 point font size, entire text should be justified (flush left and flush right). No typed page numbers, but number your pages lightly in pencil on the back of each page.

For all questions regarding the ACES Symposium please contact:
Douglas H. Werner, Technical Program Chair
The Pennsylvania State University, 211A Electrical Engineering East, University Park, PA 16802
Tel: (814) 863-2946, Fax: (814) 865-7065, E-mail: **aces@engr.psu.edu**
or visit ACES on line at: **http://aces.ee.olemiss.edu** and **www.emclab.umr.edu/aces.**

EARLY REGISTRATION FEES

ACES member	$300	Student/Retired/Unemployed	$130 (no proceedings)
Non-member	$350	Student/Retired/Unemployed	$165 (includes proceedings)

Each conference registration is entitled to publish two papers in the proceedings free of charge. Excess pages over a paper limit of 8 will be charged $15/page.

$500 BEST-PAPER PRIZE

A $500 prize will be awarded to the authors of the best non-student paper accepted for the 16th Annual Review. Papers will be judged by a special ACES prize-paper Committee according to the following criteria:

1. Based on established electromagnetic (EM) theory
2. Reliable data
3. Computational EM results
4. Practical applications
5. Estimates of computational errors
6. Significant new conclusions

$200 BEST STUDENT PAPER CONTEST

This will be for the best student paper accepted for the 16th Annual Review. (Student must be the presenter on the paper chosen). Submissions will be judged by three (3) members of the BoD. The prizes for the student presenter and his/her principal advisor will consist of: (1) free Annual Review registration for the following year; (2) one free short course taken during the 2000 or 2001 Annual Review; and (3) $200 cash for the paper.

2000 ACES Symposium Sponsored by: ACES, NPS, PSU, UNR, UTAH STATE U, MSU, UWI, SWRI
In cooperation with: The IEEE Antennas and Propagation Society,
The IEEE Electromagnetic Compatibility Society and USNC/URSI

Technical Program Chair	Symposium Co-Chair	Symposium Co-Chair	Vendor Chair	Symposium Administrator	Short Course Chair	Publicity Chair
Douglas H. Werner Penn State University	Randy Haupt Utah State University	Ping juan L. Werner Penn State DuBois Campus	Leo C. Kempel Michigan State University	Richard W. Adler Naval Postgraduate School	Susan C. Hagness University of Wisconsin	Keith A. Lysiak Southwest Research Institute

FINAL CALL FOR PAPERS

INTERNATIONAL SEMINAR

DAY on DIFFRACTION
St.Petersburg, Russia

MILLENNIUM WORKSHOP
May 29 - June 1, 2000

ORGANIZED BY
Faculty of Physics of St. Petersburg University
St. Petersburg Branch of Steklov Mathematical Institute
Euler International Mathematical Institute, St.Petersburg

JOINTLY WITH
University of Florence
University of Michigan

TECHNICALLY CO-SPONSORED BY
IEEE Antennas and Propagation Society

CO-SPONSORED BY
Russian Foundation for Basis Researches

STEERING COMMITTEE
V.M. Babich, **Steklov Math. Inst., St. Petersburg**
V.S. Buldyrev, **St. Petersburg Univ., St. Petersburg**
G. Pelosi, **Univ. of Florence, Florence, Italy**
J.L. Volakis, Univ. of Michigan, Ann Arbor, USA

LOCAL ORGANIZING COMMITTEE
I.V. Andronov (publications)
V.E. Grikurov (secretary)
A.P. Kiselev, M.A. Lyalinov
E.V. Novikova (visa support)

SESSIONS TO BE ORGANIZED

MATHEMATICAL ASPECTS OF WAVE PROPAGATION	M. Babich (Russia), S.Yu. Dobrokhotov (Russia)
NEW DIRECTIONS IN ASYMPTOTIC TECHNIQUES	G. Manara (Italy), V.S. Buldyrev (Russia)
CANONICAL DIFFRACTION PROBLEMS	V. P. Smyshlyaev (U.K.), G. Pelosi (Italy)
DIFFRACTION ON NON-SMOOTH OBSTACLES	Giraud (France), A.H. Serbest (Turkey), J.M. Bernard (France)
EM ANALYSIS TECHNIQUES	R. Tibrio (Italy)
UNDERWATER ACOUSTICS	G. Makrakis(Greece), N.S. Grigor'eva (Russia)
FLUID DYNAMICS	N.G. Kuznetsov (Russia), J. Ockendon (U.K.)
WAVES IN ELASTIC MEDIA	A.P. Kiselev (Russia)
PLATES, SHELLS AND VIBRATION	P.E. Tovstik (Russia)
NONLINEAR PHENOMENA	A. Samsonov (Russia)
NON-STATIONARY PHENOMENA	V.V. Borisov (Russia)

Proposals for session's organizing concerning various nature wave phenomena are encouraged!

Working language is English

The registration fee is 150 USD

IMPORTANT DEADLINES

Proposals for session organizing	ASAP
Papers submissions	Feb. 1, 2000
Acceptance of papers	March 1, 2000
Registration	April 1, 2000

Early registration is necessary to finalize visa formalities in time.
Registration fee is encouraged but not requested at this stage.

WAYS OF SUBMISSION

1. **Electronic submission (mostly preferred!)**

I.V. Andronov iva@aa2628.spb.edu
V.E. Grikurov grikurov@mph.phys.spbu.ru
A.P. Kiselev kiselev@pdmi.ras.ru

2. **FAX: +7-812-428-7240**
3. **Hard copies to be addressed:**

Dept. Math.& Comp.Phys.
Inst. On Physics, St.Petersburg Univ.
Ul'yanovskaya 1 198904 Petrodvoretz
Russia

We expect to receive camera-ready abstract limited, if possible, by one A4 page of 10pt font size *TeX* and *Word* documents are accepted

PUBLICATIONS

Booklet of abstracts of all papers accepted for presentation will be available at the Seminar.

Full manuscripts will be invited for the peer selection to be included into either the *Proceedings* or the special issue of *IEEE Antennas and Propagation Transactions.*

PREREGISTRATION

Pre-registration is necessary to be included into mailing list. Please fill this form (all fields are mandatory) and return it to one of addresses given above as soon as possible. Updated information and on-line pre-registration available via URL http://mph.phys.spbu.ru/DDMW

Name: _____

Affiliation: _____

Contact Address: _____

City: _____ Zip/Postal Code: _____ Country: _____

E-mail: _____ Fax: _____

I Intend to submit a paper to the Session _____

I Intend to propose a Session _____

5TH INTERNATIONAL WORKSHOP ON

FINITE ELEMENTS FOR MICROWAVE ENGINEERING

FINAL CALL FOR PAPERS

GRAND CHALLENGES FOR NEW MILLENNIUM

John Hancock Conference Center, Boston, Massachusetts, USA
June 8-9, 2000

The 5th Finite Elements Workshop for Microwave Engineering will be organized by Electrical and Computer Engineering Department, Worcester Polytechnic Institute in cooperation with University of Florence, Italy and will be held on June 8-9, 2000 at John Hancock Conference Center, Boston, Massachusetts, U.S.A.

The workshop provides an international forum for reporting and discussing recent progresses and advances in the finite element technologies for microwave engineering. The details of the workshop can be found in http://ece.wpi.edu~jinlee.

February 1, 2000: One-page Abstract due
March 1, 2000: Acceptance Notification will be mailed to the corresponding author of the paper.
April 15, 2000: Pre-Register

Authors are invited to submit an original (camera-ready) one-page abstract of no less than 250 words. The abstract should explain clearly the content and relevance of the proposed contribution. No acknowledgments should be included. Your cover letter should include the complete mailing address, telephone, fax number, and e-mail address (if available) for the corresponding author. Please mail abstracts-do not send via facsimile. Fulll paper is due at the conference and will be under regular peer review process. Accepted papers will be published in a special issue of Electromagnetics, 2001.

Each presenting author is required to register, via a non-refundable **pre-registration fee of US$100** and must be sent by April 15, 2000. The registration fee, **to be determined,** will include the Workshop program and proceedings, attendance at all technical sessions, refreshments, the opening reception, and the banquet.

Local arrangements should be directed to:
Ms. Yurong Sun
5th Finite Element Wkshop for Microwave Engineering
EM/CAD Lab, ECE Department, WPI
100 Institute Road
Worcester, MA 01609, USA
Tel: 508-831-5757 Fax: 508-831-5491
Email: ysun@ece.wpi.edu

Abstracts should be directed to:
Prof. Jin-Fa Lee
5th Finite Element Wkshop for Microwave Engineering
EMCAD Lab, ECE Dept, WPI.
100 Institute Road
Worcester, MA 01609, USA
Tel: 508-831-5778, Fax: 508-831-5491
Email: jinlee@ece.wpi.edu

ABSTRACT GUIDELINES

Submit in English. Use single-spaced, 8.5x11 inch paper; using 12 point Times Roman or and equivalent serif typeface. Set margins to 25mm (1 inch) and set paragraph indentation to 3.5mm (0.14 inch). Type title in bold letters; centered at the top. Below title, center name of the author(s) with affiliation and complete mailing address.

ADVANCE PROGRAM, AND INFORMATION SENT BY MAY 1, 2000

Registration: Travel, lodging, registration and local information will be mailed with Advance Program by May 1, 2000. The advance registration fee for all participants, including session chairpersons and authors, is US$100. The fee includes the Workshop program and proceedings, attendance at all technical sessions, refreshments, the opening reception and the banquet.

LOCATION

The Workshop is planned to be held at the John Hancock Conference Center, Boston, MA, USA, on Thursday and Friday, June 8-9, 2000. Boston is the favorite conference venue in the Northeast US and one of the most popular conference cities in the US. The city is beautiful and alive. The charm and attractions of historic Boston should create an enjoyable environment for the workshop.

ORGANIZATION

Chairs

Z.J. Cendes, Ansoft Corp., Pittsburgh, PA, U.S.A
G. Pelosi, University of Florence, Italy

Secretary

J.F. Lee, WPI, Worcester, MA, U.S.A
R. Lee, Ohio State University, Columbus, OH, U.S.A

Scientific Committee

P. Guillon, University of Limoges, France
A. Konrad, University of Toronto, Ontario, Canada
M. Koshiba, Hokkaido University, Sapporo, Japan
R. Coccioli, University of California at Los Angeles, CA, U.S.A
J.L. Volakis, University of Michigan, Ann Arbor, MI, U.S.A
J.P. Berenger, CAD-ETCA, Arcueil, France
A. Cangellaris, University of Illinois, Urbana-Champaign, IL, U.S.A
T.A. Cwik, J.P.L, Pasadena, CA, U.S.A
D.B. Davidson, University of Stellenbosch, South Africa
R.L. Ferrari, Trinity College, Cambridge, UK
R. Mittra, Penn State University, PA, U.S.A
A. Papiernik, University of Nice-Sophia Autipolis, France
M. Salazar-Palma, Polytechnic of Madrid, Spain
D.K. Sun, Ansoft, Pittsburgh, PA, U.S.A
S. Selleri, University of Florence, Italy
R. Dyczij-Edlinger, Ansoft, Pittsburgh, PA, U.S.A
J. Jin, University of Illinois, Urbana-Champaign, IL, U.S.A
E. Lucas, Northrop Grumman Corp., Baltimore, MD, U.S.A

1999 INSTITUTIONAL MEMBERS

ALLGON
Nasvagen 17, PO Box 500
Akersberga, S-18425 SWEDEN

ANDREW CORPORATION
10500 W. 153rd Street
Orland Park, IL 60462

ANSOFT EUROPE
70 London Road
Twickenham, TW1 3QS UK

BIBLIOTECA, FUNDACAO CPqD
Rod. Campinas M
Campinas, SP, BRAZIL 13083-970

BOEING NORTH AMERICAN SVCS
1745 Jefferson Davis Hwy
Arlington, VA 22202

BPLUS
100 University Ct. PO Box 1428
Blackwood, NJ 08012

BRITISH AEROSPACE
FPC 267 PO Box 5
Filton, BRISTOL, BS12 7QW UK

BRITISH AEROSPACE LAND & SEA
Newport Road
COWES, Isle of Wight, PO31 8PF UK

BRITISH BROADCASTING CO R&D
Kingswood Warren
Tadworth, SURREY, KT20 6NP UK

CENTER HP COMPUTING
PO Box 830657
Birmingham, AL 35283-0657

CHALMERS U OF TECHNOLOG
Microwave Technology
Gothenberg, S412 96 SWEDEN

CRS4 BIBLIOTECA
Z I Macchiareddu Area Casic
UTA (CA) 09010, ITALY

CST GMBH
Lauteschlagerstrasse 38
Darmstadt, D-64289 GERMANY

CULHAM LAB/AEA TECHNOLOGY
UK Atomic Energy Authority
Abingdon, OX14 3DB OXFORD, UK

FELDBERG LIB, DARTMOUTH
COLLEGE , 6193 Murdough Ctr.
Hanover, NH 03755-3560

DEFENCE TECH & PROCUREMNT
Nemp Lab, AC-Zentrum
Spiez, CH 3700, SWITZERLAND

DEFENSE RESEARCH ESTAB. LIB.
3701 Carling Avenue
Ottowa, ON, K1A 0Z4 CANADA

DEUTSCHE TELEKOM AG
PO Box 10-00-03
Darmstadt, D-64 276 GERMANY

EASTWOOD BOOKS, INC.
3250 Wilshire Blvd.
Los Angeles, CA 90010

ERA TECHNOLOGY LTD.
Cleve Road, Leatherhead
SURREY KT22 7SA UK

ERICSSON SAAB AVIONICS AB
Electromagnetic Technology
Linkoeping, SE 58188 SWEDEN

ETSE TELECOMUNICACIONES
Campus Lagoas Marcosende
Vigo, 36200 SPAIN

FACOLTA INGEGNERIA LIBRARY
Via G Duranti 89
Perugia, 06125 ITALY

FANFIELD LTD.
Braxted Park
Witham, ESSEX, CM8 3XB UK

FGAN/FHP/AUS
Neuenahrer Strasse 20
Wachtberg, Werth, 53343 GERMANY

FIRSTMARK TECHNOLOGIES
85 St. Charles Quest St.
Longueuil, PQ, J4H 1C5 CANADA

GEC MARCONI RES. CTR. LIB.
W. Hanningfield Road, Gt. Baddow
Chelmsford, ESSEX, CM2 8HN UK

GEORGIA TECH LIBRARY
225 North Avenue, NW
Atlanta, GA 30332-0001

HKUST, UNIVERSITY LIBRARY
Clear Water Bay Road
Kowloon, HONG KONG

HUGHES RESEARCH LIBRARY
3011 Malibu Canyon Road
Malibu, CA 90265-4737

HUNTING ENGINEERING LTD.
Reddings Wood, Ampthill
Bedford, MK45 2HD UK

IABG MBH, TRM
Einsteinstrasse 20
Ottobrunn, D 85521 GERMANY

IIT RESEARCH INSTITUTE
185 Admiral Cochrane Drive
Annapolis, MD 21401-7396

IMAGINEERING LTD.
95 Barber Greene Road, Suite 112
Toronto, ON, M3C 3E9 CANADA

INFORMATION CENTRE
A4 Bldg. Ively Road
Farnsborough, , GU14 0LK UK

IPS RADIO & SPACE SVC/LIBRARY
PO Box 5606
W. Chatswood, 2057 AUSTRALIA

KARGER PUBLISHERS, INC.
PO Box 888
Unionville, CT 06085-0888

KATHREIN-WERKE KG
Postbox 100 444
Rosenheim, D-83004 GERMANY

LINDA HALL LIBRARY
5109 Cherry Street
Kansas City, MO 64110-2498

McNEAL SWENDLER CO., LTD.
MSC House, Lyon Way
Camberley, Surrey, GU16 5ER UK

MISSISSIPPI STATE UNIV LIBRARY
PO Box 9570
Mississippi State, MS 39762

MIT LINCOLN LAB LIBRARY
244 Wood Street
Lexington, MA 02173-0073

MITRE CORPORATION LIBRARY
202 Burlington Road
Bedford, MA 01730-1407

MOD(PE) DGSS
Abbey Wood #54, PO Box 702
Bristol, BS12 7DU UK

MOTOROLA
2001 N. Division Street
Harvard, IL 60033

MYERS ENGINEERING INTL.
PO Box 15908, 5425 NW 24th St.
Margate, FL 33063

NATIONAL AEROSPACE LAB, NLR
Anthony Fokkerwek 2
Emmeloord, 8300 NETHERLANDS

NATL RADIOLOGICAL PROT. BD.
Chilton
Didcot, OXON, OX11 0RG UK

NAVAL RESEARCH LABORATORY
C. Office
Washington, DC 20375

NGIC
220 7th Street, NE
Charlottesville, VA 22902-5396

NIKSAR
35/45 Gilbey Road
Mt. Waverley, VIC, 3149 AUSTRALIA

NNR AIR CARGO SERVICE
Hook Creed Blvd. & 145th Avenue
Valley Stream, NY 11581

NORTEL TECHNOLOGY
London Road
Harlow, ESSEX, CM17 9NA UK

PENN STATE UNIVERSITY LIB.
Pattee Library
University Park, PA 16802

PHILIPS RESEARCH LAB LIBRARY
Cross Oak Lane, Salfords
Redhill, SURREY, RH1 5HA UK

QUEEN MARY & WESTFIELD COLL
Mile End Road
London E1 4NS UK

QUEENSLAND CTR FOR ADV.
TECH / LIBRARY
PO Box 883
Kenmore, QLD, 4069 AUSTRALIA

RADIO FREQUENCY SYSTEMS
36 Garden Street
Kilsyth, VIC, 3137 AUSTRALIA

RAND AFRIKAANS UNIVERSITY
PO Box 524, Aucklandpark
Johannesburg, 2006 S AFRICA

RAYTHEON E-SYSTEMS
PO Box 6056
Greenville, TX 75403

READMORE ACADEMIC SERVICES
901 Route 168, Suites 204-208
Turnersville, NJ 08012

RENTON TECH LIB/BOEING
PO Box 3707
Seattle, WA 98124-1563

ROCKWELL COLLINS
350 Collins Road
Cedar Rapids, IA 52498

SALISBURY DSTO
PO Box 830701
Birmingham, AL 35283-0701

SONY CORPORATION
174 Fujitsukacho, Hodogaya Ku
Yokohama MZ, 240 JAPAN

SOUTHWEST RESEARCH INST.
6220 Culebra Road
San Antonio, TX 78238

SPIKE TECHNOLOGY
1 Chestnut Street
Nashua, NH 03060

SWETS SUBSCRIPTION SERVICE
440 Creamery Way, Suite A
Exton, PA 19341

TASC - LIBRARY
55 Walkers Brook Drive
Reading, MA 01867-3297

TECHNISCHE UNIV. DELFT
Mekelweg 4, Delft
HOLLAND, 2628 CD
NETHERLANDS

TELEBRAS - CPQD, LIB.
Rod. Campinas
Campinas, SP 13088-061 BRAZIL

TELSTRA RESEARCH LABS
770 Blackburn Road
Clayton, VIC, 3168 AUSTRALIA

UNIVERSITY OF WARWICK
Gibbet Hill Road
Coventry, CV4 7AL UK

UNIV OF CENTRAL FLORIDA LIB.
PO Box 162440
Orlando, FL 32816-2440

UNIV OF COLORADO LIBRARY
Campus Box 184
Boulder, CO 80309-0184

UNIV OF MISSOURI-ROLLA LIB.
1870 Miner Circle
Rolla, MO 65409-0001

UNIVERSITY OF SAO PAULO
Av Prof Luciano
Sao Paulo, BRAZIL 05508-900

US ARMY COLD REGIONS LIB
72 Lyme Road
Hanover, NH 03755-1290

US COAST GUARD ACADEMY
15 Mohegan Avenue
New London, CT 06320-4195

VECTOR FIELDS LTD.
24 Bankside Kidlington
Oxford, OX5 1JE UK

VIT, TECHNICAL RESEARCH. CTR.
PO Box 1202
Espoo, FIN-02044 FINLAND

ACES COPYRIGHT FORM

This form is intended for original, previously unpublished manuscripts submitted to ACES periodicals and conference publications. The signed form, appropriately completed, MUST ACCOMPANY any paper in order to be published by ACES. PLEASE READ REVERSE SIDE OF THIS FORM FOR FURTHER DETAILS.

TITLE OF PAPER:

AUTHORS(S)

PUBLICATION TITLE/DATE:

RETURN FORM TO:
Dr. Richard W. Adler
Naval Postgraduate School
Code EC/AB
833 Dyer Road, Room 437
Monterey, CA 93943-5121 USA

PART A - COPYRIGHT TRANSFER FORM

(NOTE: Company or other forms may not be substituted for this form. U.S. Government employees whose work is not subject to copyright may so certify by signing Part B below. Authors whose work is subject to Crown Copyright may sign Part C overleaf).

The undersigned, desiring to publish the above paper in a publication of ACES, hereby transfer their copyrights in the above paper to The Applied Computational Electromagnetics Society (ACES). The undersigned hereby represents and warrants that the paper is original and that he/she is the author of the paper or otherwise has the power and authority to make and execute this assignment.

Returned Rights: In return for these rights, ACES hereby grants to the above authors, and the employers for whom the work was performed, royalty-free permission to:

1. Retain all proprietary rights other than copyright, such as patent rights.
2. Reuse all or portions of the above paper in other works.
3. Reproduce, or have reproduced, the above paper for the author's personal use or for internal company use provided that (a) the source and ACES copyright are indicated, (b) the copies are not used in a way that implies ACES endorsement of a product or service of an employer, and (c) the copies per se are not offered for sale.
4. Make limited distribution of all or portions of the above paper prior to publication.
5. In the case of work performed under U.S. Government contract, ACES grants the U.S. Government royalty-free permission to reproduce all or portions of the above paper, and to authorize others to do so, for U.S. Government purposes only.

ACES Obligations: In exercising its rights under copyright, ACES will make all reasonable efforts to act in the interests of the authors and employers as well as in its own interest. In particular, ACES REQUIRES that:

1. The consent of the first-named author be sought as a condition in granting re-publication permission to others.
2. The consent of the undersigned employer be obtained as a condition in granting permission to others to reuse all or portions of the paper for promotion or marketing purposes.

In the event the above paper is not accepted and published by ACES or is withdrawn by the author(s) before acceptance by ACES, this agreement becomes null and void.

AUTHORIZED SIGNATURE — TITLE (IF NOT AUTHOR)

EMPLOYER FOR WHOM WORK WAS PERFORMED — DATE FORM SIGNED

PART B - U.S. GOVERNMENT EMPLOYEE CERTIFICATION

(NOTE: If your work was performed under Government contract but you are not a Government employee, sign transfer form above and see item 5 under Returned Rights).

This certifies that all authors of the above paper are employees of the U.S. Government and performed this work as part of their employment and that the paper is therefore not subject to U.S. copyright protection.

AUTHORIZED SIGNATURE — TITLE (IF NOT AUTHOR)

NAME OF GOVERNMENT ORGANIZATION — DATE FORM SIGNED

PART C - CROWN COPYRIGHT

(Note: ACES recognizes and will honor Crown Copyright as it does U.S. Copyright. It is understood that, in asserting Crown Copyright, ACES in no way diminishes its rights as publisher. Sign only if *ALL* authors are subject to Crown Copyright.

This certifies that all authors of the above Paper are subject to Crown Copyright. (Appropriate documentation and instructions regarding form of Crown Copyright notice may be attached).

AUTHORIZED SIGNATURE TITLE OF SIGNEE

NAME OF GOVERNMENT BRANCH DATE FORM SIGNED

Information to Authors

ACES POLICY

ACES distributes its technical publications throughout the world, and it may be necessary to translate and abstract its publications, and articles contained therein, for inclusion in various compendiums and similar publications, etc. When an article is submitted for publication by ACES, acceptance of the article implies that ACES has the rights to do all of the things it normally does with such an article.

In connection with its publishing activities, it is the policy of ACES to own the copyrights in its technical publications, and to the contributions contained therein, in order to protect the interests of ACES, its authors and their employers, and at the same time to facilitate the appropriate re-use of this material by others.

The new United States copyright law requires that the transfer of copyrights in each contribution from the author to ACES be confirmed in writing. It is therefore necessary that you execute either Part A-Copyright Transfer Form or Part B-U.S. Government Employee Certification or Part C-Crown Copyright on this sheet and return it to the Managing Editor (or person who supplied this sheet) as promptly as possible.

CLEARANCE OF PAPERS

ACES must of necessity assume that materials presented at its meetings or submitted to its publications is properly available for general dissemination to the audiences these activities are organized to serve. It is the responsibility of the authors, not ACES, to determine whether disclosure of their material requires the prior consent of other parties and if so, to obtain it. Furthermore, ACES must assume that, if an author uses within his/her article previously published and/or copyrighted material that permission has been obtained for such use and that any required credit lines, copyright notices, etc. are duly noted.

AUTHOR/COMPANY RIGHTS

If you are employed and you prepared your paper as a part of your job, the rights to your paper initially rest with your employer. In that case, when you sign the copyright form, we assume you are authorized to do so by your employer and that your employer has consented to all of the terms and conditions of this form. If not, it should be signed by someone so authorized.

NOTE RE RETURNED RIGHTS: Just as ACES now requires a signed copyright transfer form in order to do "business as usual", it is the intent of this form to return rights to the author and employer so that they too may do "business as usual". If further clarification is required, please contact: The Managing Editor, R.W. Adler, Naval Postgraduate School, Code EC/AB, Monterey, CA, 93943, USA (408)656-2352.

Please note that, although authors are permitted to re-use all or portions of their ACES copyrighted material in other works, this does not include granting third party requests for reprinting, republishing, or other types of re-use.

JOINT AUTHORSHIP

For jointly authored papers, only one signature is required, but we assume all authors have been advised and have consented to the terms of this form.

U.S. GOVERNMENT EMPLOYEES

Authors who are U.S. Government employees are not required to sign the Copyright Transfer Form (Part A), but any co-authors outside the Government are.

Part B of the form is to be used instead of Part A only if all authors are U.S. Government employees and prepared the paper as part of their job.

NOTE RE GOVERNMENT CONTRACT WORK: Authors whose work was performed under a U.S Government contract but who are not Government employees are required to sign Part A-Copyright Transfer Form. However, item 5 of the form returns reproduction rights to the U.S. Government when required, even though ACES copyright policy is in effect with respect to the reuse of material by the general public.

November 1999

APPLIED COMPUTATIONAL ELECTROMAGNETICS SOCIETY JOURNAL

INFORMATION FOR AUTHORS

PUBLICATION CRITERIA

Each paper is required to manifest some relation to applied computational electromagnetics. **Papers may address general issues in applied computational electromagnetics, or they may focus on specific applications, techniques, codes, or computational issues.** While the following list is not exhaustive, each paper will generally relate to at least one of these areas:

1. Code validation. This is done using internal checks or experimental, analytical or other computational data. Measured data of potential utility to code validation efforts will also be considered for publication.

2. Code performance analysis. This usually involves identification of numerical accuracy or other limitations, solution convergence, numerical and physical modeling error, and parameter tradeoffs. However, it is also permissible to address issues such as ease-of-use, set-up time, run time, special outputs, or other special features.

3. Computational studies of basic physics. This involves using a code, algorithm, or computational technique to simulate reality in such a way that better or new physical insight or understanding is achieved.

4. New computational techniques, or new applications for existing computational techniques or codes.

5. "Tricks of the trade" in selecting and applying codes and techniques.

6. New codes, algorithms, code enhancement, and code fixes. This category is self-explanatory but includes significant changes to existing codes, such as applicability extensions, algorithm optimization, problem correction, limitation removal, or other performance improvement. **Note: Code (or algorithm) capability descriptions are not acceptable, unless they contain sufficient technical material to justify consideration**.

7. Code input/output issues. This normally involves innovations in input (such as input geometry standardization, automatic mesh generation, or computer-aided design) or in output (whether it be tabular, graphical, statistical, Fourier-transformed, or otherwise signal-processed). Material dealing with input/output database management, output interpretation, or other input/output issues will also be considered for publication.

8. Computer hardware issues. This is the category for analysis of hardware capabilities and limitations in meeting various types of electromagnetics computational requirements. Vector and parallel computational techniques and implementation are of particular interest.

Applications of interest include, but are not limited to, antennas (and their electromagnetic environments), networks, static fields, radar cross section, shielding, radiation hazards, biological effects, electromagnetic pulse (EMP), electromagnetic interference (EMI), electromagnetic compatibility (EMC), power transmission, charge transport, dielectric and magnetic materials, microwave components, MMIC technology, remote sensing and geophysics, communications systems, fiber optics, plasmas, particle accelerators, generators and motors, electromagnetic wave propagation, non-destructive evaluation, eddy currents, and inverse scattering.

Techniques of interest include frequency-domain and time-domain techniques, integral equation and differential equation techniques, diffraction theories, physical optics, moment methods, finite differences and finite element techniques, modal expansions, perturbation methods, and hybrid methods. This list is not exhaustive.

A unique feature of the Journal is the publication of unsuccessful efforts in applied computational electromagnetics. Publication of such material provides a means to discuss problem areas in electromagnetic modeling. Material representing an unsuccessful application or negative results in computational electromagnetics will be considered for publication only if a reasonable expectation of success (and a reasonable effort) are reflected. Moreover, such material must represent a problem area of potential interest to the ACES membership.

Where possible and appropriate, authors are required to provide statements of quantitative accuracy for measured and/or computed data. This issue is discussed in "Accuracy & Publication: Requiring quantitative accuracy statements to accompany data", by E.K. Miller, *ACES Newsletter*, Vol. 9, No. 3, pp. 23-29, 1994, ISBN 1056-9170.

EDITORIAL REVIEW

In order to ensure an appropriate level of quality control, papers are refereed. They are reviewed both for technical correctness and for adherence to the listed guidelines regarding information content. Authors should submit the initial manuscript in draft form so that any suggested changes can be made before the photo-ready copy is prepared for publication.

JOURNAL COPY INFORMATION

March issue	Copy deadline 13 January
July issue	Copy deadline 25 May
November issue	Copy deadline 25 September

STYLE FOR CAMERA-READY COPY

The ACES Journal is flexible, within reason, in regard to style. However, certain requirements are in effect:

1. The paper title should NOT be placed on a separate page. The title, author(s), abstract, and (space permitting) beginning of the paper itself should all be on the first page. The title, author(s), and author affiliations should be centered (center-justified) on the first page.

2. An abstract is REQUIRED. The abstract should state the computer codes, computational techniques, and applications discussed in the paper (as applicable) and should otherwise be usable by technical abstracting and indexing services.

3. Either British English or American English spellings may be used, provided that each word is spelled consistently throughout the paper.

4. Any commonly-accepted format for referencing is permitted, provided that internal consistency of format is maintained. As a guideline for authors who have no other preference, we recommend that references be given by author(s) name and year in the body of the paper (with alphabetical listing of all references at the end of the paper). Titles of Journals, monographs, and similar publications should be in boldface or italic font or should be underlined. Titles of papers or articles should be in quotation marks.

5. Internal consistency shall also be maintained for other elements of style, such as equation numbering. As a guideline for authors who have no other preference, we suggest that equation numbers be placed in parentheses at the right column margin.

6. The intent and meaning of all text must be clear. For authors who are NOT masters of the English language, the ACES Editorial Staff will provide assistance with grammar (subject to clarity of intent and meaning).

7. Unused space should be minimized. Sections and subsections should not normally begin on a new page.

MATERIAL, SUBMITTAL FORMAT AND PROCEDURE

The preferred format for submission and subsequent review, is 12 point font or 12 cpi, double line spacing and single column per page. Four copies of all submissions should be sent to the Editor-in-Chief (see inside front cover). Each submission must be accompanied by a covering letter. The letter should include the name, address, and telephone and/or fax number and/or e-mail address of at least one of the authors.

Only camera-ready original copies are accepted for publication. The term **"camera-ready" means that the material is neat, legible, and reproducible**. The preferred font style is Times Roman 10 point (or equivalent) such as that used in this text. A double column format similar to that used here is preferred. **No author's work will be turned down once it has been accepted because of an inability to meet the requirements concerning fonts and format.** Full details are sent to the author(s) with the letter of acceptance.

There is NO requirement for India ink or for special paper; any plain white paper may be used. However, faded lines on figures and white streaks along fold lines should be avoided. Original figures - even paste-ups - are preferred over "nth-generation" photocopies. These original figures will be returned if you so request.

While ACES reserves the right to re-type any submitted material, this is not generally done.

PUBLICATION CHARGES

ACES members are allowed 12 pages per paper without charge; non-members are allowed 8 pages per paper without charge. Mandatory page charges of $75 a page apply to all pages in excess of 12 for members or 8 for non-members. Voluntary page charges are requested for the free (12 or 8) pages, but are NOT mandatory or required for publication. A priority courtesy guideline, which favors members, applies to paper backlogs. Full details are available from the Editor-in-Chief.

COPYRIGHTS AND RELEASES

Each primary author must sign a copyright form and obtain a release from his/her organization vesting the copyright with ACES. Forms will be provided by ACES. Both the author and his/her organization are allowed to use the copyrighted material freely for their own private purposes.

Permission is granted to quote short passages and reproduce figures and tables from an ACES Journal issue provided the source is cited. Copies of ACES Journal articles may be made in accordance with usage permitted by Sections 107 or 108 of the U.S. Copyright Law. This consent does not extend to other kinds of copying, such as for general distribution, for advertising or promotional purposes, for creating new collective works, or for resale. The reproduction of multiple copies and the use of articles or extracts for commercial purposes require the consent of the author and specific permission from ACES. Institutional members are allowed to copy any ACES Journal issue for their internal distribution only.

APPLIED COMPUTATIONAL ELECTROMAGNETICS SOCIETY JOURNAL

INFORMATION FOR AUTHORS

PUBLICATION CRITERIA

Each paper is required to manifest some relation to applied computational electromagnetics. **Papers may address general issues in applied computational electromagnetics, or they may focus on specific applications, techniques, codes, or computational issues.** While the following list is not exhaustive, each paper will generally relate to at least one of these areas:

1. Code validation. This is done using internal checks or experimental, analytical or other computational data. Measured data of potential utility to code validation efforts will also be considered for publication.

2. Code performance analysis. This usually involves identification of numerical accuracy or other limitations, solution convergence, numerical and physical modeling error, and parameter tradeoffs. However, it is also permissible to address issues such as ease-of-use, set-up time, run time, special outputs, or other special features.

3. Computational studies of basic physics. This involves using a code, algorithm, or computational technique to simulate reality in such a way that better or new physical insight or understanding is achieved.

4. New computational techniques, or new applications for existing computational techniques or codes.

5. "Tricks of the trade" in selecting and applying codes and techniques.

6. New codes, algorithms, code enhancement, and code fixes. This category is self-explanatory but includes significant changes to existing codes, such as applicability extensions, algorithm optimization, problem correction, limitation removal, or other performance improvement. **Note: Code (or algorithm) capability descriptions are not acceptable, unless they contain sufficient technical material to justify consideration**.

7. Code input/output issues. This normally involves innovations in input (such as input geometry standardization, automatic mesh generation, or computer-aided design) or in output (whether it be tabular, graphical, statistical, Fourier-transformed, or otherwise signal-processed). Material dealing with input/output database management, output interpretation, or other input/output issues will also be considered for publication.

8. Computer hardware issues. This is the category for analysis of hardware capabilities and limitations in meeting various types of electromagnetics computational requirements. Vector and parallel computational techniques and implementation are of particular interest.

Applications of interest include, but are not limited to, antennas (and their electromagnetic environments), networks, static fields, radar cross section, shielding, radiation hazards, biological effects, electromagnetic pulse (EMP), electromagnetic interference (EMI), electromagnetic compatibility (EMC), power transmission, charge transport, dielectric and magnetic materials, microwave components, MMIC technology, remote sensing and geophysics, communications systems, fiber optics, plasmas, particle accelerators, generators and motors, electromagnetic wave propagation, non-destructive evaluation, eddy currents, and inverse scattering.

Techniques of interest include frequency-domain and time-domain techniques, integral equation and differential equation techniques, diffraction theories, physical optics, moment methods, finite differences and finite element techniques, modal expansions, perturbation methods, and hybrid methods. This list is not exhaustive.

A unique feature of the Journal is the publication of unsuccessful efforts in applied computational electromagnetics. Publication of such material provides a means to discuss problem areas in electromagnetic modeling. Material representing an unsuccessful application or negative results in computational electromagnetics will be considered for publication only if a reasonable expectation of success (and a reasonable effort) are reflected. Moreover, such material must represent a problem area of potential interest to the ACES membership.

Where possible and appropriate, authors are required to provide statements of quantitative accuracy for measured and/or computed data. This issue is discussed in "Accuracy & Publication: Requiring quantitative accuracy statements to accompany data", by E.K. Miller, *ACES Newsletter*, Vol. 9, No. 3, pp. 23-29, 1994, ISBN 1056-9170.

EDITORIAL REVIEW

In order to ensure an appropriate level of quality control, papers are refereed. They are reviewed both for technical correctness and for adherence to the listed guidelines regarding information content. Authors should submit the initial manuscript in draft form so that any suggested changes can be made before the photo-ready copy is prepared for publication.

JOURNAL COPY INFORMATION

March issue	Copy deadline 13 January
July issue	Copy deadline 25 May
November issue	Copy deadline 25 September

STYLE FOR CAMERA-READY COPY

The ACES Journal is flexible, within reason, in regard to style. However, certain requirements are in effect:

1. The paper title should NOT be placed on a separate page. The title, author(s), abstract, and (space permitting) beginning of the paper itself should all be on the first page. The title, author(s), and author affiliations should be centered (center-justified) on the first page.

2. An abstract is REQUIRED. The abstract should state the computer codes, computational techniques, and applications discussed in the paper (as applicable) and should otherwise be usable by technical abstracting and indexing services.

3. Either British English or American English spellings may be used, provided that each word is spelled consistently throughout the paper.

4. Any commonly-accepted format for referencing is permitted, provided that internal consistency of format is maintained. As a guideline for authors who have no other preference, we recommend that references be given by author(s) name and year in the body of the paper (with alphabetical listing of all references at the end of the paper). Titles of Journals, monographs, and similar publications should be in boldface or italic font or should be underlined. Titles of papers or articles should be in quotation marks.

5. Internal consistency shall also be maintained for other elements of style, such as equation numbering. As a guideline for authors who have no other preference, we suggest that equation numbers be placed in parentheses at the right column margin.

6. The intent and meaning of all text must be clear. For authors who are NOT masters of the English language, the ACES Editorial Staff will provide assistance with grammar (subject to clarity of intent and meaning).

7. Unused space should be minimized. Sections and subsections should not normally begin on a new page.

MATERIAL, SUBMITTAL FORMAT AND PROCEDURE

The preferred format for submission and subsequent review, is 12 point font or 12 cpi, double line spacing and single column per page. Four copies of all submissions should be sent to the Editor-in-Chief (see inside front cover). Each submission must be accompanied by a covering letter. The letter should include the name, address, and telephone and/or fax number and/or e-mail address of at least one of the authors.

Only camera-ready original copies are accepted for publication. The term **"camera-ready" means that the material is neat, legible, and reproducible**. The preferred font style is Times Roman 10 point (or equivalent) such as that used in this text. A double column format similar to that used here is preferred. **No author's work will be turned down once it has been accepted because of an inability to meet the requirements concerning fonts and format.** Full details are sent to the author(s) with the letter of acceptance.

There is NO requirement for India ink or for special paper; any plain white paper may be used. However, faded lines on figures and white streaks along fold lines should be avoided. Original figures - even paste-ups - are preferred over "nth-generation" photocopies. These original figures will be returned if you so request.

While ACES reserves the right to re-type any submitted material, this is not generally done.

PUBLICATION CHARGES

ACES members are allowed 12 pages per paper without charge; non-members are allowed 8 pages per paper without charge. Mandatory page charges of $75 a page apply to all pages in excess of 12 for members or 8 for non-members. Voluntary page charges are requested for the free (12 or 8) pages, but are NOT mandatory or required for publication. A priority courtesy guideline, which favors members, applies to paper backlogs. Full details are available from the Editor-in-Chief.

COPYRIGHTS AND RELEASES

Each primary author must sign a copyright form and obtain a release from his/her organization vesting the copyright with ACES. Forms will be provided by ACES. Both the author and his/her organization are allowed to use the copyrighted material freely for their own private purposes.

Permission is granted to quote short passages and reproduce figures and tables from an ACES Journal issue provided the source is cited. Copies of ACES Journal articles may be made in accordance with usage permitted by Sections 107 or 108 of the U.S. Copyright Law. This consent does not extend to other kinds of copying, such as for general distribution, for advertising or promotional purposes, for creating new collective works, or for resale. The reproduction of multiple copies and the use of articles or extracts for commercial purposes require the consent of the author and specific permission from ACES. Institutional members are allowed to copy any ACES Journal issue for their internal distribution only.